Rock Magnetism *and* Paleogeophysics

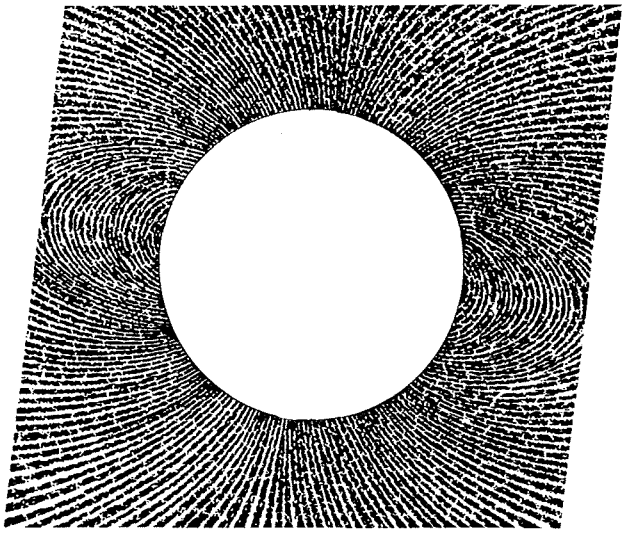

Volume 17

December 1990

Published by

Rock Magnetism and Paleogeophysics
Research Group in Japan

Preface

This volume is the annual progress report of the Rock Magnetism and Paleogeophysics Research Group in Japan for the year of 1990. We have published annual reports with a title *Annual Progress Report of the Rock Magnetism (Paleogeophysics) Research Group in Japan* in 1963, 1964, 1965, and 1967. Since 1973, the title changed to *Rock Magnetism and Paleogeophysics* and the reports were published annually (except 1976).

As the previous report were so, this volume contains a collection of summaries, extended abstracts or brief notes of research works carried out in our group this year. Many reports contain materials which may undergo a significant change or may be revised as the research activity continues. In this respect, readers are warned to regard them as tentative and are also requested to refer from a complete paper if published as a final results. (Names of journals appear at the end of individual articles if they are in press, submitted, or in preparation for submission to some scientific journals).

The editor of *Rock Magnetism and Paleogeophysics* has been Professor Masaru Kono of Tokyo Institute of Technology since 1973, that is from the first volume. Last year, he decided himself to retire from the editorial charge. There were some debate about the continuation of the annual report in our group. Finally, we decided to continue the publication on two *one-year shift* editors system: by M. Torii of Kyoto University for an even-number year, and by Y. Hamano of University of Tokyo for an odd-number year . Although it is difficult to state how long the publication will be maintained by our group, the editors are expecting to continue the annual report for more several years.

This publication is partly supported by a Grant-in-Aid for Scientific Research on Priority Areas (Central Core of the Earth) from the Japanese Ministry of Education, Science and Culture (No. 02246105).

Kyoto
December 1990

Masayuki Torii
Editor of 1990

Rock Magnetism and Paleogeophysics
Research Group in Japan

Rock Magnetism and Paleogeophysics, Volume 17
Table of Contents

Preface i

Table of Contents ii

Rock Magnetism and Paleogeophysics Symposium 22 iv

Rock magnetism

T. Yamazaki, I. Katsura, and K. Marumo 1
Origin of stable remanent magnetization of siliceous sediments in the central equatorial Pacific

M. Funaki, H. Sakai, T. Matsunaga, and S. Hirose 5
The S pole distribution on magnetic grains in pyroxenite determined by magnetotactic bacteria

M. Torii, H. Oda, and J. E. T. Channell 11
Some whole-rock magnetic properties of Pleistocene marine sediments from the Boso peninsula, central Japan

Archeomagnetism

T. Nishitani 17
Archeomagnetic investigation of Kami-Kumanosawa remain in Akita Prefecture

K. Maenaka 21
Archeomagnetic secular variation in Southwest Japan

Paleomagnetism: Geomagnetic application

C. Itota, M. Hyodo, and K. Yaskawa 26
Rotational sense of the geomagnetic vectors from paleosecular variation

M. Hyodo, W. Sunata, and E. E. Susanto 31
A long-term geomagnetic excursion from the Plio-Pleistocene sediments in Java

Y. Fujiwara and T. Kanamatsu 38
Magnetostratigraphy of the Nemuro Group, East Hokkaido, Japan

H. Oda, H. Shibuya, A. Hayashida, and M. Torii 42
An objective deconvolution scheme of pass-through measurement

Paleomagnetism: Tectonic application

H. Momose, M. Torii, and H. Tanaka 47
Counter-clockwise paleomagnetic direction from the Gongenyama Formation (N9-N10) on the coastal area of Northeast Japan

D. Miki and K. Hirooka 51
Deformation of the central part of the Honshu island inferred from paleomagnetic study
A. Hayashida, T. Fukui, and M. Torii 57
Paleomagnetism of the Early Miocene Kani Group in Southwest Japan and its implication for the opening of the Japan Sea
Y. Kanaori, S. Kawakami, and K. Yairi 59
An angle of a block rotation caused by left-lateral faulting in the Inner belt of central Japan
K. Fukuma and M. Torii 65
Paleomagnetic pole from late Cretaceous Koto Rhyolites, Southwest Japan
N. Ishikawa 73
Differential rotation of the western part of Southwest Japan: Paleomagnetic study in the northern part of the Kyushu Island
M. Koyama and S. M. Cisowski 80
Paleomagnetic evidence for northward drift and clockwise rotation of the Izu-Bonin forearc since the Late Oligocene
M. Miki, M. Furukawa, Y. Otofuji, S. Tsao, and T. Huang 83
Tectonics of an arc-arc junction: Paleomagnetic study of northern Taiwan
Z. Zheng, M. Kono, and J. Shao 86
The amalgamative history of eastern Asia inferred from paleomagnetism of the North China
Y. Otofuji, J. Kadoi, S. Funahara, F. Murata, and X. Zheng 94
Deformation of southern Tibet: Paleomagnetic study of the Quxu pluton of the Gandese belt

Paleogeophysics: miscellaneous

R. Morijiri, M. Makino, S. Okuma, and T. Nakatsuka 96
A study of ground magnetic and apparent susceptibility survey around Gozaisho-Takanuki metamorphic rocks
T. Fujiwara, S. Ogura, R. Morijiri, and H. Kinoshita 100
The crustal structure of the southern part of Boso Peninsula based on magnetic anomaly study
Y. Tatsumi and N. Kimura 105
Intermittent upwelling of asthenosphere beneath the Kenya Rift

Authors Index 109

Rock Magnetism and Paleogeophysics Symposium 22

The 22th Annual Symposium of Rock Magnetism and Paleogeophysics was held between 18th and 20th of July, at Naniwa Kaikan, Osaka (Convener: H. Shibuya).

Wednesday 18, July

H. Morinaga (Himeji Institute of Technology)
Paleoclimatic change in Central Tibet as inferred from stable isotope analysis of lake sediments.
H. Momose (Kyoto University)
Counter-clockwise rotation of NE Japan inferred from paleomagnetic directions of the Gongenyama Formation, Akita.
N. Niitsuma (Shizuoka University)
Paleomagnetic study on the rheology of the crust
H. Uchimura and H. Tanaka (Tokyo Institute of Technology)
Paleomagnetic and paleointensity database.
H. Sakai (Toyama University)
Paleomagnetic results of ODP Leg 119
T. Yamazaki (Geological Survey of Japan)
Grain size distribution of magnetic minerals in the deep-sea sediments.
K. Hirooka (Toyama University)
Paleomagnetism of sands extruded at a paleo-earthquake.
S. Nomura (Gunma University) and Paleomagnetic Research Group for Nojiri-ko Excavation
An evidence of different magnetization of some beds which had deposited in same age.
M. Koyama (Shizuoka University) and ODP Leg 126 Shipboard Scientific Party
Paleomagnetism of the Izu-Bonin-Mariana arc and its tectonic implication
H. Morinaga (Himeji Institute of Technology)
A geomagnetic excursion record in a stalagmite.

Thursday 19, July

H. Morisada (Toyama University)
Paleo-secular variation from the Holocene sediments.
K. Fukuma (Kyoto University)
ARM acquisition process in single domain grains.
H. Shibuya (University of Osaka Prefecture)
Bayesian statistics, how it works.
H. Oda (Kyoto University)
Deconvolution of long-core remanence data on the basis of Bayesian statistics.
H. Tsunakawa (Tokai University)
Bayesian approach to smoothing the paleomagnetic data.
J. Kirschvink (California Institute of Technology)
New biogenic magnetites in bacteria and fish

J. Kirschvink (California Institute of Technology)
Magnetostratigraphic constraints on the formation of Gondwana during Cambrian time.
Y. Kanaori (Gifu University)
Strike-slip block rotation of Southwest Japan
M. Nakanishi (University of Tokyo)
Source layer of marine magnetic anomaly lineations (Review)
M. Hyodo (Kobe University)
A review of paleomagnetic secular variation studies.
Y. Hamano (University of Tokyo)
Dynamo theory and the busy Earth's core.
Y. Honkura (Tokyo Institute of Technology)
Report on SEDI symposium.

Friday 20, July

Y. Honkura (Tokyo Institute of Technology)
Spatial dependence of the declination and inclination inferred from a model of geomagnetic secular variation.
H. Oda (Kyoto University)
Short polarity transition within Matuyama Chron.
A. Hayashida (Doshisha University)
Timing of the tectonic rotation of NE Japan.
C. Itota (Kobe University)
Identification of rotational sense of the geomagnetic vectors from paleosecular variation.
M. Torii (Kyoto University)
Some notes on rock magnetic study of sediments.

ORIGIN OF STABLE REMANENT MAGNETIZATION OF SILICEOUS SEDIMENTS IN THE CENTRAL EQUATORIAL PACIFIC

Toshitsugu YAMAZAKI [1], Ikuo KATSURA [2] and Katsumi MARUMO [3]

[1] Geological Survey of Japan, Tsukuba, Ibaraki 305
[2] Department of Geology and Mineralogy, Kyoto University, Kyoto 606
[3] Department of Geology, University of Toronto, Ontario, M5S 3B, Canada

Siliceous sediments distributed in the central equatorial Pacific are known to have stable remanent magnetization regardless of age or depth (Opdyke et al., 1974; Theyer and Hammond, 1974; Yamazaki, 1986). This is in contrast with the unstable remanence of unfossiliferous red clay (defined as "pelagic clay" here) which accumulates in the middle latitudes of the Pacific (Opdyke and Foster, 1970; Kent and Lowrie, 1974; Yamazaki and Katsura, 1990). We conducted a rock-magnetic study of the siliceous sediments to clarify the magnetic carriers of the stable remanence. For this purpose, we combined magnetic granulometry by the suspension method (Yoshida and Katsura, 1985) and observation of magnetic grains with a transmission electron microprobe (TEM). The advantage of the former is that the magnetic extraction procedure, which is inevitable for the latter, is not required for obtaining size distribution of magnetic grains in sediments.

Figure 1 shows the remanent magnetization of a siliceous-sediment core P225 from the central equatorial Pacific (position: 3°13.32N, 169°41.65W, water depth 5427m). The TEM observation (Fig. 2) revealed that most of the magnetic extracts from the core are identical in size and shape to magnetosomes of bacteria (Towe and Moench, 1981; Mann et al., 1987; Vali et al., 1987). The magnetic granulometry proved that the magnetic assemblages of the siliceous sediments of both Quaternary and early Miocene age have mean diameters of around 0.05μm (Fig. 3), which is within the single-domain range of magnetite (Butler and Banerjee, 1975), and have narrow size distribution compared with the pelagic clay (Fig. 4). These characteristics can be explained well if we consider that the magnetofossils found by the TEM observation are the major constituent of their magnetic grains, and these magnetites have been preserved for a long period of time. The difference in the stability of the remanent magnetization between the siliceous sediments and the pelagic clay can be explained by the difference in the size distribution of magnetic grains, which would reflect difference in their sources, biogenic vs. detrital (eolian).

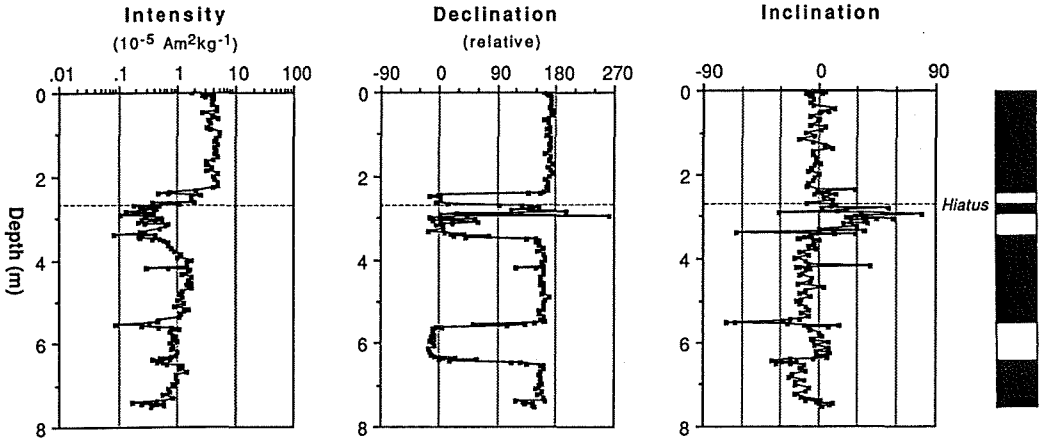

Fig. 1 Remanent magnetization of Core P225 after the alternating field demagnetization of 7.5 mT in a peak field (after Yamazaki, 1986). Declination is relative because the core was not oriented azimuthally. The intensity is normalized by the weight of solids. The right column is the magnetostratigraphic interpretation.

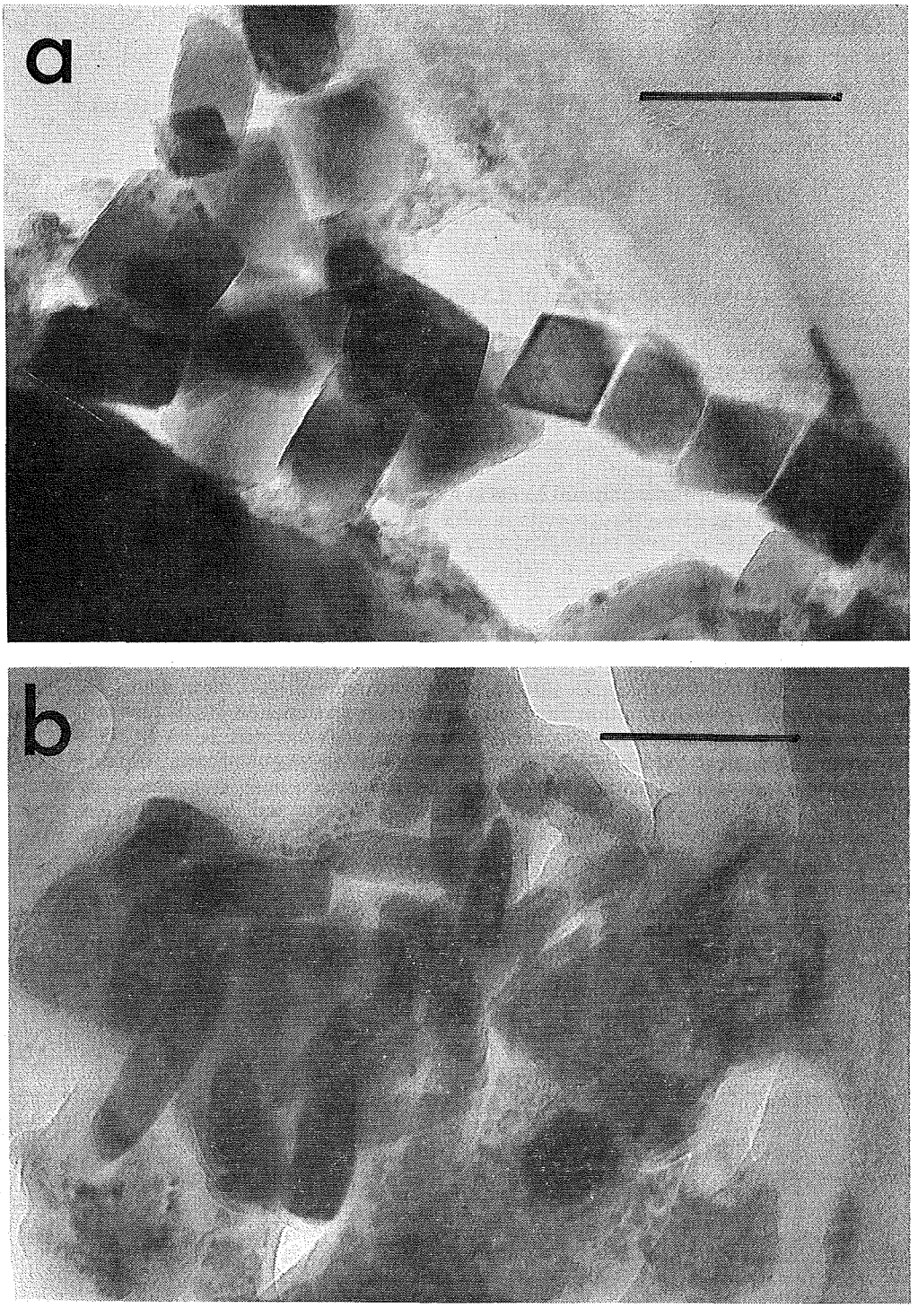

Fig. 2 TEM images of magnetic extracts from the siliceous sediments of early Miocene age (Core P225, 7.0 to 7.5m in depth); octahedra (rectangular in projection) (a), bullet-shaped grains (b). The shape and size of these grains are identical to magnetosomes in magnetotactic bacteria. Scale bars represent 0.1 μm.

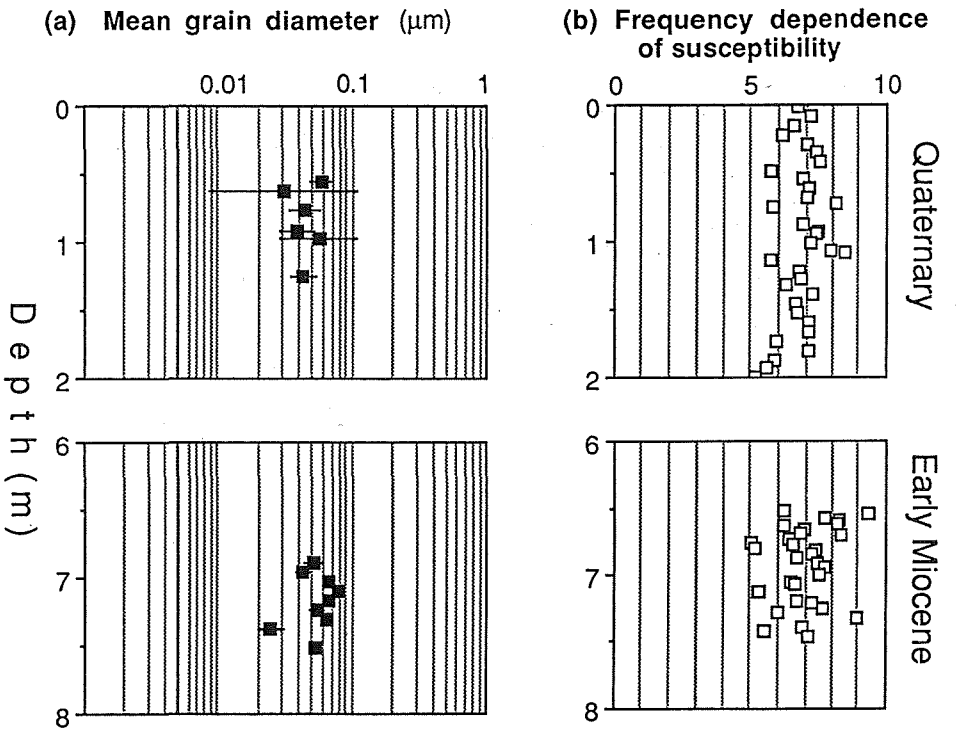

Fig. 3 (a) The mean diameter of magnetic grains in Core P225 calculated from the mean magnetic moment determined by the suspension method. The bar attached to the mean represents its uncertainty which propagated from the uncertainty of the mean magnetic moment. (b) The frequency dependence of magnetic susceptibility defined as 100 x $(\chi_L-\chi_H)/\chi_L$, where χ_L and χ_H are low-frequency (0.47 kHz) and high-frequency (4.7 kHz) susceptibility, respectively.

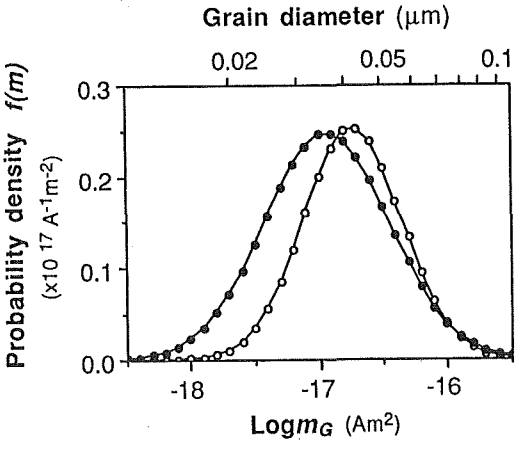

Fig. 4 Examples of the shapes of the probability density function of the magnetic moment distribution (a lognormal distribution was assumed). The samples having approximately equal mean moment are compared; a curve with open circles represents a sample of the siliceous-sediment core P225 (m_G =4.0x10^{-17}Am^2 (d =0.054μm), a = 3.8 (Table 1)), another curve with solid circles represents sample No. 888 of the pelagic-clay core P411 (m_G =4.1x10^{-17}Am^2 (d =0.055μm), a = 6.8; Yamazaki and Katsura, 1990).

References

Butler, R.F. and S.K. Banerjee (1975) J. Geophys. Res., 80, 4049.
Kent, D.V. and W. Lowrie (1975) J. Geophys. Res., 79, 2987.
Mann, S., N.H.C. Sparks and R.P. Blakemore (1987) Proc. R. Soc. Lond. B, 231, 469.
Opdyke, N.D. and J.H. Foster (1970) Mem. Geol. Soc. Amer., 126, 83.
Opdyke, N.D., L.H. Burckle and A. Todd (1974) Earth Planet. Sci. Lett., 22, 300.
Theyer, F. and S.R. Hammond (1974) Earth Planet. Sci. Lett., 22, 307.
Towe, K.M. and T.T. Moench (1981) Earth Planet. Sci. Lett., 52, 213.
Vali, H., O. Förster, G. Amarantidis and N. Petersen (1987) Earth Planet. Sci. Lett., 86, 389.
Yamazaki, T. (1986) Geol. Surv. Japan Cruise Rept., 21, 173.
Yamazaki, T. and I. Katsura (1990) J. Geophys. Res., 95, 4373.
Yoshida, S. and I. Katsura (1985) Geophys. J. R. astr. Soc., 82, 301.

(Submitted to Earth Planet. Sci. Lett.)

THE S POLE DISTRIBUTION ON MAGNETIC GRAINS IN PYROXENITE DETERMINED BY MAGNETOTACTIC BACTERIA

Minoru FUNAKI[1], Hideo SAKAI[2], Tadashi MATSUNAGA[3] and Shigehisa HIROSE[4]

1: National Institute of Polar Research, 9-10 Kaga 1-chome, Itabashi-ku, Tokyo 173.
2: Department of Earth Science Faculty of Science, Toyama University, Gofuku, Toyama 390.
3: Tokyo University of Agriculture and Technology, 24-16 Nakamachi 2-chome, Koganei City, Tokyo 184.
4: Tokyo Institute of Technology, 12-1 Ookayama 2-chome, Meguro-ku, Tokyo 152.

1. Introduction

The direction of the natural remanent magnetization (NRM) of magnetic grains in rocks gives some meaningful information for the NRM acquisition mechanisms. The NRM of rocks is measured by SQUID, spinner, astatic and other magnetometers, but the value shows an average NRM without any directional information of magnetic grains. If the grains can be taken out with orientations from the rock, it is possible, the procedure is usually extremely difficult because of too small grains.

Funaki et al. (1990) discussed a possibility to identify the fine magnetic structures of iron-nickel grains in chondrite by north seeking magnetotactic bacteria (NSB) which migrate to the only S pole. In the paper following evidences were elucidated.

(1): The bacteria are sensitive magnetic sensors to detect the S poles.
(2): The direction of dipole moment of the magnetic grains may be identified using both of the NSB and south seeking bacteria (SSB).
(3): The directions of lines of magnetic force radiated from the grains can be observed.
(4): The magnetic coercive force may be measured by the bacteria.

They pointed out that these evidences can be applied in principal to terrestrial rocks having relatively strong NRM. We have studied the S pole distributions in magnetite rich pyroxenite using the NSB. The result is introduced in this paper, although some fundamental examinations for the bacteria are still lacked.

We used the cocci type magnetotactic bacteria in this study, because of their high sensitivity to the magnetic field and the technic of enrichment. The bacteria with spherical shape of about 1 μm in diameter were confirmed.

2. Magnetic properties of a pyroxenite

A pyroxenite included 50-800 μm in size of magnetite grains which were cut by hercynite lamellae from 5 to 20 μm in width. A sliced sample (7.0x7.4x2.2 mm in size) was polished completely in order to observe the bacterial configuration on the surface.

The sample has been magnetized to relatively strong NRM as

intensity (R)=5.64x10^{-3} Am^2/kg, inclination (I)=75° and declination (D)=243°. The NRM was easily demagnetized by AF field; the NRM changed to R=1.02x10^{-5} Am^2/kg, I=-5.5° and D=325.9° to 60 mT. When the sample acquired saturation isothermal remanent magnetization (SIRM) to the north direction by 1.0 T of the steady magnetic field (H), the SIRM of R=7.79x10^{-1} Am^2/kg, I=-31.6° and 349.3° was very stable against the AF demagnetization.

The magnetic minerals in the rock were identified by thermo-magnetic analyses from room temperature to 700°C in 1.0T of the magnetic field under 8x10^{-2} Pa in atmospheric pressure. The results indicated that the rock included only single phase of pure magnetite with Curie point at 580°C.

Magnetic hysteresis properties were obtained between ±1.4T under the room temperature, indicating saturation magnetization (I_S)=25.2 Am^2/kg, saturation remanent magnetization (I_R)=1.02 Am^2/kg, coercive force (H_C)=4.15 mT and remanent coercive force (H_{RC})=15.3 mT.

3. Experimental procedure

The NSB were enriched by the S pole of a small hand-magnet in cultural bottles. A cluster of the NSB was pumped up with water by a glass tube, then the NSB were dropped on the sample in the controlled geomagnetic field to about 4μT. Although it is difficult to estimate the number of the NSB in a droplet, we estimated that more than several million in population were enriched in the droplet. The migration of NSB was recorded immediately by a video tape and photographs, if necessary, in order to analyze the S pole distribution on the sample. The S pole distributions were investigated in a natural state (NRM), after treatments by the AF demagnetization to 60 mT and acquisition of SIRM at H=1.0 T.

4. Experimental results

The main magnetite grains in the pyroxenite sample were marked from "a" to "z", as shown in Figs. 1 and 2. The dark-field microscopical observations were adopted to clearly detect the bacterial distributions as shown in Photo 1 (A, B, C, D), while it is not so clear under the bright-field observation.

The NSB made dense clusters not only at edges but also at interior in limited areas of the particular grains "a, d, e, l, u, v, y and z" in the NRM state. Some clusters were also observed on silicate areas, denoted "A" in the Fig. 1 . The density and size of clusters decreased clearly with time for some clusters on the grain "a" denoted "B" in Fig. 1, although other clusters did not changed drastically during 10 minute experiment. The most obvious cluster was formed at upper part of the grain "v" as shown in the Photo. 1(B). The representative feature of feeble cluster is shown at downward right side of the grain "d", as shown in Photo. 1(A). On the other hand, the NSB sparsely scattered throughout every magnetite grains, such as downward side in grain "v" and upward left one in the grain "d", as shown in the Photo. 1(A, B).

After AF demagnetization to 60mT, only sparse bacteria were observed on the every magnetite grain, while any bacterial

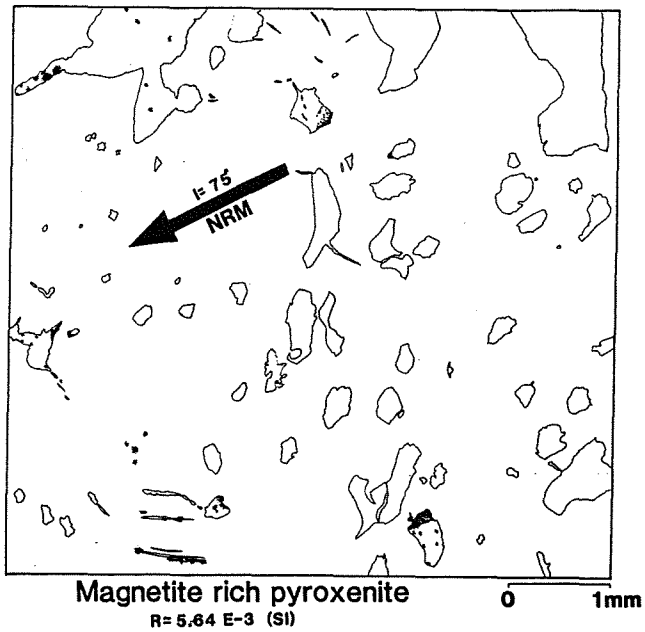

Fig. 1: Distribution of the magnetite grains and the lculsters of the NSB (bright or dotted areas) in the NRM state of thrpyroxenite sample. The NRM intensity of the sample: $R=5.64x10^{-3}$ Am^2/kg, arrow: direction of the declination, I: inclinationof the NRM.

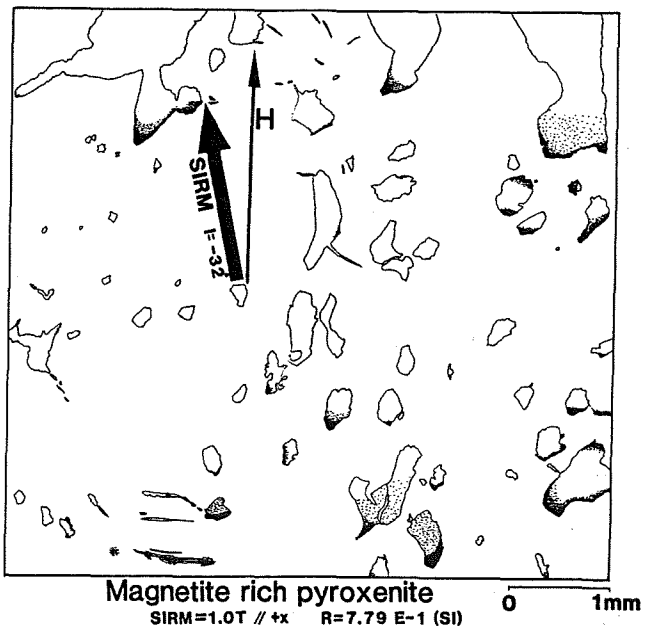

Fig. 2: Distribution of the bacterial clusters (bright areas) for the sample acquireing the SIRM (SIRM//+x=1.0 T). The SIRM intensity: $7.79x10^{-1}$ Am^2/kg, H: Applied field direction, Arrow: Declination, I: inclination of the SIRM.
clusters did not appear. Almost all NSB migrated to the boundary

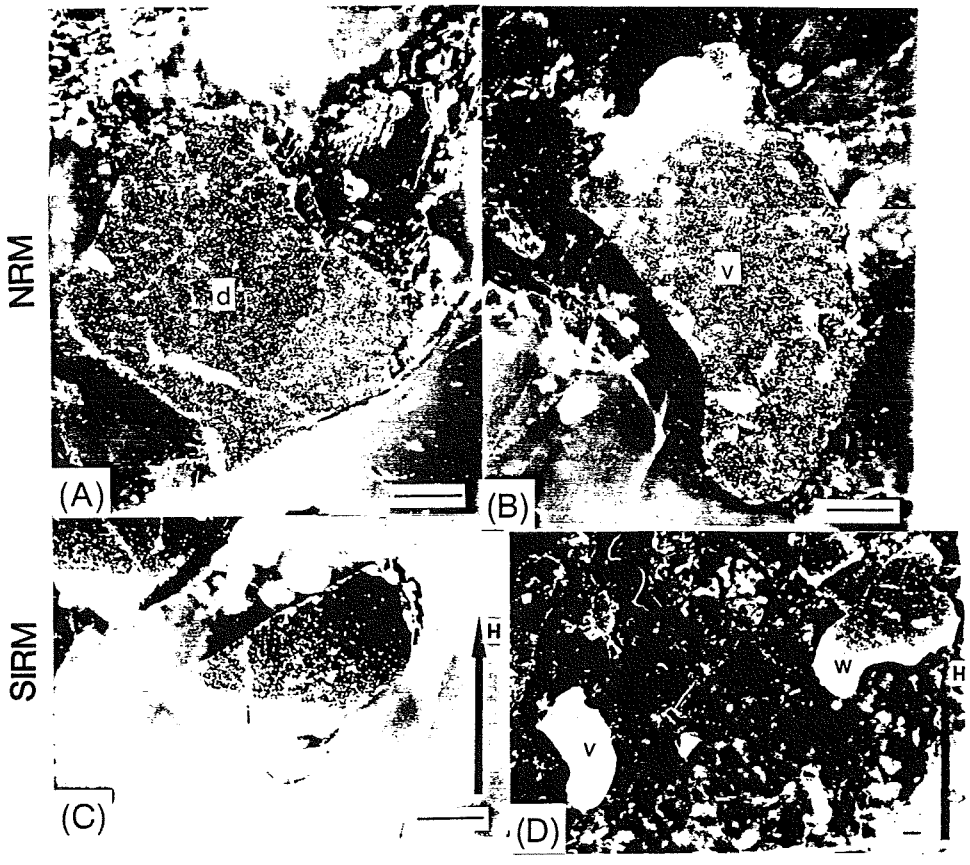

Photo. 1. The pictures were taken under the dark-field microscopical observation (pictures A, B, D and E) and the bright-field one (picture C). (A, B): the clusters of the NSB (bright areas) and the scattered ones (bright dot) on the magnetite grains in the NRM state. (C, D, E): the clusters of the NSB on the magnetite grains acquireing the SIRM. Arrows: applied filed direction. Scale: 0.1 mm.
of the droplet through the sample and gathered at their terminal.

When the sample acquired the SIRM (H=1.0 T//+x), the NSB formed the clusters as shown in Fig. 2, and following 4 kinds of the clustering features appeared.

Type 1: A dense cluster was formed at the S pole side (opposite direction to the H) as observed in many magnetite grains.

Type 2: An extremely dense cluster was formed at the S pole side and a relatively dense one was formed throughout the grains "u, v", as shown in Photo. 1(D) (grain "v").

Type 3: Dense and relatively dense clusters were formed at the S pole side and N pole one (parallel to the H) respectively

as observed on grains "h" and "w" (Photo. 1(D)).
Type 4: A few small clusters were formed along lamella-like grain "z".

Almost no sparse bacterial distributions were observed in the absent area of the clusters on the grains for the types 1 and 3. However, some grains did not take any clusters and took a small population of sparse bacteria even if the SIRM was acquired.

5. Discussions

The AF demagnetization curve indicated 2 components of the soft and the hard NRMs. The both components may not be believed paleomagnetically, because the magnetite grains are classified into multi-domain structure from the ratios of I_R/I_S=0.04 and H_{RC}/H_C=3.69 (Day et al., 1977). However, large magnetite grains with the strong NRM is available for the observation of the bacterial migrations in detail.

The NRM direction of original sample inclined steeply to downward direction (I=74.5°); the S poles exposed dominantly on the upper side of the sample (observed surface). The variable distribution of the bacterial clusters on the surface (Fig. 1) is explained by its steep downward inclination. Namely, a probability of the S pole occurrence is higher but its distribution is controlled with lower limitation for alignment to the declination. Four clusters in the silicate area "A" seems to have convergence of magnetic flux through silicate phase into the hidden magnetite grains. The decreasing density and size of clusters (denoted "B") on the grain "a" during the experiment seems to be caused by viscous remanent magnetization (VRM), because the magnetite grains consist of multidomain structure; the NRM intensity decreased in the controlled magnetic field (4 μT) by the VRM.

The acquired SIRM direction was I=-32° and D=349°, which was not parallel to the applied magnetic field. The reason is caused by magnetic shape anisotropy of the sample. The S pole distribution determined by the NSB (Fig. 2) has been classified into 4 types in this paper. Type 1 is obedient magnetite behavior; the SIRM is acquired toward the opposite direction to the applied magnetic field as expected. Many magnetic grains having this type distribution may indicate that the NSB can be detect the S poles on the fine magnetic grains. Types 2 is explained by the magnetization acquired toward the downward direction due to excessive magnetic anisotropy. Consequently the only S pole appeared on the observing surface of the grains. Type 3 is the grains having the S pole at the both side of grains along the applied field direction. As we do not know the polarity in absent area of the NSB on the grains, the distribution of the S poles cannot be explained in present. But it may relate to more complicate internal structures such as exsolution of lamellae and/or the anisotropy. Type 4 is the clusters formed on lamellar magnetite. As the magnetite situated to the perpendicular direction with the H, the cluster should locate either edges of the lamellae. If the lamellae extend to the downward direction, it may be possible to form the cluster at any place on the surface of lamellae. The SIRM of the sample is upward direction with I=-32°, so the N poles should rather

dominate on the observing surface. These magnetite grains without clusters may be result from the upward magnetization. Since the SIRM intenstiy at the clustering area may be extremely strong, it suggests that the NSB around the cluster must be strongly drawn to the cluster by the magnetic gradient. This may be one of the reason why almost all sparse bacteria were not recognized in a part of area of grains in the types 1 and 3.

We could not use the SSB in this study because of the cultivation problems. If the SSB are applied to this study, we can estimate the dipole direction of each magnetic grains. The size of the magnetotactic bacteria used in this study was 1 μm in diameter. So we can detect the S poles more than 10 μm in diameter of the magnetic substances. Since the smallest magnetotactic bacteria are 0.5 μm in diameter as reported by Lins de Barros and Esqivel (1985), it is possible to deteft further detailed magnetic structures.

6. Concluding remarks

The NSB can be applied to detect the S pole determination on polished rock samples under the dardk-field microscope. The NSB formed clusters at the various places on the magnetite grains in natural state (NRM=5.64×10^{-3} Am^2/kg), but did not form any clusters after AF demagnetization to 60 mT (NRM=1.02×10^{-5} Am^2/kg). However, the scattered NSB distributed on the whole magnetite grains, resulting from magnetic field of the domain walls. In the SIRM state (SIRM=7.79×10^{-1} Am^2/kg), very dense clusters were formed at the S Pole side on grains. The evidence indicated that the NSB are able to detect the S poles formed fine magnetic grains. The effect of magnetic anisotropy of grains was estimated from the formation of clusters, and that of the VRM was also observed by variation of density and size of the clusters. Here we estimated the fine magnetic structures of pyroxenite using the NSB. If the SSB are applied to this study, further detailed magnetic structures may be elucidated.

References

Blakemore, R., (1975) Science, **190**, 377-379.

Blakemore, R., (1982) Ann Rev. Microbiol. **36**, 217-238.

Blakemore, R, Frankel, R.B. and Kalmijn, Ad.J., (1980) Nature **286**, 24, 384-358.

Day, R., Fuller, M. and Schmidt, V.A., (1977) Phys. Earth Plan. Inter., **13**, 260-267.

Funaki, M., Sakai, H. and Matsunaga, T., (1990) J. Geomag. Geoelect., **41**, 77-87.

Lins de Barros, H.G.P. and Esquivel, D.M.S., (1985) in: Magnetite biomineralization and magnetoreception. Plenum Press, New York, pp289-309.

SOME WHOLE-ROCK MAGNETIC PROPERTIES OF PLEISTOCENE MARINE SEDIMENTS FROM THE BOSO PENINSULA, CENTRAL JAPAN

M. TORII, H. ODA and J. E. T. CHANNELL*

Dept. Geology & Mineralogy, Kyoto University, Kyoto 606, Japan
*Dept. Geology, University of Florida, Gainesville, FL32611, USA

Introduction

A thick sedimentary sequence of high-sedimentation rate is a good target for studying past geomagnetism. If we can continuously measure the remanent magnetism of homogeneous sediments, we will hopefully reveal time-variation of the past geomagnetism and resolving power for such an analysis is basically controlled by the sedimentation rate of the samples. Cenozoic marine sediments of the Boso peninsula deposited in extremely high sedimentation rate. The highest sedimentation rate so far reported from the Boso sediments is 370 cm/ka (Okada and Niitsuma, 1989). Niitsuma (1976) proposed revised magnetostratigraphy spanning from Pleistocene to upper Miocene for the Boso sediments . He also suggested a number of short polarity reversals which have been not correlated to the established subchrons of the geomagnetic reversal time scale so far.

We will hereafter just focus on the samples from the horizons between Jaramillo and Olduvai subchrons according to the magnetostratigraphy by Niitsuma (1976). The sediments from this horizon were deposited during the Matuyama reversed chron. This situation make it simple to find possible record of short polarity reversal phenomena. If we take samples from the normal polarity zone, it is rather difficult to discriminate normal overprinted samples on the basis of standard demagnetization techniques. Our final goal of the study is to decipher transitional field directions for those short polarity reversals. For this purpose, we have to find an optimum condition of demagnetization procedures based on the rock magnetic characteristics.

Sample and experimental procedure

We sampled at 127 sites along two river sections, Yoro river and Hirasawagawa river at the central area of the Boso peninsula. Samples were mostly collected from the fresh out crop of clay, silt and tuff layers on the river bed by using a portable drilling machine.

As a laboratory routine procedure, we selected two pilot samples for progressive AF and thermal demagnetizations from each site. We found that more than half of the samples were degraded by stable overprintings of the normal (present) field. It is generally accepted that thermal demagnetization is rather effective in eliminating secondary overprintings even for the case of

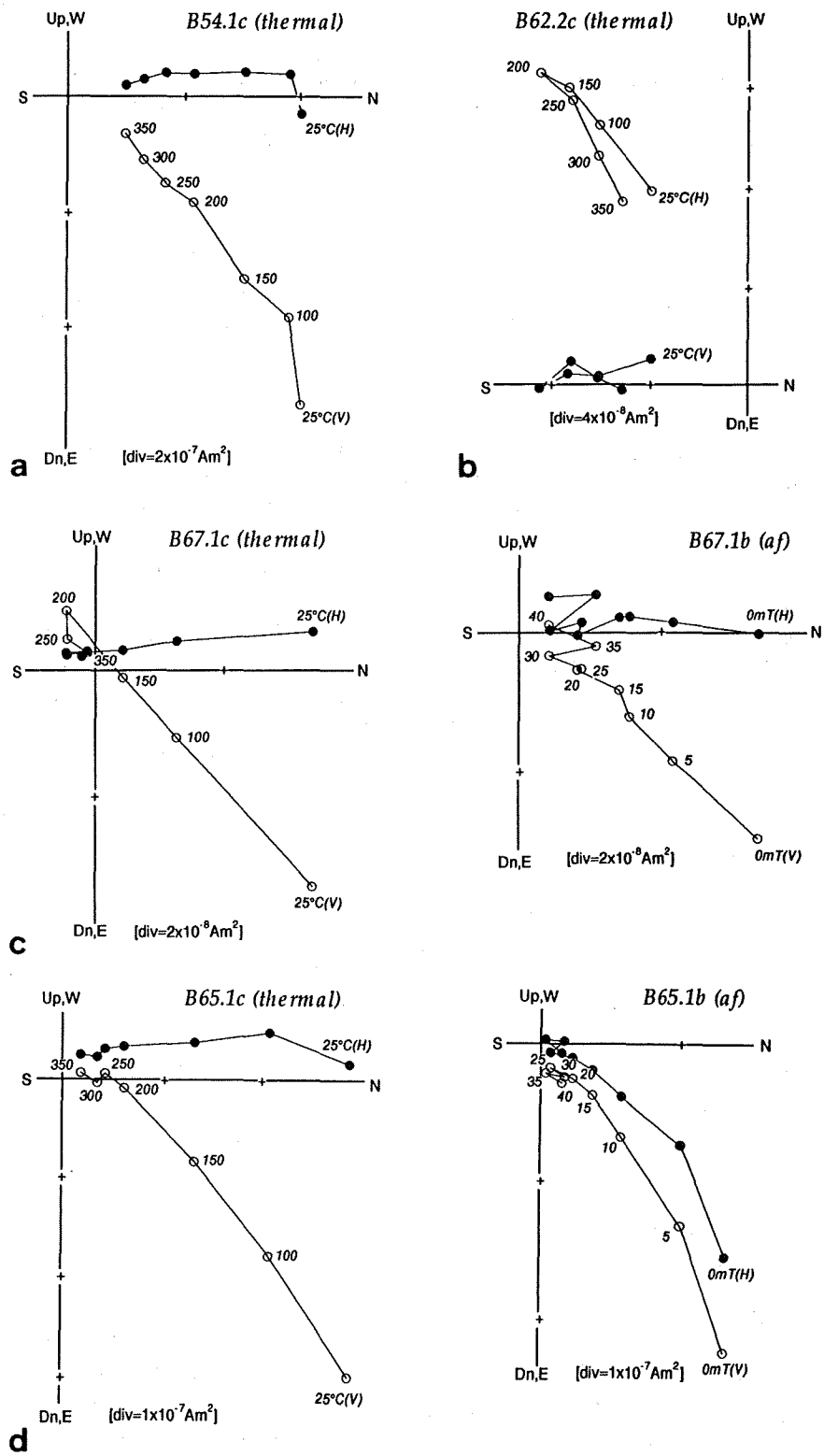

Fig. 1 Vector demagnetization plots of thermal and AF demagnetization. a: is typical example of N->N class samples. b: is R->R, and c: is N->R. d: is an example of unsuccessful demagnetization (N->?).

unconsolidated sediments (e.g., Torii et al., 1986; Vallet et al., 1988). For the case of the Boso samples, AF demagnetization could not bring linear decay to the origin of Zijderveld diagram for the most of cases (Fig. 1 c, d). Thermal demagnetization sometimes succeeded to reveal reversed component at the moderate temperature range (Fig. 1 c). However we could not extend heating higher than 350°C. Above that temperature, the remanent vectors showed irregular behavior. We measured initial susceptibility at each step of thermal demagnetization to detect change in magnetic property using Bartington M.S.2. susceptibility meter. The increase of susceptibility was observed for most of samples (Fig. 2). This thermal behavior can be attributed to the production of new magnetic minerals from iron-bearing non-magnetic minerals. We therefore ceased most of thermal treatment up to 350°C. This experimental difficultly is a one of reasons that we could not effectively remove the secondary overprintings.

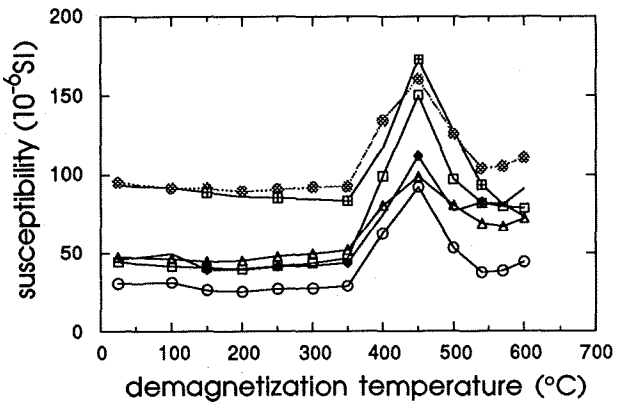

Fig. 2 Initial susceptibility measured after each step of thermal demagnetization.

We tentatively classified samples into four groups on the basis of pilot demagnetization results: N->N, R->R, N->R, and N-> ?. N->N is an abbreviation to represent the class of samples which have a normal polarity before demagnetization and hold normal polarity after demagnetization at a moderate temperature (Fig. 1 a). R->R and N->R are abbreviated with the same manner (Fig. 1 b, c). N-> ? is to symbolize ambiguous (unconvincing) results of thermal demagnetization (Fig. 1 d). The whole-rock samples were then tested by various rock magnetic methods as described below.

One of the pilot samples was subjected to stepwise alternating field demagnetization. ARM was then given to the AF demagnetized samples; with 100 mT AC field biased by 0.1 mT DC field. Acquired ARM was then demagnetized. IRM up to 1.3 T, by back field method, was then imposed and followed by AF demagnetization. Those procedure give us information about remanence coercivity and domain state of the magnetic minerals as know by "modified Lowrie Fuller test" (Johnson et al., 1975). After AF demagnetization of IRM, the sample was again magnetized along the z-axis of sample by 1.3 T DC field. Immediately after, 0.4 T IRM was superimposed along the y-axis, and further 0.12 T IRM was given to the x-direction. The composite IRMs was then

thermally demagnetized in a stepping mode above 600°C. This procedure is known as *orthogonal* IRM experiment which was recently introduced by Lowrie (1990). When we applied this method, we can get certain idea about unblocking temperature spectrum for three coercivity fractions at once. The rest of pilot samples was progressively demagnetized in the demagnetization oven.

Result and discussion

Rock magnetic study of sediments is generally not simple and has been not well organized. It is mainly because of rather complicated nature of the magnetic minerals in the sediments. We can not easily assume chemical characteristics and grain size distribution of the magnetic minerals in sediments as it sometimes possible for the case of igneous rocks. The orthogonal IRM method is one of the powerful tools to identify magnetic minerals in the sediments (Lowrie, 1990). Some typical examples of the orthogonal IRM experiment are shown in Fig. 3. It can be said that magnetic constituents in those samples are having one distinct (~550°C) and less prominent (~300°C) blocking temperature regardless with the coercivity fractions. We can find wide variation of intensity ratios between the soft component and the medium one (or the medium and the hard component) at each temperature (Fig. 3 a, b, c). However comparison among normalized curves for each coercivity fraction elucidates that there is no significant deviation of the unblocking temperature distribution (Fig. 3 d, e, f). All samples show an identical blocking temperature spectrum. For the hard component, relatively large fluctuation comes form extremely small value of the original IRM. This

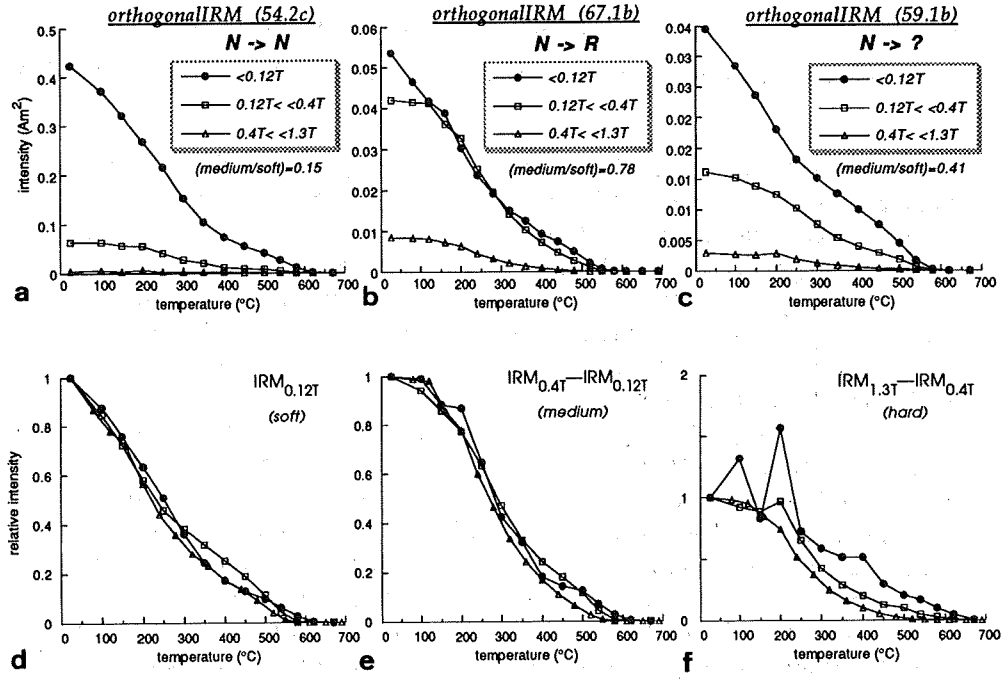

Fig. 3 Three examples of thermal demagnetization of orthogonal IRM (a, b, and c). Normalized intensities are plotted for each fraction of coercivity (d, e, and f).

pattern of the unblocking temperature is observed throughout all samples we studied. Thus we can safely conclude that the magnetic minerals in the studied samples have similar chemical composition.

Results of the modified Lowrie and Fuller test (Johnson et al., 1975) shows *roughly* identical pattern throughout the samples. If we can assume a single magnetic constituent, most of the samples seem to have grains as small as single and/or psuedo-single domain size.

We examined correlation among several rock magnetic properties such as a remanent coercivity (Bcr), MDF of ARM and IRM, ratio between medium IRM (0.4 T< <0.12 T) and soft IRM (<0.12 T) at the room temperature of the orthogonal IRM experiment, and so on. Diagrams in Fig. 4 are some examples of the correlations among those factors. We first found a good linear relationship between the intensity of SIRM and ARM (Fig. 4 a). Such a linear relationship is also found between some intensive factors such as Bcr, MDF of ARM, and MDF of SIRM (Fig. 4 c, d). There is however no clear correlation between Bcr and ARM intensity (Fig. 4 b). These lines of evidence suggest that the dominant magnetic minerals in the samples is unique (possibly Ti-magnetite), and the grain size distribution is rather continuous from single to psuedo-single domain size.

Negative correlation of Bcr with the ratio between MDF of ARM and that of IRM is illustrated in Fig. 4-e. This diagram may imply saturation of MDFs ratio to 1.0 at the higher range of Bcr. At the higher Bcr range, the grains are possibly in single domain size and thus MDFs of ARM and SIRM are almost compatible. Fig. 4-f shows linear increase of the ratio between the medium IRM (subtracting IRM acquired in 0.4 T field at room temperature from IRM in 0.4 T)

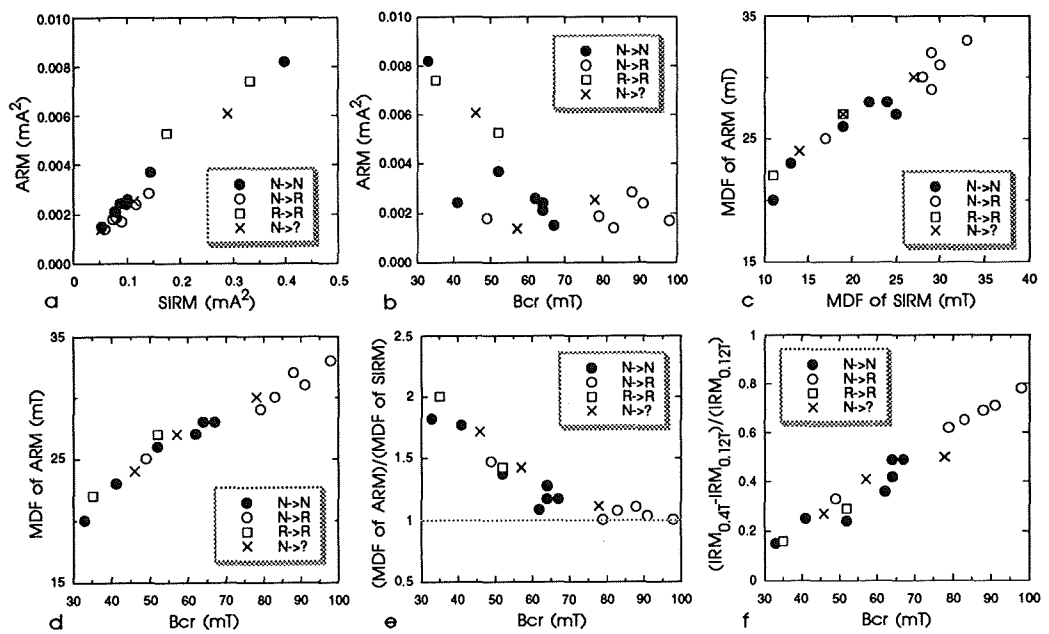

Fig. 4 Trial correlations among rock magnetic properties determined on whole-rock samples. See text for detailed explanation.

and the soft IRM (IRM in 0.12 T) to Bcr. This suggests continuous distribution of magnetically hard components in the samples.

In the Fig. 4, we used four different symbols which represent demagnetization behaviors as typically shown in Fig. 1. If we can find any trend or cluster of a particular symbol in the diagrams, it can be used as a diagnosis to the demagnetization experiments. It is quite natural that the samples of high coercivity (Bcr and MDFs) represent successful results (Fig. 4 c, d, e, and f). The samples of low Bcr are tend to have larger intensity (Fig. 4 b), and brought successful results. This may indicate relatively larger abundance of magnetic minerals in the samples. The unsuccessful samples are distributed on the medium coercivity range of the diagrams. There scattered some of N->N class samples. Those N->N samples correspond to the unknown short reversals of the Boso magnetostratigraphy. We are now planning to make farther experiments for those "marginal" samples.

References:

Johnson, H. P., H. Kinoshita, and R. T. Merrill (1975) Geol. Soc. Am. Bull., *86*, 412.

Lowrie, W (1990) Geophys. Res. Lett., *17*, 159.

Niitsuma, N (1976) J. Geol. Soc. Japan, *82*, 163.

Okada, M and N. Niitsuma (1989) Phys. Earth Palnet. Inter., *56*, 133.

Torii, M., H. Shibuya, A. Hayashida, I. Katsura, S. Yoshida, T. Tagami, Y. Otofuji, Y. Maeda, S. Sasajima, and S. Horie (1986) Proc. Japan Acad., Ser. B, *62*, 333.

Vallet, J.-P., L. Tauxe, and D. R. Clark (1988) Earth Planet. Sci. Lett., *87*, *463*.

ARCHEOMAGNETIC INVESTIGATION OF KAMI-KUMANOSAWA REMAIN IN AKITA PREFECTURE

Tadashi NISHITANI

Institute of Applied Earth Sciences, Mining College,
Akita University, Akita 010 Japan

Archeomagnetic investigations were performed at Kami-kumanosawa Remain. Kami-kumanosawa (39°8.6'N, 139°54.4'E) located near Kisakata city in Akita prefecture (Fig.1).

Total 78 specimens were collected in 8 furnaces using a plastic case (Fig.2). Archeologist indicates all samples in figure 2 are in the middle of Jyomon period (about 4000 B.C.) except SI-01, which has the age of Jyomon to Yayoi (about 2300 B.C.). Three pilot samples from each furnaces were demagnetized progressively up to a peak alternating field of 45 mT and an optimum alternating field (ODF) was determined. Other specimens were demagnetized using this optimum alternating field. Fig.3 shows results of this treatment.

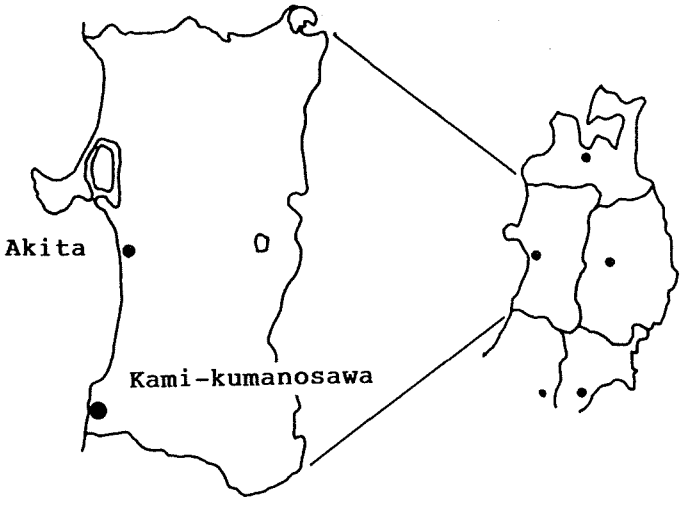

Fig.1 Kami-Kumanosawa is in the southern part of Akita Prefecture in Japan.

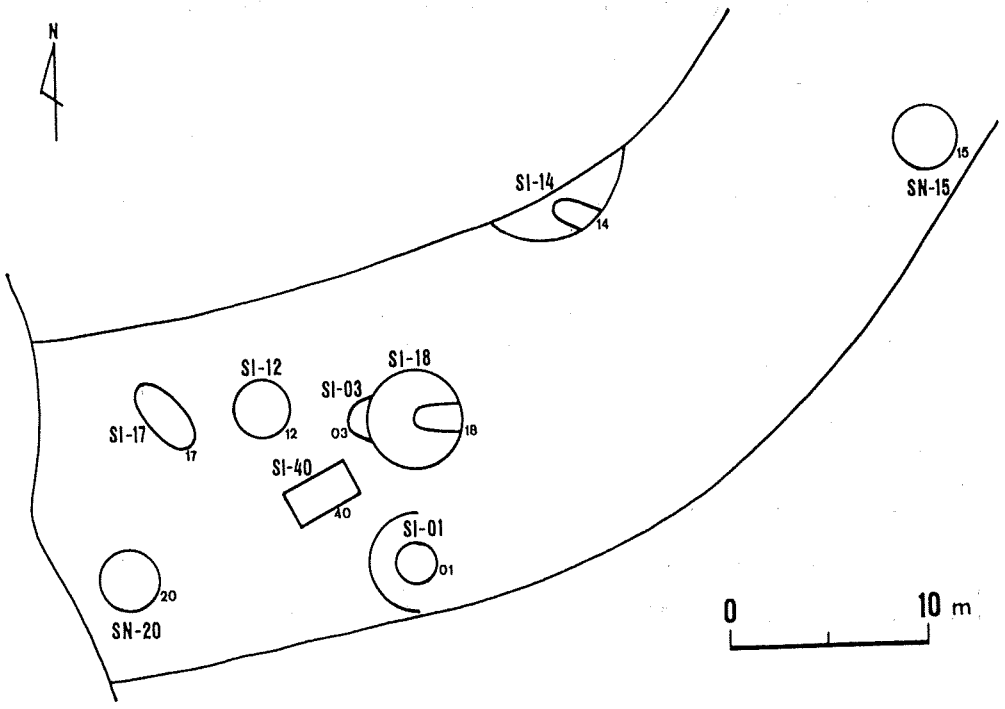

Fig.2 SI and SN mean furnaces. Samples were collected from these furnaces.

Table I Archeomagnetic results of Kami-kumanosawa remain.

Sample	N	ODF	Dec	Inc	k	α_{95}
SN-20	7	8	14.58	67.77	188.27	4.41
SI-01	15	7	-6.46	42.44	191.69	2.77
SN-15	10	6	-	-	-	-
SI-14	10	6	17.22	56.88	116.34	4.50
SI-18	7	6	0.53	55.47	104.89	5.92
SI-03	4	6	-3.77	62.45	270.06	5.60
SI-40	3	6	-	-	-	-
SI-12	9	5	10.89	56.68	128.34	4.56

Note: N: Analyzed data number, ODF: Optimum demagnetizing field (mT), Dec: Declination, Inc: Inclination, k: precision parameter, α_{95}: 95% confidence circle.

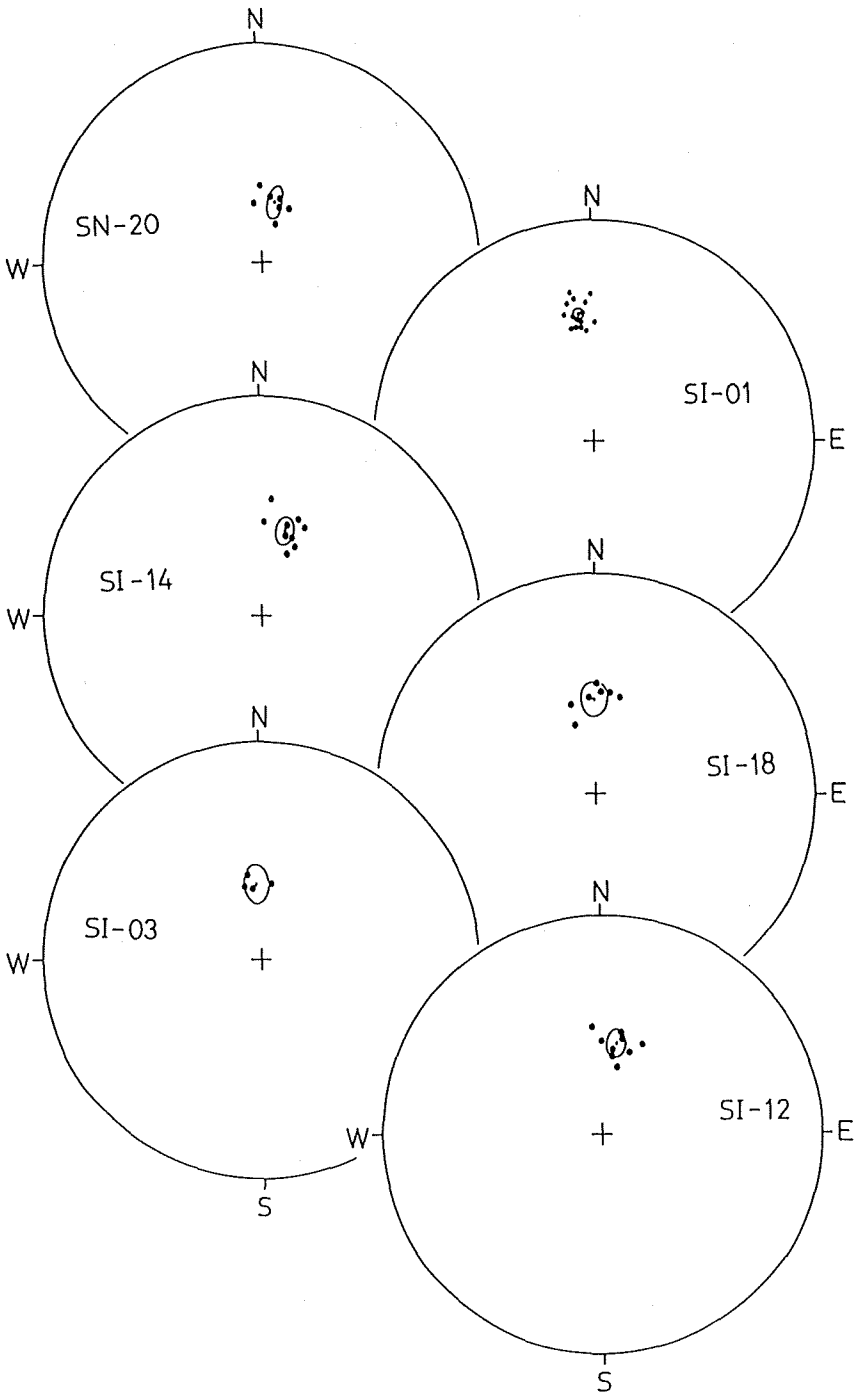

Fig.3 Results obtained after alternating field demagnetization. α_{95} confidence circle is also indicated.

Table I summarized the results. Figure 4 showed the mean inclinations and declinations. In this figure declination 0° means magnetic north direction. Archeomagnetic data in Jyomon and Yayoi period are not so popular because of the difficulty of age determination. The absolute age is not obtained in Kami-kumanosawa area in the present stage, but it will be obtained in the near future. The position of A.D.0 in the results of Hirooka (1971) is indicated in figure 4.

Reference

Hirooka, K. (1971) Mem. Fac. Sci., Kyoto Univ., Ser. Geol. Mineral., 38, 167.

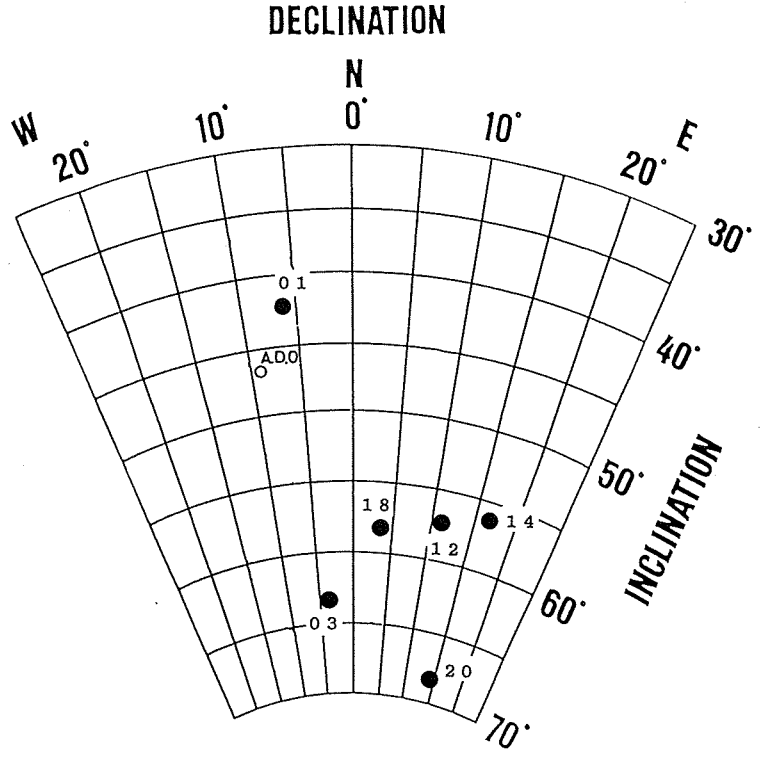

Fig. 4 Results of mean inclinations and declinations.

ARCHAEOMAGNETIC SECULAR VARIATION IN SOUTH WEST JAPAN

Kazuaki MAENAKA

Hanazono College, Nishinokyo-Tsubonouchi, Nakagyo, Kyoto 604

INTRODUCTION

A study of secular variation of the geomagnetic field gives the basis of paleomagnetic dating of archaeological remains. In Japan, the first trial to infer the secular variation of the geomagnetic field by means of archaeomagnetism was carried out by Watanabe (1959). He measured the magnetization of many baked clays of known age to correlate the secular geomagnetic variation to archaeological chronology. After then, Kawai et al. (1964) began to measure a number of samples from kilns and hearths excavated in Southwest Japan. As a dating tool, archaeomagnetism in Southwest Japan obtained fruitful results (Hirooka, 1971; Shibuya, 1980). However, ten years have passed since the geomagnetic secular variation in Southwest Japan was inferred by Shibuya (1980). Increase of data make it necessary to revise the basic values to draw the secular variation curve in Southwest Japan.

In this report, some new archaeomagnetic results obtained by the writer are presented, and then so far reported archaeomagnetic results are compiled with new data.

SAMPLING LOCATION

More than five hundred samples are collected from seventy-three sites of various locations in Southwest Japan as follows.

1) Aichi Prefecture
   1. NN-307 Kiln (Hirahari, Tenpaku-ku, Nagoya City)
   2. NN-259 Kiln (Shiratsuchi, Midori-ku, Nagoya City)
   3. H-G-6B (Ageha, Chigusa-ku, Nagoya City)
   4. H-G-6C1 (Ageha, Chigusa-ku, Nagoya City)
   5. H-G-6C2 (Ageha, Chigusa-ku, Nagoya City)
2) Nara Prefecture
   1. IK Sue Kiln (Ikoma City)
   2. Jikouin Urayama (Jikouin, Yamatokoriyama City)
   3. Shimogaito (Shimogaito, Heguricho)
   4. Hatsukayama (Hatsukayama, Heguricho)
   5. Haniwa Kiln (Sugawarahigashi, Nara City)
3) Osaka Prefecture
   1. A-2-103 OD (Fuseo, Sakai City)
   2. A-2-105 OD (Fuseo, Sakai City)
   3. A-2-106 OD (Fuseo, Sakai City)
   4. A-3-16 OD (Fuseo, Sakai City)
   5. A-3-70 OD (Fuseo, Sakai City)
   6. Sue Kiln (Hekiso, Sakai City)
   7. Haniwa Kiln (Hekiso, Sakai City)
   8. Obadera (Obadera, Sakai City)
4) Kyoto Prefecture
   1. EJX-A-02 (Abada, Takenogun)
   2. EJX-A-30 (Abada, Takenogun)
   3. EJX-A-31 (Abada, Takenogun)

4. EJX-C-2 (Enjo, Takenogun)
5. EJX-C-3 (Enjo, Takenogun)
6. EJX-C-4 (Enjo, Takenogun)
7. EJX-C-7 (Enjo, Takenogun)
8. EJX-C-9 (Enjo, Takenogun)
9. EJX-C-10 (Enjo, Takenogun)
10. EJX-E-2 (Enjo, Takenogun)
11. EJX-E-3 (Enjo, Takenogun)
12. EJX-E-4 (Enjo, Takenogun)
13. EJX-F-2 (Enjo, Takenogun)
14. EJX-F-7 (Enjo, Takenogun)
15. EJX-F-10 (Enjo, Takenogun)
16. EJX-F-20 (Enjo, Takenogun)
17. EJX-G-2 (Enjo, Takenogun)
18. EJX-G-3 (Enjo, Takenogun)
19. EJX-G-4 (Enjo, Takenogun)
20. EJX-G-5 (Enjo, Takenogun)
21. EJX-J-10 (Enjo, Takenogun)
22. EJX-J-11 (Enjo, Takenogun)
23. EJX-J-20 (Enjo, Takenogun)
24. EJX-J-21 (Enjo, Takenogun)
25. EJX-K-01 (Enjo, Takenogun)
26. EJX-L-01 (Enjo, Takenogun)
27. EJX-N-01 (Enjo, Takenogun)
28. EJX-N-02 (Enjo, Takenogun)
29. EJX-O-01 (Enjo, Takenogun)
30. EJX-O-02 (Enjo, Takenogun)
31. EJX-O-03 (Enjo, Takenogun)
32. EJX-O-04 (Enjo, Takenogun)
33. EJX-S-5 (Enjo, Takenogun)
34. EJX-T-1 (Enjo, Takenogun)
35. EJX-T-2 (Enjo, Takenogun)
36. EJX-V-10 (Enjo, Takenogun)
37. EJX-X-01 (Enjo, Takenogun)
38. EJX-X-02 (Enjo, Takenogun)
39. EJX-X-03 (Enjo, Takenogun)
40. EJX-X-04 (Enjo, Takenogun)
41. EJX-X-06 (Enjo, Takenogun)
42. EJX-X-07 (Enjo, Takenogun)
43. EJX-X-12 (Enjo, Takenogun)
44. EJX-Z-1 (Enjo, Takenogun)
45. Toridani-1 (Toridani, Takenogun)
46. Toridani-2 (Toridani, Takenogun)

5) Hyogo Prefecture
1. Shimizu (Tatsuno City)

6) Kagawa Prefecture
1. Maedahigashi (Takamatsu City)
2. Nakamura (Takamatsu City)
3. Ayanami Sue Kiln (Tokameyama, Ayautagun)
4. SF01 (Kusui, Takamatsu City)
5. SF02 (Kusui, Takamatsu City)
6. ST02 (Kusui, Takamatsu City)
7. SB4 (Tokameyama, Ayautagun)
8. KM (Kametani, Ayautagun)

MEASUREMENT AND RESULT

The remanent magnetizations of the baked earth specimens with the size of 35mm prepared from the collected samples were measured by a ring-core type spinner magnetometer (SSM-85). The secondary magnetizations can be removed by the progrressive alternating field demagnetization method. The reliable primary magnetization was discreted by the Zijderveld (1967) projection. The mean directions of the remanent magnetizations after magnetically cleaning were calculated by Fisher's statics (Fisher, 1953). The obtained result is given in Table 1.

Table 1. The result of measurement of the remanent magnetization of the baked earth specimens. Age is archaeologically estimeted.

Age	Site	Intensity of NRM ($\times 10^{-5}$emu/g)	N	D(° E)	I (°)	α_{95}	K
0	Jikouin	0.8~ 69.4	18	3.6	46.2	5.5	41
50	Fuseo A-3-160D	0.8~ 1.4	2	15.7	53.0	2.4	10882
75	Fuseo A-2-1050D	38 ~ 75	2	21.2	45.4	10.0	629
125	Fuseo A-2-1060D	2.4~ 43	9	3.7	51.7	3.5	215
150	Fuseo A-2-1030D	32 ~ 50	4	16.2	62.5	6.4	206
250	Fuseo A-3-700D	0.4~ 1.2	3	14.6	47.3	10.7	134
500	EJX-J-10	1.4~166	7	−13.4	56.9	6.6	85
500	EJX-J-11	3.6~150	11	−14.2	52.5	2.1	481
500	EJX-J-02	2.6~ 20	9	−12.7	52.0	4.3	225
525	Heki Sue Kiln	21 ~318	5	−16.5	47.1	4.6	276
550	Heki Haniwa Kiln	0.3~ 3.4	8	−13.9	55.1	3.4	259
575	EJX-L-01	3.9~ 42	6	− 9.0	57.9	3.2	430
575	EJX-O-01	0.3~ 29	11	−10.6	50.0	4.5	104
575	EJX-O-02	0.8~ 5.2	5	−12.7	51.5	5.7	180
575	EJX-O-03	0.7~ 52	8	−13.0	53.0	3.6	235
775	IK Sue Kiln	1.7~ 5.6	10	−13.4	54.4	3.2	224
800	EJX-A-02	3.7~ 33	11	−16.0	53.1	1.8	677
800	EJX-A-30	15 ~ 37	10	−12.8	54.3	2.3	440
925	NN-259	0.5~ 60	13	−18.0	41.7	4.1	101
975	Maedahigashi	52 ~ 80	6	−19.4	56.9	2.5	868
1100	H-G-6B	24 ~130	13	− 0.3	56.4	1.7	604
1100	H-G-6C1	80 ~535	9	2.1	56.9	2.0	680
1100	H-G-6C2	5.4~233	9	− 3.8	57.2	3.2	255
1150	Ayanami Sue Kiln	1.1~ 46	12	−10.2	55.5	1.9	507
1225	NN-307	4.5~ 31	14	0.9	59.1	1.8	496
1400	SF01	11 ~ 83	8	8.9	52.6	3.8	215
1500	Shimogaito	1 ~ 37	7	6.0	42.4	3.0	408

Table 2. List of mean directions of archaeomagnetic data at intervals of 25 years in Southwest Japan.

Median Age	Number of Sites	Dec(° E)	Inc(°)	α_{95}	K	Median Age	Number of Sites	Dec(° E)	Inc(°)	α_{95}	K
25	3	2.0	38.9	9.9	156	950	5	−16.1	46.1	5.3	210
50	3	− 4.7	55.5	18.2	47	975	4	−17.6	53.4	5.4	200
75	2	−15.4	55.5	23.9	117	1000	4	−16.2	52.3	7.9	138
100	2	8.0	46.5	41.3	39	1025	2	−11.3	50.1	23.2	118
125	2	− 1.1	48.9	18.0	195	1050	2	−15.5	48.2	9.8	655
150	3	7.1	60.8	13.7	83	1075	8	− 5.0	52.2	3.5	258
175	2	9.6	65.2	17.4	209	1100	13	− 3.1	53.5	2.1	394
200	2	5.3	62.0	9.2	742	1125	6	− 2.2	54.4	2.8	592
225	2	5.3	62.0	9.2	742	1150	6	− 1.8	59.1	4.1	268
250	6	8.3	51.6	5.6	143	1175	14	0.1	59.3	2.1	359
275	6	8.3	51.6	5.6	143	1200	15	1.1	59.0	1.9	424
300	1	− 9.1	58.3	.....	.....	1225	14	2.0	57.6	2.0	398
325	3	4.8	49.2	25.8	24	1250	9	3.5	57.3	2.2	525
350	3	3.9	48.7	25.8	24	1275	7	9.6	58.3	3.9	241
375	1	−11.7	56.4	.....	.....	1300	9	7.9	60.3	3.7	196
400	1	− 7.1	47.7	.....	.....	1325	8	8.9	58.5	4.5	150
425	10	− 7.2	45.2	3.2	233	1350	8	8.0	55.3	2.8	383
450	38	− 5.9	45.5	1.8	169	1375	6	4.7	56.4	3.7	332
475	53	− 6.1	47.8	1.5	167	1400	3	3.2	50.9	14.3	76
500	29	− 8.8	49.8	1.7	250	1425	1	8.9	52.6	.....	.....
525	12	−10.8	47.8	2.9	219	1450	1	2.9	40.6	.....	.....
550	27	−11.2	49.4	2.2	162	1475	1	2.9	40.6	.....	.....
575	33	−12.8	52.4	1.8	191	1500	1	6.0	42.4	.....	.....
600	27	−15.6	54.7	2.1	174	1525	3	6.4	43.4	1.4	7264
625	23	−12.4	60.0	2.2	193	1550	6	8.9	39.9	5.2	165
650	20	−13.0	59.4	2.3	201	1575	5	9.3	38.8	6.1	160
675	20	−13.5	58.9	2.3	219	1600	4	5.8	39.3	4.7	391
700	16	− 9.5	56.9	2.4	247	1625	5	4.5	38.8	3.4	494
725	9	−10.6	55.5	3.4	230	1650	10	4.1	40.0	2.5	380
750	38	−10.1	54.0	1.5	237	1675	12	4.9	40.4	2.3	351
775	48	−12.0	52.7	1.4	208	1700	9	5.1	41.5	2.1	611
800	14	−14.2	48.3	1.8	422	1725	6	4.2	41.8	2.0	1136
825	10	−13.4	49.8	2.4	342	1750	2	2.1	37.1	19.7	163
850	11	−13.5	49.9	2.7	281	1775	2	1.5	37.7	22.2	129
875	4	−15.3	51.7	5.4	294	1800	1	1.6	42.7	.....	.....
900	1	−14.5	42.0	.....	.....	1825	...	.....	.....	.....	.....
925	5	−15.2	43.8	3.5	469	1850	4	− 1.3	45.3	3.2	829

The baked earth specimens listed in Table 1 are collected from widely distributed locations in Southwest Japan. The archaeologically estimated ages also are ranged between 0 and 1500 AD. The intensity of the natural remanent of the baked earth specimens seems to be stronger than that of the volcanic rocks. The variation of the direction at the collecting sites in this work, however, has been known as within a few degrees, as the samples were obtained mainly from Kyoto and the areas around it. So, the present data are not corrected except the reduction from geomagnetic north to geographic north in declination.

For the purpose of obtaining the revised values to draw secular variation curve, the present data with those listed in Shibuya (1980) are analysed. To obtaining better results some rigorous criteria were applied through data processing.

(1) Median years were set at intervals of 25 years.
(2) The data whose archaeological age fell in the period between 25 years before and after each median year, were averaged by the method given by Fisher (1953).
(3) Mean directions which have a radius of 95% confidence circle larger than 11° were rejected.
(4) In the calculation, the datum whose most distant value from the mean direction exceeds ten degrees is removed, and then the mean direction of the remainders is computed. Thus the result whose most distant value from the mean direction is within ten degrees is adopted.

Table 2 gives the results of this calculation. From the viewpoint of archaeomagnetic dating, there are larger alpha-95 in the age before 400 AD, 900-1050 AD, and 1400-1500 AD. More accumulation of data in that ages is desired.

REFERENCES

Fisher, R.H. (1958) Proc. R. Soc. Lond., A217, 295.
Hirooka, K. (1971) Mem. Fac. Sci., Kyoto Univ., Ser. Geol. & Minerl., 38, 167.
Kawai, N., K. Hirooka, S. Sasajima, K. Yaskawa, H. Ito, and S. Kume (1964) Ann. Prog. Rep. Rock Mag. Res. Group Japan, 39.
Shibuya, H. (1980) M.E. Thesis, Fac. Eng. Sci., Osaka Univ., 54.
Watanabe, N. (1959) J. Fac. Sci. Univ. Tokyo, Sec. V, 2, 1.
Ziderveld, J.D.A. (1967) Method in Paleomagnetism, 254.

ROTATIONAL SENSE OF THE GEOMAGNETIC VECTORS FROM PALEOSECULAR VARIATION

Chizu ITOTA, Masayuki HYODO and Katsumi YASKAWA

The Graduate School of Science and Technology, Kobe University, Kobe 657, Japan

1. Introduction

Dominance of westward motion of drifting nondipole fields is one of the most important features in the present geomagnetic field. It is also recognized from the spherical harmonic analyses of the historical geomagnetic fields for the past 300 years (Bullard et al., 1950 ; Yukutake and Tachinaka, 1968). Extension of this feature farther in the past can be examined in paleomagnetic secular variations. A westward-drifting nondipole source makes the geomagnetic field vector rotate in a clockwise sense on the earth's surface (Runcorn, 1959). Exact secular variation records, however, show complex motions of field vectors mixed with clockwise and counter-clockwise rotations (Creer and Tucholka, 1983 ; Smith and Creer, 1986 ; Creer et al.., 1986 ; Verosub et al.., 1986).

We introduce a new method to examine the rotational sense of a field vector in a time-series data. The method is based on the idea that the complex motion of field vector is due to mixture of various field components with different periodicities. A paleosecular variation record from southwest Japan (Hyodo et al., in preparation) was used to test the method. The record is a stacked secular variation at 50-years intervals covering the duration from 11,500 years B.P. to 400 years B.P..

2. Method and results

The time series data of pairs of declination and inclination were transformed into those in the new coordinate system (X,Y,Z) defined as follows. The X-axis coincides with the direction of the geocentric axial dipole field at the site. The Y-axis is a horizontal axis perpendicular to the X-axis. The Z-axis is perpendicular to both X- and Y-axes (figure 1). A unit vector along a paleomagnetic field direction is separated into two components in this coordinate system. One is east-west (E-W) component defined by the angle between the X-axis and a vector projected on to the X-Y plane. The other is up-down (U-D) component expressed by the angle from the X-Y plane. A pair of these two components is preferred for the present analysis to the traditional one, a pair of declination and inclination, because the effect of latitude on the relative amplitude and degrees of scatter is compensated (Turner and Thompson, 1981). Secular variation of field directions is to be seen as an orbit of end points of unit vectors projected on to the Y-Z plane, which is here viewed along the X-axis from negative toward positive.

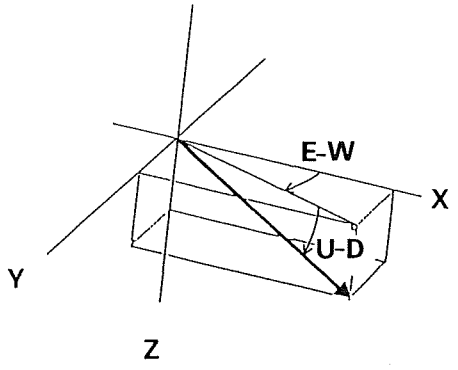

Figure 1

The new coordinate system. The X-axis coincides with the direction of the geocentric axial dipole field. The Y-axis is a horizontal axis perpendicular to the X-axis. The Z-axis is perpendicular to the X- and Y- axes.

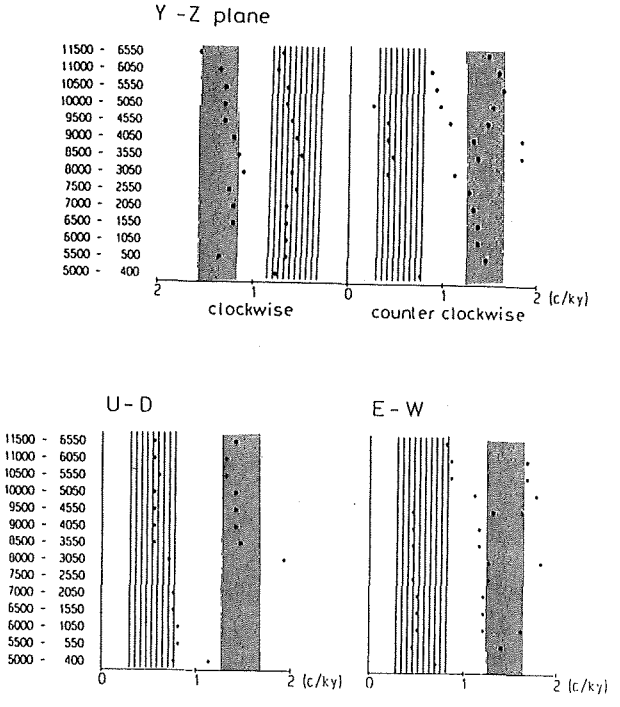

Figure 2

Results of spectral analyses for the new time-series data of secular variation within a running window 5000 years wide shifted by 500 years. Spectral peaks are obtained in two bands of periods 600-800 and 1200-3500 years shown by striped areas.

Spectral analysis was carried out on the E-W and U-D components, separately using the maximum entropy method [MEM] (Burg, 1967). Periodicities and sense of loopings on the Y-Z plane have been revealed by the MEM analysis of complex numbers [Y+i Z where $i=(-1)^{1/2}$] developed by Denham (1975). Both analyses were applied to the new time-series of secular variation within a running window 5000 years wide, shifted by 500 years. The results are summarized in figure 2. The periods of spectral peaks plotted with circles seem to concentrate in two bands. One is the period 600-800 years which is shown by thin striped areas in Figure 2. The other is the band 1200-3500 years which is shown by bold striped areas in Figure 2. The present secular variation data will be treated with band-pass filters of these periods in the later calculation.

Figure 3

Curvature of secular variation of field vectors calculated from three successive data points.

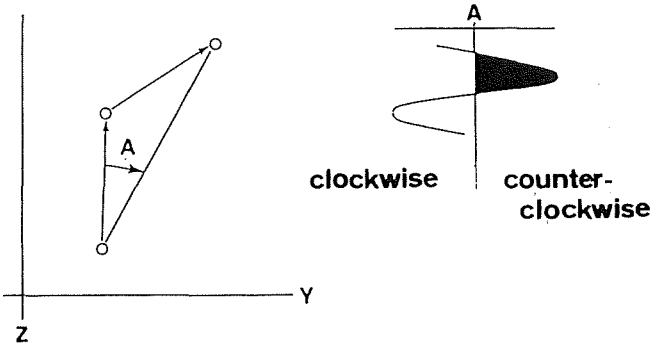

Calculation of curvature is one of the methods to see the sense of rotation of field's vector. Curvature is quantified by the angle 'A' in figure 3 calculated from three successive data points projected on to the Y-Z plane. This definition of curvature was given for virtual geomagnetic pole paths by Creer et al.. (1986).

The curvature was calculated for three sets of secular variation data ; the original one and two sets of secular variation data treated with band-pass filters of periods 600-800 and 1200-3500 years, respectively. The data sets and results of curvature calculation are represented in Figures 4 and 5, respectively.

Curvature of the original secular variation, without band-pass filters, represents complex pattern of change. The sense of rotation frequently changes and duration time of persistence of one rotational sense is only about several hundred years.

For the secular variation components of band of periods 600-800 years show that one sense of rotation continues more steadily. Durations of persistence of one rotational sense, for both clockwise and counter-clockwise, are extended to longer than one thousand years.

Curvature of the secular variation components of band of periods 1200-3500 years represents a simple pattern of persistence in rotational sense. Clockwise sense of rotation persists for about 4000 years twice in the past 11500 years : one is between 11500 years B.P. to 8050 years B.P. and the other is between 4550 years B.P. to 600 years B.P.. From 8050 years B.P. to 4550 years B.P., both rotational senses alternate in short intervals. The components of this band of periods has a nature of predominance of clockwise sense of rotation.

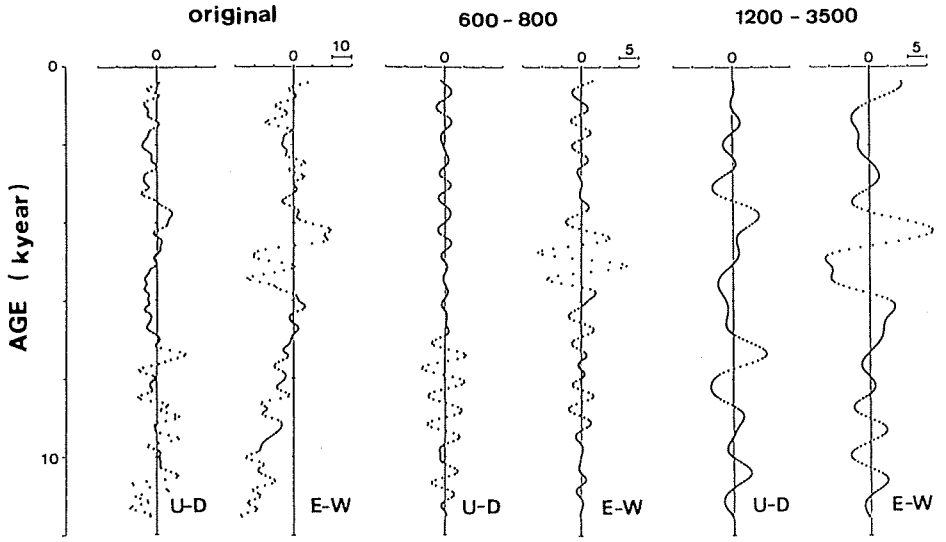

Figure 4

Analyzed data sets of secular variation ; original (left), the secular variation components of band of periods 600-800 years (middle) and the secular variation components of band of periods 1200-3500 years(right).

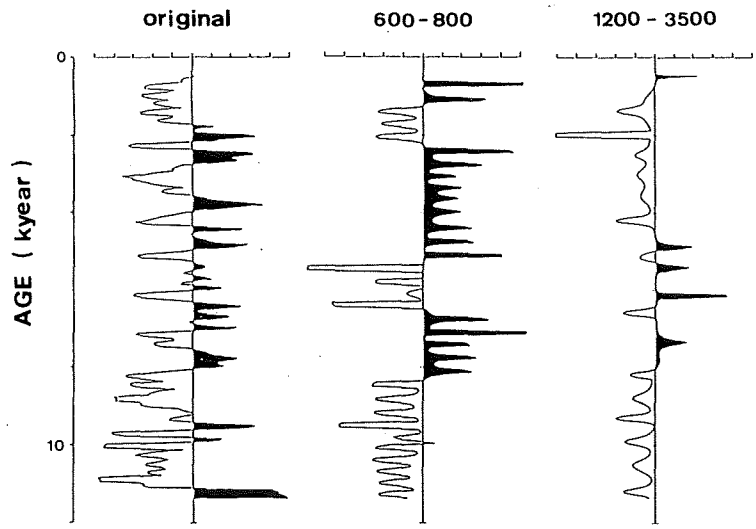

Figure 5

Plots illustrating the sense of curvature, clockwise sense is shown in white and counter-clockwise sense is shown in black. Curvature of field direction paths for the original secular variation (left), the secular variation components of band of periods 600-800 years (middle) and the secular variation components of band of periods 1200-3500 years (right).

3. Discussion

The motion of the geomagnetic field vector is very complex as shown by the vector motion without filtering in figure 5. This complexity may be caused by existence of various field components with different periodicities. Curvatures calculated for two sets of data treated with band-pass filters of periods, concentrated with MEM spectral peaks, do confirm this In the secular variation components of band of periods 600-800 years, both clockwise and counter-clockwise rotations continue for more than one thousand years. The stability of them seems to be equivalent. The components of band of periods 1200 to 3500 years shows predominance of clockwise sense of rotation. Thus our method seems to be useful to investigate the geomagnetic secular variation composed with various components.

Analyses of the geomagnetic data for the last 300 years revealed that the observed secular variation was considerably caused by the westward drift of the non-dipole field (Yukutake,1962). Velocity of westward-drifting has been estimated about 0.2~0.4°/year from historical geomagnetic records (Bullard et al.., 1950 ; Yukutake, 1962, 1968). The duration needed for one cycle is about 1800~900 years. If the nature of westward drifting of non-dipole fields has continued in the past several thousands or several tens thousands years,the effect should be observed in paleosecular variation data. The dominance of clockwise sense of rotation in the components of band periods 1200 to 3500 years suggests that the westward drifting is dominant in the past 10000 years.

Looping motions of a field vector can also be produced by stationary oscillating radial dipoles (Creer and Tucholka, 1982). The sense of curvature is depend on the phase difference

in oscillation of sources. Secular change of phase difference will make a curvature pattern includes alternations of rotational sense, as observed in curvature for the band of periods 600 to 800 years (figure 5). A westward drifting radial dipole with no intensity change can generate a counter-clockwise rotational motion of the local field vector under certain site - source geometry (Dodson, 1979). This phenomenon may be observed in some area under the present geomagnetic field (Thompson and Barraclough, 1982).

A recent examination using Gauss coefficients of geomagnetic fields at various epoches revealed that in the equatorial dipole component the eastward drifting components predominates over westward drifting one (Yukutake, 1987). Counter-clockwise sense of rotation may support the existence of the eastward drifting components. On the other hand, the addition of fluctuating components to standing and drafting non-dipole fields yields a good model for Gauss coefficients and requires no eastward drifting fields (Matsushima and Honkura, 1988). Eastward drifting non-dipole components are still on a debate for their existence in the present field.

It is hard at present to define the origin of curvature pattern because there are many possible sources. But through the analyses using our new method we have at least found a remarkable feature of curvature, a long term persistency of one rotational sense. The durations of one sense of rotation would indicate the stabilities of one condition in the earth's core, probably around the core surface, from where the sources of secular variation are originated.

References

Bullard, E.C., C. Freedman, H. Gellman and J. Nixon (1950) Phil.Trans. Roy. Soc. Lond. A, 243, 67-92

Burg, J.P. (1967) 37th ann. int. meet. Soc. Explor. Geophys.,Oklahoma City

Creer, K.M. and P. Tucholka (1982) Phil. Trans. R. Soc. Lond. A 306, 87-102

Creer, K.M. and P. Tucholka (1983) Geophys. J. R. astr. Soc., 74, 223-238

Creer, K.M., G. Smith, P. Tucholka, E. Bonifay, N. Thouveny and E. Truze (1986) Geophys. J. R. astr. Soc., 86, 943-964

Denham, C.R. (1975) J. Geophys. Res., 80, 1897-1901

Dodson, R.E. (1979) J. Geophys. Res., 85, 2625-2683

Matsushima, M. and Y. Honkura (1988) Geophys. J., 94, 35-50

Runcorn, S.K. (1959) Annls. Geophys., 15, 87-92

Smith, G. and K.M. Creer (1986) Phys. Earth Planet. Int., 44, 1-14

Thompson, R. and D.R. Barraclough (1982) J. Geomag. Geoelectr., 34, 245-263

Turner, G.M. and P. Thompson (1981) Geophys. J. R. astr. Soc., 65, 703-725

Verosub, K.L., P.J. Mehringer, Jr. and P. Waterstraat (1986) J. Geophys. Res., 91, 3609-3623

Yukutake, T. (1962) Bull. Earthq. Res. Inst., 40, 1-65

Yukutake, T. (1968) J. Geomag. Geoelectr., 20, 403-414

Yukutake, T. (1987) Hinrich-Herz Int. Rep. 21, 7-20

Yukutake, T. and H. Tachinaka (1968) Bull. Earthq. Res. Inst. Univ. Tokyo, 46,1027-1074

A LONG-TERM GEOMAGNETIC EXCURSION FROM THE PLIO -PLEISTOCENE SEDIMENTS IN JAVA

Masayuki Hyodo[1], Wahyu Sunata[2] and Eko. E. Susanto[2]

[1]The Graduate School of Science and Technology, Kobe University, Kobe 657, Japan
[2]G.R.D.C., Jl. Diponegoro No. 57, Bandung, Indonesia

1. Introduction

Geomagnetic secular variation and reversals represent two modes of change of the earth's magnetic field. The former shows steady fluctuations of the field due to small fluctuations of major entire flow, and generation, decay and/or drift of turbulent flows in the outer core. The latter may arise from drastic change of the entire flow in the core. Paleomagnetic observations on lacustrine sediment cores (Creer et el., 1983) suggests that secular variations are dominated by random and local sources. Detailed records of reversal transition field by recent observations from lavas (Mankinen et al., 1985) and sedimentary rocks (Valet et al., 1986 ; Okada and Niituma, 1989) have enabled to make some models for transitional field geometries and then indicate that some local fields make important role during reversals. Thus a number of paleomagnetic observations have developed our knowledge on these two major behaviors of the geomagnetic field.

Geomagnetic excursion has been still obscure comparing with the above two phenomena. Cox (1969) regarded excursions as large scale secular variations occurring at random which trigger reversals or as aborted reversals. Excursional fluctuations frequently observed around polarity transition (Clement and Kent, 1985) support this model. On the contrary, few excursions independent on a reversal have been observed.

We report duplicate records of a geomagnetic excursion from two different sites 200 km distant in Java, Indonesia. The excursion is characterized by a simple large-scale motion in the field direction and its long duration ($>10^5$yr). We discuss a possibility of correlation with some excursions or short events reported from other places on the globe and estimate possible sources.

2. Sampling and experimental techniques

Paleomagnetic samples have been taken by handwork. Sediments 10-20 cm deep from surface were outcropped and then a flat level about a few hundreds cm^2 was constructed using nonmagnetic tools, from which five to seven small cubic specimens were cut out. Sometimes a large block sample was collected and later in laboratory seven small cubic specimens were cut from each block sample. All the specimens were put in acrylic cubic capsules 2.5 cm on a side.

Paleomagnetic samples were mainly collected from fine clays and sometimes from fine tuffs. Silty clays were also sampled only when fine sediments were unobtainable. Sampling was made on the Plio-Pleistocene sediments in Sangiran, central Java and Mojokerto, east Java, both of which unearth hominid fossils (*Pithecanthropus*). Geological stratigraphies in both areas have been established in details (Watanabe and Kadar, 1984), so that stratigraphic levels of sediments at distant sampling sites are well correlated.

All the specimens were progressively demagnetized in alternating fields (AF) up to 80 mT in average at intervals of 5 - 20 mT. We adopted AF-demagnetization technique rather than thermal demagnetization to isolate stable primary remanence because most of sediments were still wet or preserved some moisture. Thermal demagnetization was applied only to the remanences of samples possessing anomalous paleomagnetic directions to test their stability.

3. Results from Sangiran

The Sangiran area (7.5°S, 110.8°E) is characterized by a dome structure which was truncated by erosion. Because of the truncated dome structure, older sediments are exposed concentrically, the oldest sediments being located at the center. The Kalibeng formation is overlain by the Pucangan Formation which mainly consists of black clays (Fig.1).
Depositional environment of this formation gradually changed from shallow marine to lagoonal and then to lacustrine. The Pucangan Formation is overlain by the Kabuh Formation which is

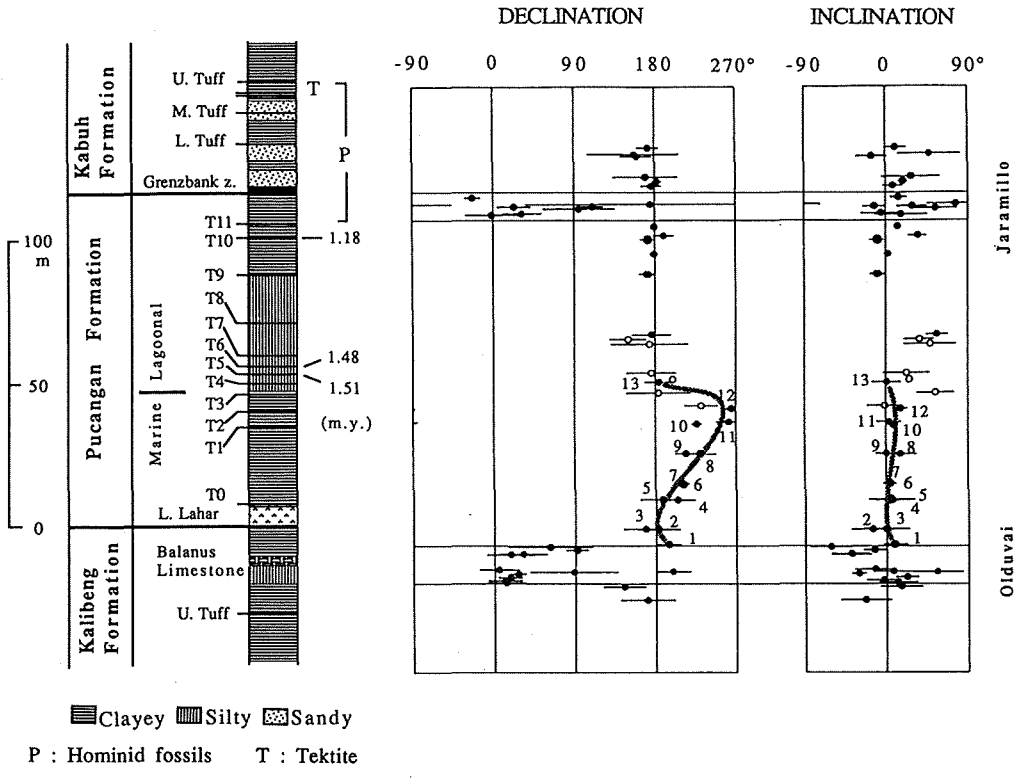

Fig.1 A columnar section and paleomagnetic results from Sangiran. Declination and inclination are of an average of converged higher-coercivity components of five to seven specimens in a horizon. Closed circles show magnetizations in the present study and open circles are those of previous work (see text). Error bars represent limits of 95%-confidence circle. The sequence of westerly deflected fields are numbered 1-13. The absolute ages of tuffs are those by fission-track dating.

composed of fresh water sediments. The discovery of a Tektite by excavation (Watanabe & Kadar, 1984) suggests that the Brunhes/Matuyama geomagnetic polarity boundary at 0.73 Ma (Mankinen & Dalrymple, 1979) is between the Middle and the Upper Tuffs in the Kabuh Formation. A total of 286 specimens from 45 horizons have been taken in the Kalibeng, Pucangan and Kabuh Formations.

Remanence of samples from the Pucangan Formation keeps stable direction until 60 mT in AF and the direction begins to scatter above the AF-level. A typical demagnetization behavior of remanence of samples from the Pucangan Formation is represented in Fig.2. Strong magnetizations often observed in the Kabuh Formation have been intensively affected by secondary viscous magnetization. Demagnetization behavior of such samples is like the typical of tuffaceous clays in Mojokerto as in the bottom of Fig.2. In both cases, all specimens in the same horizon exhibit consistent demagnetization patterns as in the right hand of Fig.2.

Declination and inclination of a mean of converged higher coercivity remanences are plotted in Fig.1. Two normal zones around the Balanus Limestone and below the Grentzbank zone may be correlated with the Olduvai and Jaramillo events, respectively. These are consistent with the results of fission-track dating (Suzuki et al., 1984) as in Fig.1,

A remarkable feature of paleomagnetic direction has been found in the declination just above the Olduvai event. There is a large scale change over a 50 m thick zone from just below the Lower Lahar up to the Tuff T4. The paleomagnetic directions somewhat westerly deflected just above the Olduvai event once returns to south and then gradually move westward again. After the maximum deflection (D= 264.9°, I=17.0°, a_{95} = 6.4°), it suddenly returns to south. Inclination keeps low values during the large change of declination.

4. Results from Mojokerto

The sampling area (7.5°S, 112.5°E) is located near the Perning village located 9 km north - east of Mojokerto City at the Kedungwaru Anticline. Older sediments are exposed by erosion of the ridge crest symmetrically in the north and south wings of the anticline, the oldest one being located at the axis. The Pucangan and Kabuh Formations are distinguished in this area. A total of 162 specimens over 28 horizons have been taken from clays, tuffaceous clays and tuffaceous silty clays.

Declination and inclination of horizon means of stable remanence after AF-demagnetization are shown in Fig.3. A zone of normal and intermediate magnetizations around the hominid fossil layer can be correlated with the Jaramillo event. The intermediate magnetizations are governed by easterly and downward directions. This is consistent with the Jaramillo event in Sangiran suggesting that the intermediate remanence is not due to insufficient removal of secondary remanence but represents the exact geomagnetic phenomena. The zone of normal and intermediate directions in the Moluscan Horizon II may represent the uppermost part of the Olduvai event. The large scale westward deflection of declination above the Olduvai event has also been obtained in Mojokerto.

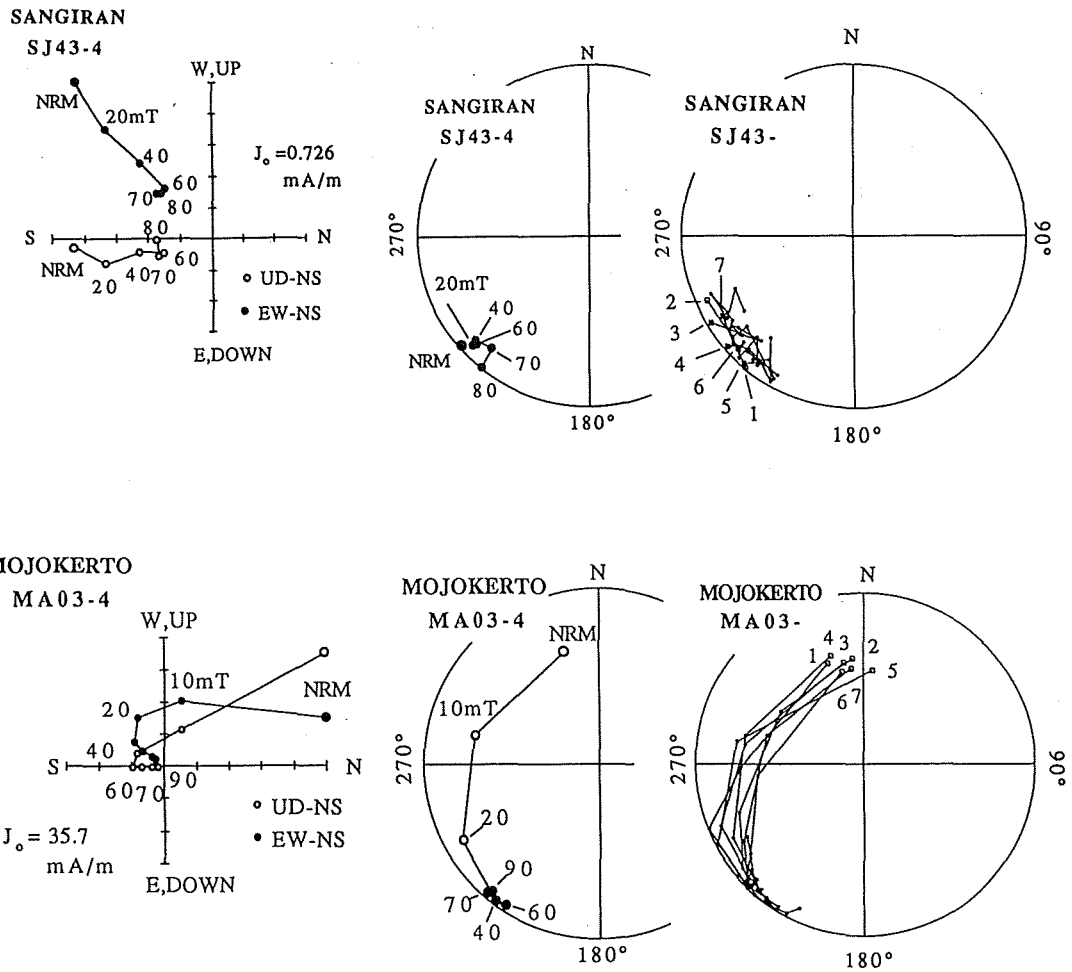

Fig.2 Typical AF-demagnetization patterns of samples from the black clay of the Pucangan Formation in Sangiran (top) and a tuffaceous clay in Mojokerto (bottom). Orthogonal and Equal area (middle) plots of remanence are on the same specimen. The equal area plot (Right) exhibits the consistent demagnetization patterns in the same horizon.

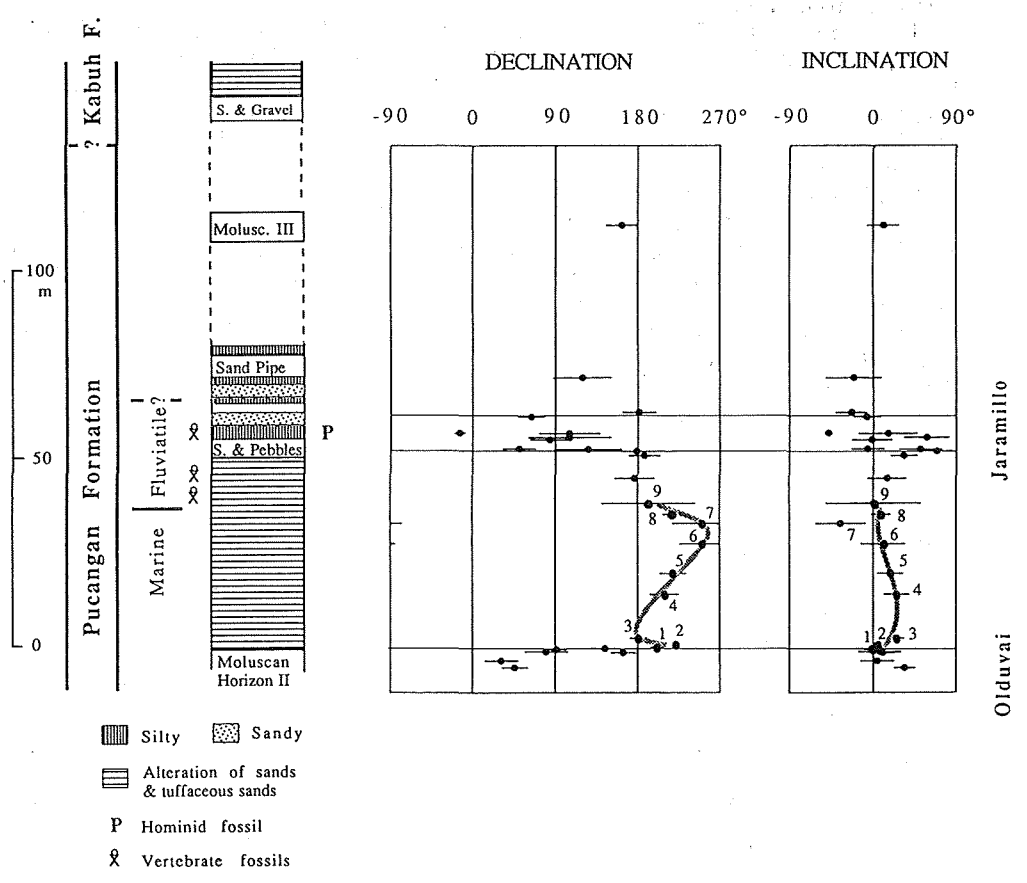

Fig.3 A columnar section and paleomagnetic results from Mojokerto. Declination and inclination are of an average of converged higher-coercivity components of five to seven specimens in a horizon. Error bars represent limits of 95%-confidence circle. The sequence of westerly deflected fields are numbered 1-9.

5. Geomagnetic excursion

Thermal demagnetization was applied to the remanence after AF-demagnetization of the marine sediments in the lower part of Pucangan Formation from both areas showing fairly westerly deflected directions. The remanence does not show significant changes in direction throughout the progressive thermal demagnetizations. The isothermal remanent magnetization (IRM) acquisition curves for the marine sediments in the lower part of the Pucangan Formation from both areas all attain saturation at about 0.5 T, indicating that the dominant magnetic mineral is magnetite or titano-magnetite. Sudden intensity drop at 300°C in the progressive thermal demagnetization also suggests that titano-magnetite is dominant. It seems that major magnetic carriers are titano-magnetite and the westerly deviated remanence in the marine sediment should be primary one.

The westerly biased fields above the Olduvai event are recognized at multiple sites suggesting that the anomalous fields are not caused by local disturbances of sedimentary structure. Since we sampled fine clays widespread in the area along the river Puren in Sangiran, the sampling sites are spacing sometimes several tens meters laterally. For example, the sites of the samples Nos.11 and 12 (Fig.2), the most westerly deflected data, are distant about 100 m. Further, a previous work (Shimizu et al., 1984) has also observed a westerly declination at a site 1.8 km south west of our site (Fig.1).

The stratigraphic positions of the Jaramillo and Olduvai events in Sangiran are quite convincing owing to many absolute age controls. There is no reliable dating in Mojokerto, but the upper normal zone should be defined as the Jaramillo event because it includes a Pithecanthropus fossil. All the discoveries of Pithecanthropus fossils in Sangiran range above the lower boundary of the Jaramillo event (Fig.1). Thus, the sequences of westerly deflected fields in Sangiran and Mojokerto are regarded as records of a same geomagnetic phenomenon between the Jaramillo and the Olduvai events. This is consistent with the positions of the boundaries from marine to lacustrine or fluviatile sediments in each sites (see Figs. 1 and 3).

Geomagnetic excursions are generally defined to have occurred when the VGP calculated from the field direction at the locality departs more than 45° from its time-averaged position for that epoch and is not associated with a polarity transition (Merrill and McElhinny, 1983). The present definition of geomagnetic excursion includes no condition on its duration of time. The VGP's of average reverse fields except the westerly deflected ones are at 82.9°S in latitude and 136.7°W in longitude (N=17) for Sangiran and at 81.1°S in latitude and 129.2°W in longitude (N=7) for Mojokerto. The geomagnetic fields which departs more than 45° in VGP from these averages are Nos. 8, 9, 10, 11 and 12 for Sangiran and Nos. 2, 5, 6, 7 and 8 for Mojokerto (Fig.4).

We here define that the sequence of the westerly deviated fields is a geomagnetic excursion which spans the fields Nos. 2-13 in Sangiran (Fig.1) and the fields Nos. 3-9 in Mojokerto (Fig.3). We exclude the fields in the basal parts which may be associated with a polarity transition. The sections span 44.7 m in thickness in Sangiran and 36.8 m in Mojokerto. The period of the excursion is estimated 130 Kyr (1.52-1.65 Ma) for the Sangiran record assuming a constant sedimentation rate between the tuff T5 dated at 1.51Ma and the upper boundary of the Olduvai event at 1.67 Ma (Mankinen and Dalrymple, 1979). The sequence of the most deviated fields which depart more than 45° in VGP spans 16.1 m in thickness in Sangiran, which is estimated 50 Kyr (1.55-1.60 Ma) assuming the same sedimentation rate. We here propose that the geomagnetic excursion be named the Sangiran Excursion. The black clay from just below the Lower Lahar to the Tuff T4 along the river Puren near the village Pablengan in Sangiran is here designated the type section.

The motion of field vectors during the excursion shows a simple large clockwise swing with some small clockwise and anticlockwise fluctuations and VGP's move on a simple circle (Fig.4).

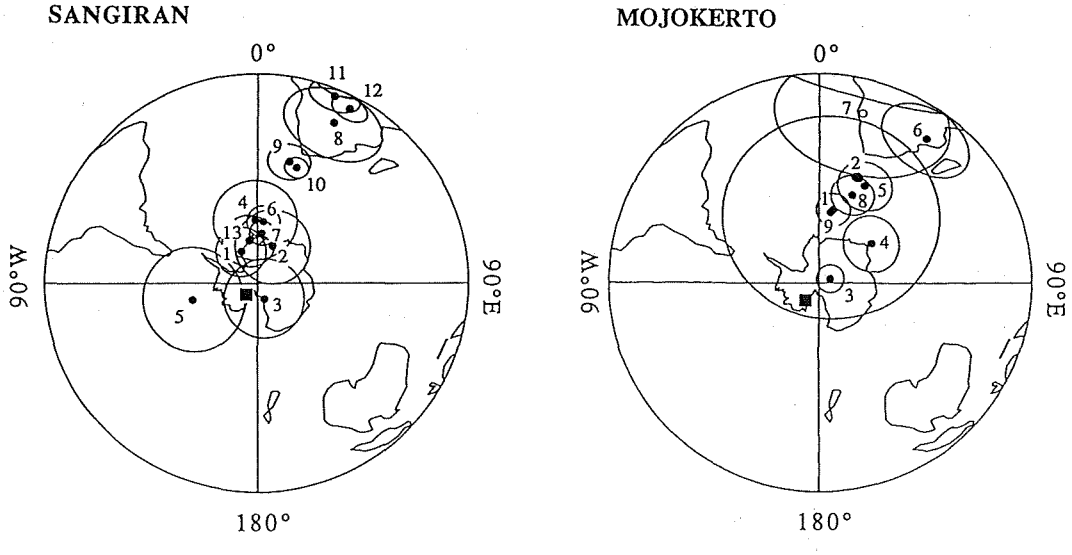

Fig.4 Equal area plot of VGP's during the westerly deflected fields with a 95%-confidence circle. Closed/open circles show southern/ northern hemispheres. Squares represent VGP positions of average reverse fields except the geomagnetic excursion in Matuyama epoch for each area.

6. Discussion

The Sangiran Excursion somewhat differs from others suggesting that there are intrinsic differences in their sources. The estimate of duration 130 Kyr is quite long in comparison with others', usually a few thousands years. The geomagnetic behavior of the Sangiran Excursion is rather simple. The Mono Lake Excursion shows an overall counterclockwise looping of field directions and steepening of inclination (Denham, 1974). The Laschamp Excursion includes full reverse fields (Bonhomet and Babkine, 1967). The only similarity in the geomagnetic behavior can be seen in the Lake Mungo Excursion, Australia in which field vectors with shallow inclination and some of them have westerly declination 230°-270° (Barbetti and McElhinny, 1976).

No geomagnetic excursion corresponding to the Sangiran Excursion has been observed at present. There have been reported many short events between the Jaramillo and Olduvai events. The short events at Cobb Mountain, California (Mankinen et al., 1978), at Komyoike, Japan (Maenaka, 1979) and at Coso Range, California (Mankinen and Gromme, 1982) should be the same one at 1.1 Ma. Two events, one corresponding to the Cobb Mountain event and a new one spanning 40 Kyr at about 1.4 Ma, have been found in a long core of lacustrine sediments from California (Liddicoat et al, 1980). Tauxe et al. (1983) reported an event at 1.3 - 1.4 Ma from Pleistocene sediments in southern Italy. Any of these events appear to be chronologically irrelevant to the Sangiran Excursion.

The Sangiran Excursion thus appears not to be a global phenomenon. We attempt to account for the excursion by a simple model with a geocentric dipole and an eccentric radial dipole (Alldredge and Hurwitz, 1968). We simulate the geomagnetic behavior calculating a field produced by a central axial dipole (c.a.d.) in the reverse polarity position and a standing eccentric radial dipole (e.r.d.) at the core/mantle boundary. The exact procedure of calculation is to obtain the position and the strength of an eccentric radial dipole with offset 0.54 earth's radius.

We have first searched an e.r.d. position on mesh points 5° in both latitude and longitude to obtain a field with almost westerly and horizontal direction resulting in many solutions over wide area. We have next calculated magnetic fields to account for the shallowly inclined fields with declination changing between 180° and 270°. Two solutions have been obtained, an upward-pointing e.r.d. at 35°S in latitude and 135°E in longitude (Model A) and a downward-pointing e.r.d. at 25°N in latitude and 80°E in longitude (Model B). Table 1 represents results of calculation of field directions for variaous moment ratios. Strength of e.r.d. moment relative to the c.a.d. moment changes up to 0.25 for Model A and up to 0.4 for Model B.

The Model A appears to produce more effectively shallowly inclined westerly fields. Models in conjunction with decrease in a geocentric dipole moment would be more realistic and further a pair of adjacent radial sources in opposite signs (Coe, 1977) also account for the deflected fields more effectively.

If strengths of nondipole fields are constant in all latitude, excursions more easily occur in low-latitude areas where a dipole field is small. Schneider and Kent (1988) showed that the time-averaged fields in low-latitude during the Plio-Pleistocene times deviate from the geocentric axial dipole fields. The deviation is expressed by negative inclination anomaly, which is equivalent with the existence of upward-pointing magnetic fluxes around the equator. The nondipole fields due to a radial source like the Model A may contribute to the geomagnetic inclination anomaly in low-latitude. Standing nondipole sources persisted for times as long as 100 Kyr may be associated with the dynamo model anchoring to the lowermost mantle by either thermal or topographic coupling (Gubbins & Richard, 1986 ; Bloxam & Gubbins, 1987).

Table 1. Eccentric radial dipole model. M/M0 ; moment ratio of e.r.d. relative to c.a.d.

Model A (35°S, 135°E)			Model B (25°N, 80°E)		
M/M0	Dec(°)	Inc(°)	M/M0	Dec(°)	Inc(°)
0.10	203	12	0.10	194	17
0.15	223	8	0.20	215	17
0.20	245	3	0.30	240	16
0.25	265	-3	0.40	268	15

In this study, we defined the geomagnetic excursion following the conventional definition based on only behaviors of change of the field direction, in spite of its long duration. We consider that conditions on its time duration and source mechanisms are not necessary like secular variations whose periods range from several tens to several thousands years produced by various sources.

7. Conclusions

(1) The paleomagnetic records from Sangiran and Mojokerto represent a large-scale deflection in the field direction between the Olduvai and Jaramillo events. The motion of the field directions in reverse polarity shows a simple clockwise swing with a maximum deflection more than 70° from the axial dipole field. We propose that the geomagnetic behavior be named the Sangiran Excursion. The black clay from just below the Lower Lahar to the Tuff T4 along the river Puren near the village Pablengan in the Sangiran area is designated the type section.

(2) The excursion is younger than the upper boundary of the Olduvai event and older than 1.51 Ma. The full duration is roughly estimated 130 Kyr (1.52 - 1.65 Ma) and the span of extremely deviated fields 50 Kyr (1.55-1.60 Ma) assuming a constant sedimentation rate.

(3) Neither geomagnetic excursion nor geomagnetic event corresponding to the Sangiran Excursion has been reported at present.The Sangiran Excursion should be a local phenomenon.

(4) The geomagnetic behavior during the excursion is accounted by a standing eccentric radial dipole at the core-mantle boundary changing its strength. Upward-pointing eccentric radial dipole model is plausible being consistent with possible sources for the inclination anomalies in the time-averaged fields of the Plio-Pleistocene times around the equatorial areas.

References

Alldredge, L. R. and L. Hurwitz (1964) J. Geophys. Res., 69, 2631-2640.

Barbetti, M.F. and M.W. McElhinny (1976) Phil. Trans. R. Soc. London, 281, 515-542.

Bloxam, J. and D. Gubbins, Nature, 325, 511-513, 1987.

Bonhommet, N. and J. Babkine (1967) C. R. Acad. Sci. Paris, B264, 92-94.

Clement, B. M., and D. V. Kent (1985) Phys. Earth Planet. Inter., 39, 301-313.

Coe, R. S. (1977) Nature, 269, 49-51.

Cox, A. (1969) Science, 163, 237-245.

Creer, C. M., P. Tucholka and C. E. Barton (Eds.) (1983) Geomagnetism of baked clays and recent sediments (Elsevier, Amsterdam) 324.

Denham, C. R. (1974) J. Geomag. Geoelect., 26, 487-498.

Gubbins, D., and M. Richard, Geophys. Res. Lett. (1986) 13, 1521-1524.

Liddicoat, J. C., N. D. Opdyke, and G. I. Smith (1980) Nature, 268, 22-25.

Lund, S. P., and S. K. Banerjee, J. Geophys. Res. (1985) 90, 803-825.

Maenaka, K., Geophys. Res. Lett. (1979) 6, 257-260.

Mankinen, E. A. and G. B. Dalrymple (1979) J. Geophys. Res., 84, 615-626.

Mankinen, E. A., J. M. Donnelly, and C. S. Gromme (1978) Geology, 6, 653-656.

Mankinen, E. A., and C. S. Gromme, Geophys. Res. Lett. (1982) 9, 1279-1282.

Mankinen, E. A., M. Prevot, C. S. Gromme and R. S. Coe (1985) J. Geophys. Res., 90, 10379-10417.

Merrill, R. T., and W. McElhinny (1983) The Earth's magnetic field (Academic Press, London) 401.

Okada, M. and N. Niituma (1989) Phys. Earth Planet. Inter., 56, 133-150.

Schneider, D. A., and D. V. Kent (1988) J. Geophys. Res., 93, 11621-11630.

Shimizu, Y., B. Muburoto, H. Siagian and M. Untung (1984) in Quaternary Geology of the Hominid Fossil Bearing Formations in Java (G.R.D.C., Spec. Publ. 4, Bandung) 275-308.

Suzuki, M., Wikarno, Budisantoso, I.Saefudin and M.Iitihara (1984) in Quaternary Geology of the Hominid Fossil Bearing Formations in Java (G.R.D.C., Spec. Publ. 4, Bandung)309-357.

Valet, J.-P., C. Laj, and Tucholka (1986) Nature, 322, 27-32, 1986.

Tauxe, L., N. D. Opdyke, G. Pasini, and C. Elmi (1983) Nature, 304, 125-129.

Watanabe, N. and D. Kadar (eds.) (1984) Quaternary Geology of the Hominid Fossil Bearing Formations in Java (Geol. Res. Dev. Centre, Spec. Publ. 4, Bandung) 378.

(Submitted to J. Geophys. Res.)

MAGNETOSTRATIGRAPHY OF THE NEMURO GROUP, EAST HOKKAIDO, JAPAN

Yoshiki FUJIWARA and Toshiya KANAMATSU

Department of Geology & Mineralogy Faculty of Science
Hokkaido University Sapporo, 060 JAPAN

Thick shallow marine and turbidite deposits intercalated with basic volcanic rocks are extensively developed in the Nemuro Peninsula eastern Hokkaido. These deposits have been called the Nemuro Group and considered to range in age from the Upper Cretaceous to Paleogene. The Nemuro Group has been divided into 8 Formations from their lithologic nature;
The Nokkamappu, Ohtamura, Monshizu, Hamanaka, Akkeshi, Tokotan and Kiritappu Formation in ascending order (Kiminami, 1978). Almost complete succession ranging from the upper Cretaceous to Paleogene is represented. Kiminami (ibid) suggested that the Cretaceous tertiary time boundary (K-T boundary) may be determined in the middle part of the Akkeshi Formation on the basis of fossil evidence. Saito et al. (1986) described the existence of a clay layer that marks the boundary between the Cretaceous and Tertiary period in the Shiranuka district, about 120 Km westward from the Nemuro Peninsula. We made magnetostratigraphic analysis of these formations to get further useful informations concerning to the K-T boundary layer.

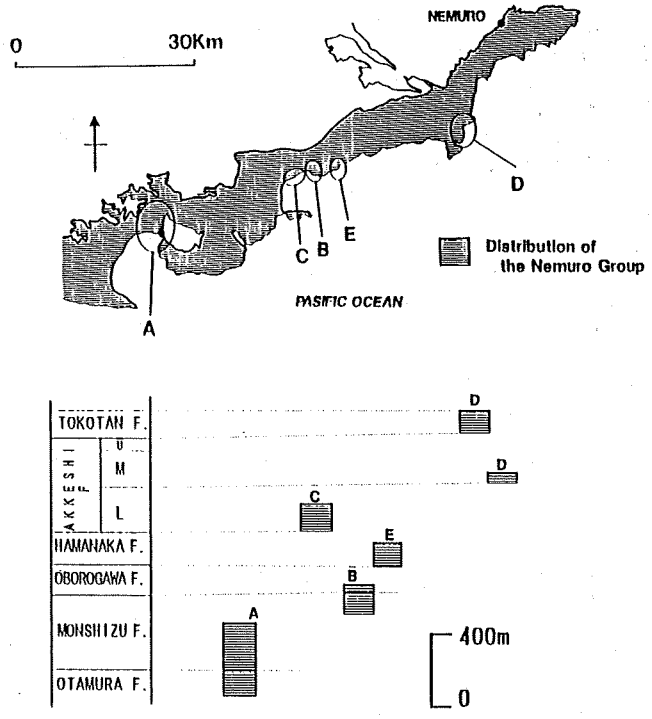

Fig. 1. Locations of the sampling sites and their stratigraphic positions. Distribution of the Nemuro Group in the Nemuro Peninsula is also shown.

Paleomagnetic determinations were made on 129 specimens from 14 sites from upper Cretaceous and Paleogene rocks in the Nemuro Peninsula. Their locations and the stratigraphic positions are presented in Fig. 1. Both alternating field demagnetization (AFD) and thermal demagnetization (THD) have been used to reduce a secondary component of magnetization. Mostly, the progressive AFD, at least one specimen from each site was demagnetized in stepwise up to 60 mT, effectively removes the soft components (Fig. 2). THD was carried out on specimens already subjected to AFD which represent no directional change.

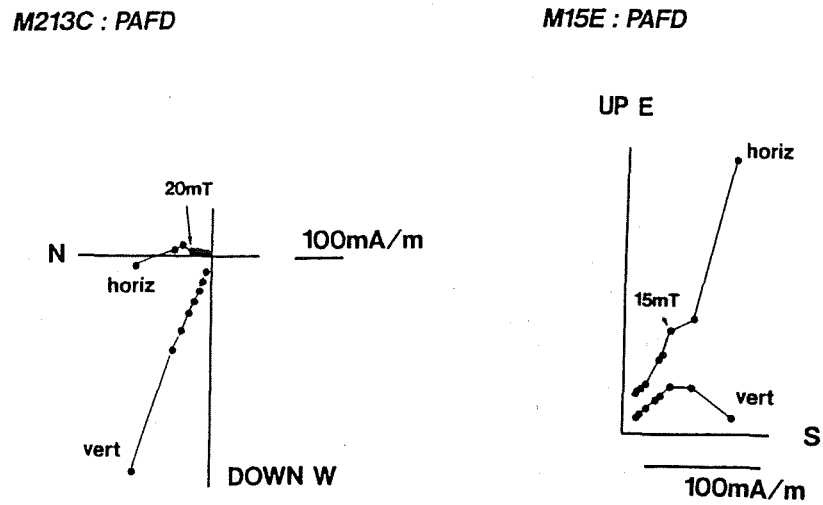

Fig. 2. Examples of results of stepwise AF demagnetization.

Tilt corrected site mean directions with corresponding ovals of 95% confidence are presented in Fig. 3. As clearly shown in the figure, the presence of antipodal steep negative inclinations can be inferred. The present results are approximately the same as the result reported by Tanaka and Uchimura (1989).

The K-Ar age was determined upon monzonite which considered to be intruded during deposition of the Ohtamura Formation (Shibata, 1985) This K-Ar age (70 Ma) indicate that the normal zone found from the upper Ohtamura Formation to the middle of the Monshizu Formation is tentatively correlated with the polarity chron 32. Therefore, the reversed zone inferred from the Oborogawa Formation ought to be precisely correlated with the chron 31R. The magnetic poralities of the Hamanaka Formation are predominantly normal and a short reversed zone is found in the middle part. There is a large possibility that this short reversed zone represents the chron 30N. Available K-Ar ages of volcanic rocks which suggesting the age of deposition of the Hamanaka Formation are also support this interpretation (Shibata, ibid). Magnetic porality of most of the Lower Akkeshi Formation is undoubtedly reverse. This reversed zone may accordingly be correlated with the chron 29R.

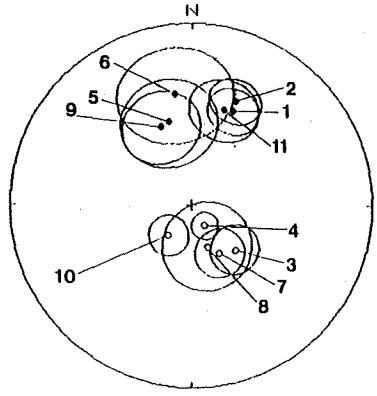

SITE No.	HORIZON	Dic	Inc	α 95	N	DEMAGTYPE(LEVEL)
1	OTAMURA F. (UPPER)	23	38	11	5	AFD(10mT)
2	MONSHIZU F. (LOWER)	19	44	15	11	AFD(10～20mT)
3	MONSHIZU F. (UPPER)	195	-62	11	7	AFD(20mT)
4	OBOROGAWA F.	147	-79	6	10	AFD(10～20mT)
5	HAMANAKA F. (LOWER)	344	51	21	3	THD(230°C)
	HAMANAKA F. (LOWER)	230	-46	56	4	THD(230°C)
	HAMANAKA F. (UPPER)	75	51	37	6	THD(230°C)
6	HAMANAKA F. (UPPER)	351	38	24	5	THD(230°C)
7	AKKESHI F. (LOWER)	149	-65	11	15	AFD(10mT)
8	AKKESHI F. (LOWER)	159	-70	20	6	AFD(10mT)
9	AKKESHI F. (MID)	338	52	17	5	THD(200°C)
10	TOKOTAN F. (LOWER)	217	-73	9	5	AFD(10mT)
11	TOKOTAN F. (UPPER)	24	43	11	2	AFD(10mT)

Fig. 3. Site mean directions and corresponding ovals of 95% confidence from 11 sites.

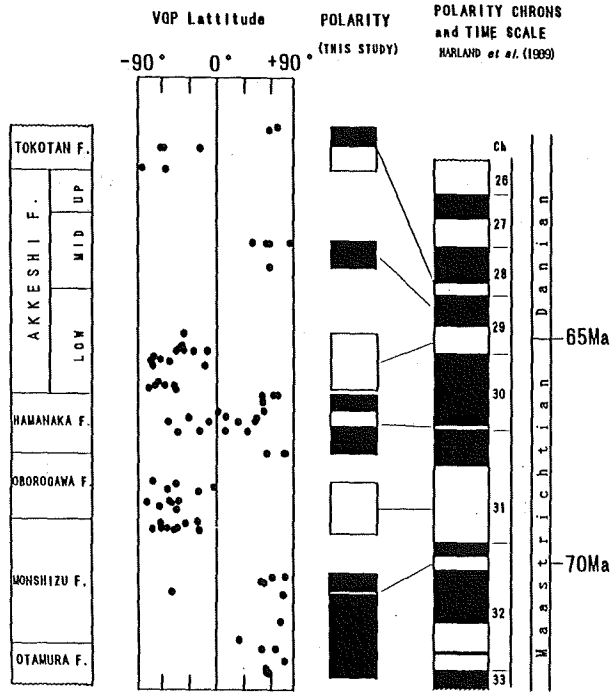

Fig. 4. Summary of magnetic polarity of the Nemuro Group. Correlation with the polarity time scale is based upon Harland et al. (1989).

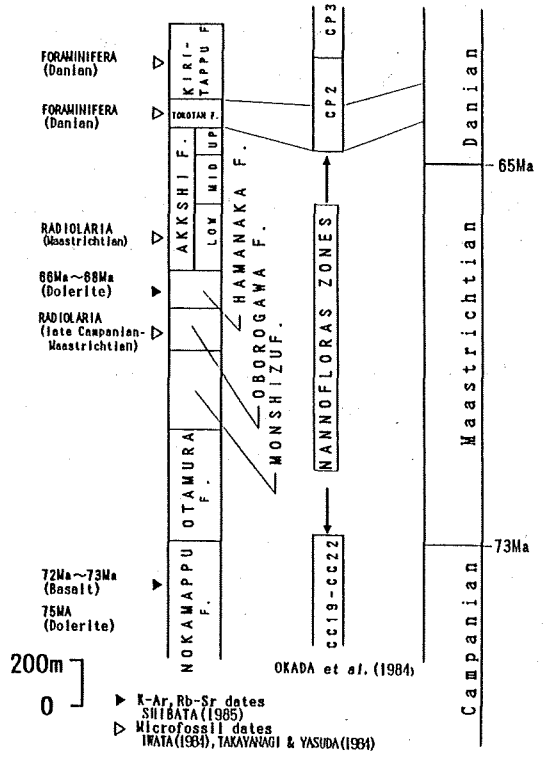

Fig. 5 K-Ar ages and biostratigraphic correlation of the Nemuro Group.

It is generally believed that the age of the boundary between Cretaceous and Tertiary has been discussed to be 65 Ma (Harland et al., 1989). The boundary point estimated to be placed at the polarity chron 29R, although there are no dated magnetic anomalies.

Therefore, our magnetostarigraphic interpretation strongly suggests that the K-T boundary point to be placed at the Lower Hamanaka Formation.

References

Harland, W. B., Armstrong, R. L., Cox, A. V., Craig, L. E., Smith, A. G. & Smith, D. G. (1989) A geologic time scale, Cambridge Univ. Press
Kiminami, K. (1983) J. Geol. Soc. Japan, 89, 607-624
Saito, T., Yamanoi, T. and Kaiho, K. (1986) Nature, 323, 253-255
Shibata, K. (1985) Memoirs Geol. Soc. Japan, 26, 119-133
Tanaka, H. and Uchimura, H. (1989) Chikyu Mothly, 11, 5, 298-305

AN OBJECTIVE DECONVOLUTION SCHEME OF PASS-THROUGH MEASUREMENT

Hirokuni ODA*, Hidetoshi SHIBUYA**, Akira HAYASHIDA***
and Masayuki TORII*

*Department of Geology and Mineralogy, Kyoto University, Kyoto 606, Japan
**Department of Earth Sciences, University of Osaka Prefecture, Sakai 591, Japan
***Laboratory of Earth Science, Doshisha University, Kyoto 602, Japan

Introduction

A pass-through measurement is a potential method to obtain a sequence of the high resolution remanent magnetizations from sediment core samples. Because the sensors of the cryogenic magnetometer has broad responses, the data sequence of pass-through measurement does not indicate magnetization itself but the convolution of the magnetization. Deconvolution must be performed to get real remanent magnetizations from the magnetometer data. It has been accomplished by Fourier transformation (Dodson et al., 1974), for the sake of easy calculation. However, conventional method has a subjectivity of selecting the L.P.F. We developed an objective method using Bayesian statistics. The scheme is tested compareing a path-through and thin slice measurements.

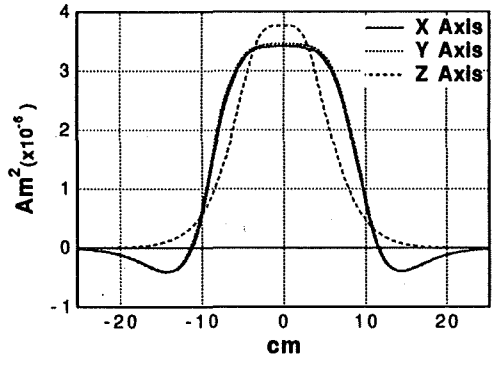

Fig.1: Sensor response curves of SQUID magnetometer (HOXAN SRM). A rock fragment of basalt ($3.61 \times 10^{-6} Am^2$) is used for the standard sample.

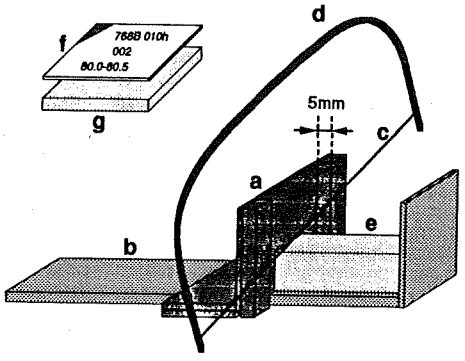

Fig.2: Slicing tools and thin section. (a)slider, (b)plate, (c)phosphor bronze wire, (d)frame, (e)U-channel sample, (f)Pyrex glass plate, (g)thin section.

Principles of Deconvolution using Bayesian Statistics

Since the pick up coils of the cryogenic magnetometer have fairly broad response curves (Fig. 1), the magnetic data measured on a long core sample is equivalent to the convolution of the magnetizations of the corresponding thin slices. Thus, the deconvolution of the magnetometer output with the sensor response gives real values of magnetization along the core. The sensor output is expressed mathematically by a matrix equation as,

$$\mathbf{Y} = \begin{pmatrix} y_1 \\ y_2 \\ \vdots \\ y_n \end{pmatrix} \qquad \mathbf{X} = \begin{pmatrix} x_1 \\ x_2 \\ \vdots \\ x_m \end{pmatrix} \qquad \mathbf{R} = \begin{pmatrix} R_l & & 0 \\ \vdots & \ddots & \\ R_0 & & R_r \\ \vdots & \ddots & \vdots \\ R_{-r} & & R_0 \\ 0 & \ddots & \vdots \\ & & R_{-l} \end{pmatrix}$$

$$\mathbf{Y} = \mathbf{RX}$$

where Y, R and X represents magnetometer output, sensor response and magnetization, respectively. Number of total data points, data points of magnetization, half of sensor data points and leading or trailing data points are represented as n, m, r, and l, respectively. The magnetizations are obtained solving the equation Y=RX by the least square method. Because of the sensor frequency characteristics of the sensor curve, this calculation is very unstable against high frequency noise. Low pass filtering must be applied to get meaningful solution. This filtering is the source of the subjectivity in the conventional method. For the purpose of giving objectivity, we developed an alternative method using Bayesian statistics. We assumed that the second order difference of magnetization have a Gaussian distribution (Akaike, 1980). Second order difference is expressed by the following matrix D as

$$\mathbf{DX}, \qquad \mathbf{D} = \begin{pmatrix} a & & & & & \\ b & -b & & 0 & & \\ 1 & -2 & 1 & & & \\ & 1 & -2 & 1 & & \\ & 0 & \ddots & \ddots & \ddots & \\ & & & 1 & -2 & 1 \end{pmatrix}$$

where a and b is properly chosen constants.

To obtain magnetization applying Baysian statistics, we have to solve the equation

$$s^2 = || \mathbf{Y} - \mathbf{RX} ||^2 + u^2 || \mathbf{DX} ||^2$$

where u is a parameter which controls smoothness of magnetizations. The meaning of this calculation is to fit RX to Y and DX to zero, simultaneously. In order to select the parameter u, Akaike(1980) proposed ABIC (Akaike's Bayesian Information Criterion) as a criterion for Bayesian modeling. For this case, ABIC is expressed as

$$ABIC = n\log s^2 - m\log u^2 - \log|\mathbf{D}^t\mathbf{D}| + \log|\mathbf{R}^t\mathbf{R} + u^2\mathbf{D}^t\mathbf{D}| + n - n\log n + n log 2\pi$$

Magnetization of the maximum likelihood is obtained for the u value which minimizes ABIC.

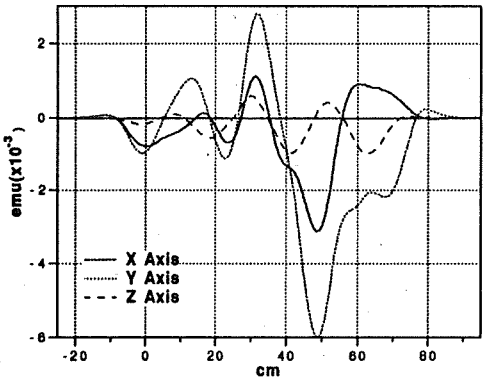

Fig.3: Magnetometer data by pass-through measurement.

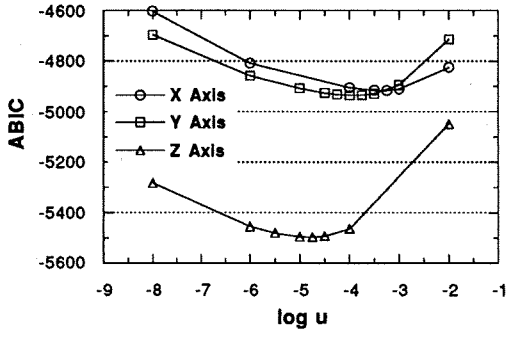

Fig.4: ABIC values versus log u for each axis.

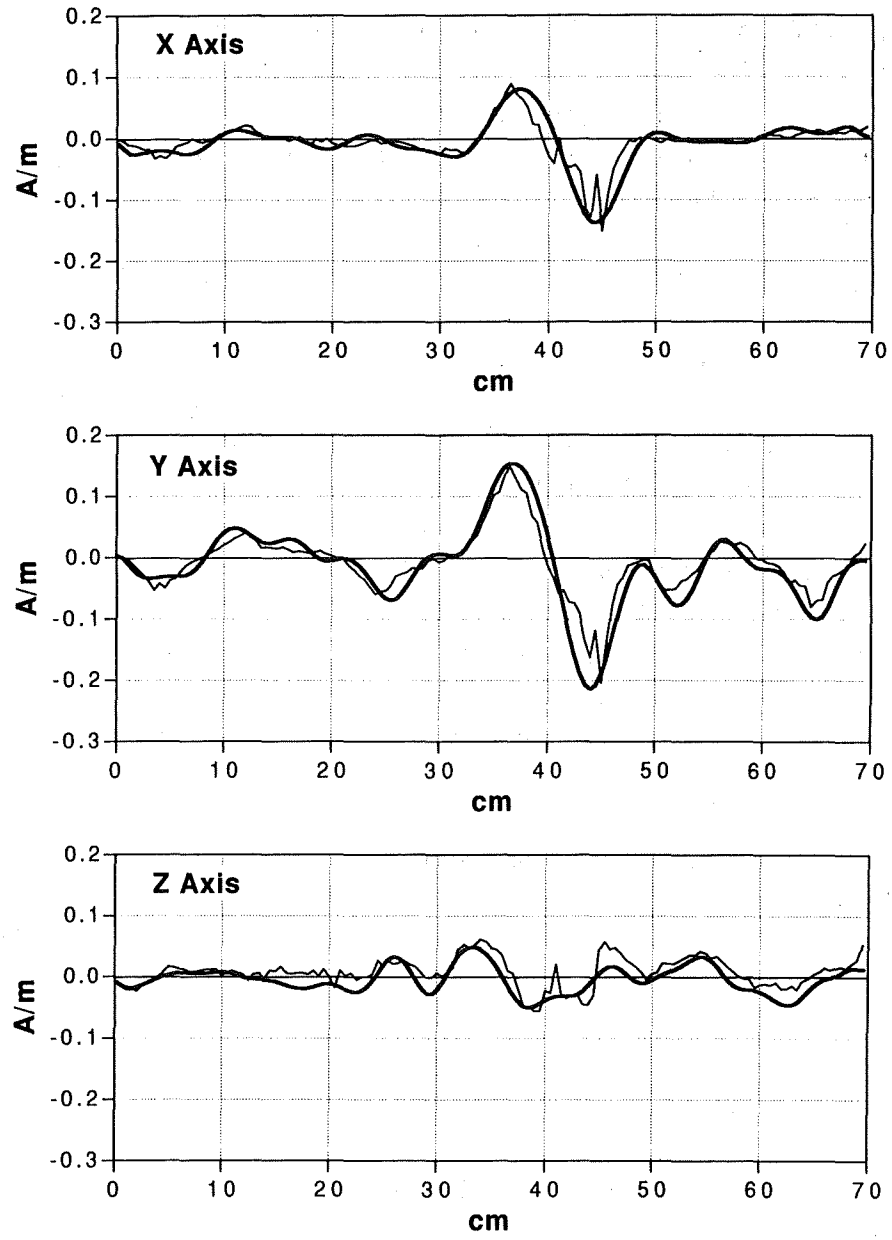

Fig.5: Magnetizations of the U-channel sample. Thick line represents magnetizations obtained by deconvolution of pass-through data. Thin line represents magnetizations of thin sections.

U-channel sample and magnetic measurements

A U-channel sample of 70 cm long with a square cross-section of 24mmx24mm from ODP Leg 124 was used for this study (124-768B-10H-2, 80-150cm; Rangin et al., 1990). The sample has high magnetic intensity of the order of 0.1-0.01 A/m.

The pass-through magnetic measurement was carried out at every 5mm by using a horizontally placed, three axes cryogenic magnetometer of Doshisha University (HOXAN SRM). We also measured both leading and trailing space (25cm) of the U-channel sample. The U-channel sample was fixed on a non-magnetic guide which is L shaped long angle of polyvinyl chloride. The sample was inserted with the L-angle into the bore hole of the magnetometer.

The U-channel sample was cut into thin slices after pass-through measurement. We modified the method developed by Kawai et al. (1976) (Fig. 2). Slider made of acrylic plastic moves on the plate made of polyvinyl chloride. Two acrylic guide plates of 5mm thickness are attached on the front side of the slider, which enables us to make 5mm thick slices. The U-channel sample is sliced by 0.2mm thick non-magnetic phosphor bronze wire. Each specimen is 5mmx24mmx24mm rectangular in shape, put on a 0.5mm thick Pyrex glass plate, and wrapped by aluminum foil. The remanent magnetizations of the specimens were measured with a cryogenic magnetometer of Kyoto University (ScT C-112). The magnetic intensity was normalized to the wet weight of the specimen.

Results

The results of pass-through measurements of the U-channel sample are shown in Fig. 3 for each axis. Deconvolution is then performed on the data. ABIC values versus log u for X,Y, and Z axes are shown in Fig. 4. The magnetizations obtained for the u values minimizing ABIC and NRMs of thin sections are shown in Fig. 5 for comparison. Thick curve (deconvolved) and thin curve (thin slice) are almost compatible for each X,Y, and Z axis. This shows that the Bayes modeling is effective on the deconvolution of pass-through data of sediment core samples.

References

Akaike, H. (1980) : in *Bayesian Statistics*, Univ. Press, Valencia, Spain, 143.

Dodson, R., M. Fuller, and W. Pilant (1974) : *Geophys. Res. Lett.*, **1**, 185.

Kawai, N., Y. Otofuji, and K. Kobayashi (1976) : *J. Geomag. Geoelectr.*, **28**, 395.

Rangin, C., Silver, E., A., von Breymann, M.T., et al.(1990). *Proc. ODP, Init. Repts.*, **124**, College Station, TX(Ocean Drilling Program).

COUNTER-CLOCKWISE PALEOMAGNETIC DIRECTION FROM THE GONGENYAMA FORMATION (N9-N10) ON THE COASTAL AREA OF NORTHEAST JAPAN

Hiroshi MOMOSE, Masayuki TORII, and Hiroyuki TANAKA

Department of Geology & Mineralogy, Kyoto University, Kyoto 606, Japan

1. Introduction

A number of paleomagnetic data, (e.g., Otofuji et al., 1985; Tosha and Hamano, 1988), indicate that Northeast (NE) Japan was rotated counter-clockwise during middle Miocene, meanwhile Southwest (SW) Japan was rotated clockwise. This contrasting movement of the land blocks has been regarded as a "double door mode" suggested by Otofuji et al. (1985). There are, however, some paleomagnetic directions in different manner, such as reported by Yamazaki (1989) and by Oda et al. (1989). These discordant data may imply clockwise rotation or no significant rotation of some part of NE Japan. Precisely age dated paleomagnetic directions from the Miocene strata are crucial to understand detailed feature of the opening mode of the Japan Sea. A few paleomagnetic data have been so far reported from the rocks of the age between 16 and 20 Ma.

We, therefore, studied the Gongenyama Formation for the purpose to obtain paleomagnetic directions from the sedimentary sequence whose age can be estimated precisely with biostratigraphy.

2. Sample collection

The Gongenyama Formation is exposed on the coastal area of Akita Prefecture, along the Fudo-no-taki anticline (Fig. 1). This region is characterized by intense folds and reverse faults with the general trend of N-S direction, which is a typical aspect of the so-called "Oil Field Structure".

The Gongenyama Formation is mainly consist of mud stones and thick pumiceous tuff layers. The sediments are intruded by dolerite sills which are exposed near the anticline axis. Fujioka et al. (1976) reported occurrence of planktonic foraminifera fossils of *G.praemenardii, G. peripheroacuta,* and *Orburina,* which correspond to N9 and N10 zone of Blow (1969) as shown in Fig. 2. Occurrence of diatom fossils, *D. hustedtii,* are also reported from the Onnagawa Formation which overlies the Gongenyama Formation. Therefore, geologic age of the Gongenyama mud stones is estimated to be 14 to 15 Ma.

Paleomagnetic samples are collected at 32 sites from the both limbs of the Fudo-no-taki anticline of the Gongenyama Formation along Fukumata river and Hebi river (Fig. 1).

3. Paleomagnetic directions

We could not successfully isolate stable component with progressive thermal demagnetization for the case of sediment samples of the Gongenyama Formation. On the basis of thermomagnetic analysis, magnetic minerals in the sample are found to be altered when heated above 300 or 400°C. Therefore, we carried out alternating field demagnetization for all the samples to estimate stable component of the remanence. We could not extend demagnetization to

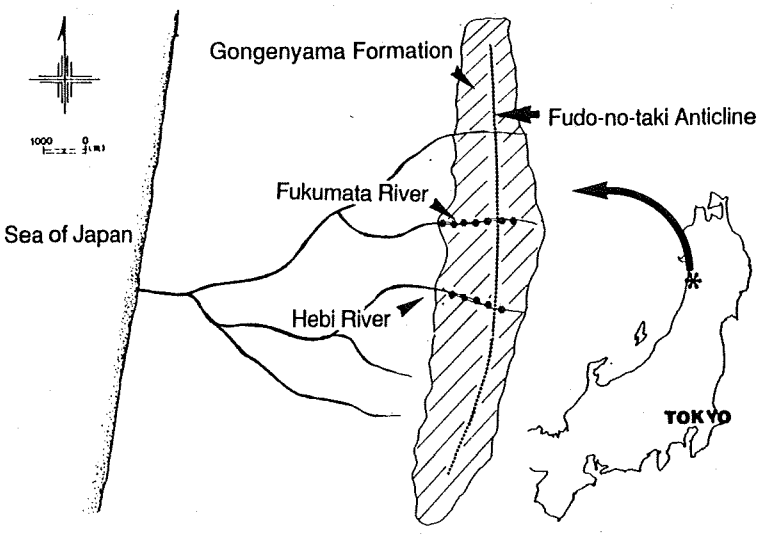

Fig. 1 Geological Map of the studied area

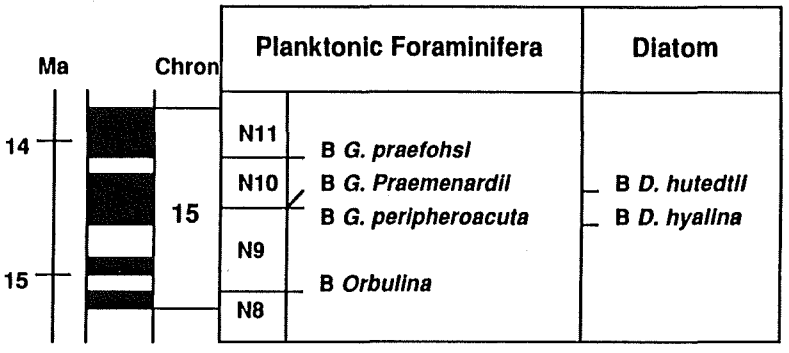

Fig.2 Standard biostratigraphy of NE Japan (Oda, 1986)

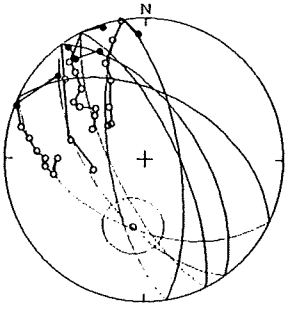

Fig. 3 Schematic diagram of great circle fitting method on equal area projection. Data points are selected from one real sampling site. Cross point of great circles and 95 percent confidence limit are calculated along the procedure mentioned in McFadden and McElhinny (1988).

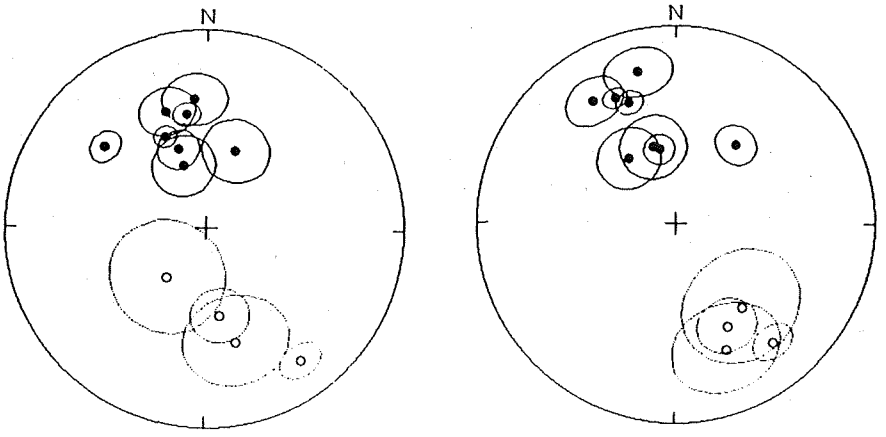

Fig. 4 Site mean directions of before (left) and after (right) tilt correction on equal area projection. Open circle and solid circle indicate upper and lower hemisphere respectively. Small circles show 95 percent confidence limit.

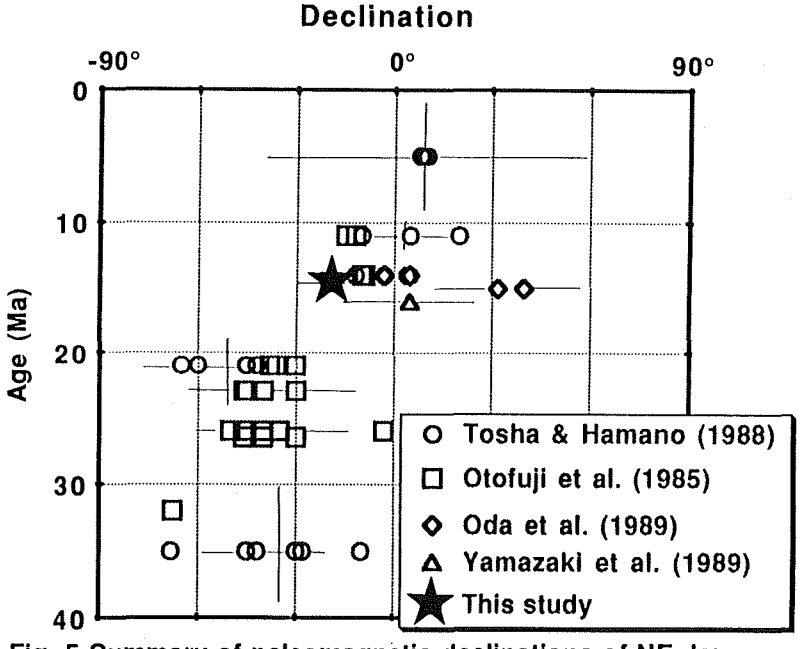

Fig. 5 Summary of paleomagnetic declinations of NE Japan. Error bars of declination indicate 95 percent confidence limit.

higher level for samples that intensity is very weak. For such samples, we applied the great circle fitting method proposed by McFadden and McElhinny (1988). Typical example is shown in Fig. 3.

We employed following two rejection criteria. Sample of single component whose direction is parallel to the present geomagnetic field is discarded. Such a magnetization is highly possible to be VRM origin. We also reject the site of larger dispersion, that 95 percent confidence limit exceeds 30°. Finally, 11 site-mean directions (Fig. 4) are obtained as characteristic directions. After tilt correction, site-mean directions make tight clusters on northwest and southeast quadrants on the equal area projection with antipodal relationship. These site-mean directions can be regarded as primary directions. Overall-mean direction is calculated averaging 11 site-mean directions as follows: Declination = -19.6°, Inclination = 40.6°, and 95 percent confidence limit = 10.6°.

4. Discussion

Paleomagnetic declination of the Gongenyama Formation is concordant with that of Otofuji et al. (1985), and Tosha and Hamano (1988) as illustrated in Fig. 5. Our data suggest counter-clockwise rotation of NE Japan at about 15 Ma. Meanwhile, middle Miocene paleomagnetic directions from the eastern coast of NE Japan (Yamazaki, 1989; Oda et al., 1989) are discordant with the present data. For the case of SW Japan, coherent pre-Cenozoic structure suggests single block rotation of clockwise sense. For NE Japan, coherent basement structure can not be geologically recognized and paleomagnetic directions dated middle Miocene indicate different sense of rotation between sampling sites. It is possible to assume several rotated blocks among NE Japan during the period of Japan Sea formation.

5. Conclusion

(1). Primary paleomagnetic directions are obtained from the upper part of the Gongenyama Formation.

Declination = -19.6°, Inclination = 40.6°, and α_{95} = 10.6°

(2). Paleomagnetic direction from the Gongenyama Formation implies that NE Japan was subjected to counter-clockwise rotation after 14-15 Ma (N9-N10). It constraints the duration of the rotation more precisely on the basis of biostratigraphy.

6. Reference

Blow, W. H. (1969) Proc. 1st Intern. Conf., Plankt. Microfossils, Geneva, 1, 199-422.

Fujioka, K., A. Ozawa, and Y. Ikebe (1976) Quadrangle Series, Akita, Geology of the Ugo and Wada district, Geological Survey of Japan.

McFadden, P., L. and M.W. McElhinny (1988) Earth Planet. Sci. Lett., 21, 315-320.

Oda, H., M. Torii, and A. Hayashida (1988) Rock Mag. Paleogeophys., 4, 65-71.

Oda, M. (1986) Prof. Kitamura Commemorative Volume, 297-312.

Otofuji, Y. T. Matsuda, and S. Nohda (1985) Earth Planet. Sci. Lett., 75, 265-277.

Tosha, T. and Y. Hamano (1988) Tectonics, 7, 653-662.

Yamazaki, T. (1989) J. Geomag. Geoelectr., 41, 533-548.

DEFORMATION OF THE CENTRAL PART OF THE HONSHU ISLAND INFERRED FROM PALEOMAGNETIC STUDY

Daisuke MIKI* and Kimio HIROOKA**

*Dept. Geol. Mineral., Fac. Sci., Kyoto Univ., Kyoto 606, Japan
**Dept. Earth Sci., Fac. Sci., Toyama Univ., Toyama 930, Japan

Introduction

Recent paleomagnetic studies revealed that the Japanese Islands experienced the bending of its main Island Honshu caused by the opening of the Sea of Japan at about 15 Ma (*e.g.* Otofuji and Matsuda, 1983; Otofuji *et al.*, 1985). The central part of the Honshu Islands is located in between the southwestern and northeastern blocks which rotated oppositely. Very complex tectonic deformation is, therefore, expected in the region. The subject of this study is to clarify the tectonic deformation took place in this region. A paleomagnetic study was carried out on the Late Cretaceous to Paleogene acidic volcanic rocks, the Nohi Rhyolite and its correlatives, which are distributed in the region.

Geological Setting and Sampling

The distribution of the Late Cretaceous to Early Paleogene acidic volcanic rocks in the central part of the Honshu Island is shown in Fig. 1. These rocks unconformably overlie on the Paleozoic and Mesozoic series of the Hida, the Circum-Hida and the Mino tectonic terranes, and consist mainly of rhyolitic and rhyodacitic welded tuffs and a small amount of tuffs, lavas and unwelded pyroclastic deposits. Paleomagnetic samples collected from twenty-one sites of five rock units; such as the

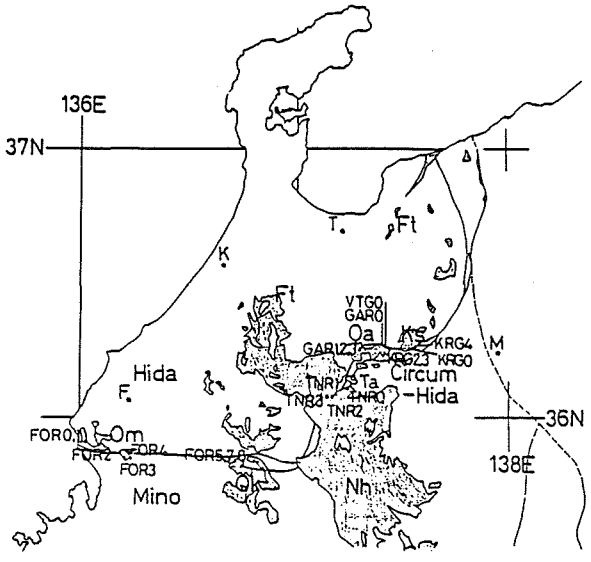

Figure 1. Distribution of the Late Cretaceous to Paleogene acidic volcanic rock units (shaded zone) and pre-Neogene tectonic terranes (after Yamada *et al.* eds., 1982), and localities of sampling sites (dots). Nh, Ok, Oa, Ks, Om, Ft: see caption of Table 2; T: Toyama, K: Kanazawa, F: Fukui, Ta: Takayama, M: Matsumoto.

Nohi Rhyolite, the Okumino Acid Igneous Complex, the Oamamiyama Group, the Kasagatake Rhyolite and so-called 'Omodani Rhyolite'. Four rock units except for the Omodani Rhyolite have very similar petrologic features and volcanic history. Harayama *et al.* (1985) divided Cretaceous to Paleogene magmatism of this region into five stages of I to V, and above-mentioned four rock units fall under the Stage II or Stage III.

In each paleomagnetic sampling site, ten to fifteen oriented hand samples were collected, and the direction of strike and dip angle of the strata was measured for the tilt correction. From some of those sampling sites, fission track ages, listed in Table 1, are obtained (Iwano *et al.*, 1989; Nakajima and Iwano, 1987; Nakajima *et al.*, 1988;).

Paleomagnetic Measurements and Results

Remanent magnetizations of most of specimens were measured by means of a cryogenic magnetometer (Cryogenic Consultants Limited, GM-401) and the rest of specimens of strongly magnetized were measured by two types of spinner magnetometers (Schonstedt Instrument Company, SSM-1A; and Natsuhara Giken, SMM-85).

Progressive alternating field demagnetization (AFD) and thermal demagnetization (ThD) of pilot specimens were carried out, after measurements of Natural Remanent Magnetizations (NRM) of all specimens. Typical behaviors of remanent magnetizations of pilot specimens against demagnetizations are shown in the orthgonal plot diagrams (Zijderveld, 1967) in Fig. 2.

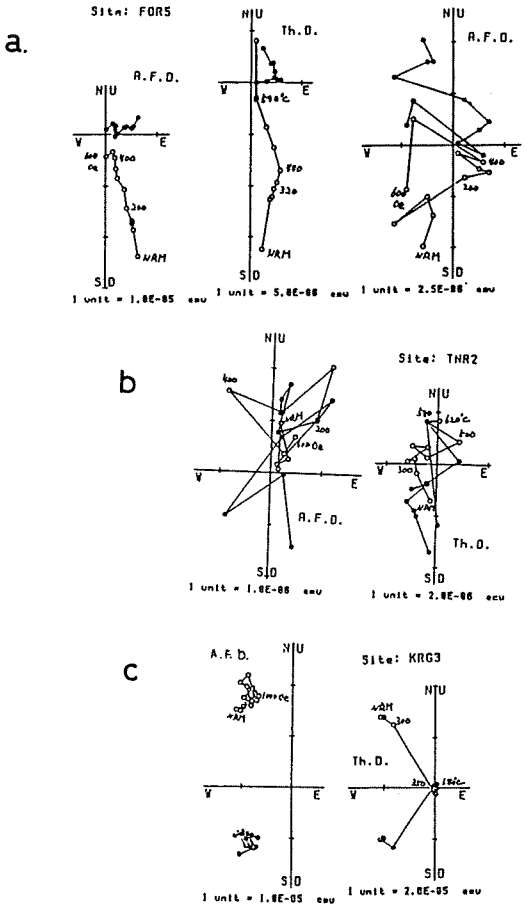

Figure 2. Typical behaviors of remanence of pilot specimen against demagnetization plotted on orthogonal vector diagrams (Zijderveld, 1967). solid circles: horizontal plane, open circles: vertical plane.

Site	N	D (°E)	I (°)	α_{95} (°)	k	ODF ODT	Rock Type	Age (Ma)
Nohi Rhyolite								
TNR0	10	19.0	65.0	2.3	428.5	15mT	W.T.	69.8 ± 4.0
TNR1	10	176.3	-71.5	5.3	85.5	40mT	tuff	68.1 ± 3.8
Okumino Acid Igneous Complex								
FOR5	8	43.2	53.6	5.0	125.0	15mT	W.T.	65.5 ± 4.2
FOR7	9	45.9	64.8	4.7	123.6	20mT	W.T.	
FOR8	9	60.1	50.6	3.6	208.6	15mT	sand	
Oamamiyama Group								
VTG0	9	63.3	37.3	9.7	29.4	15mT	tuff	63.8 ± 3.4
GAR2	4	-133.6	-71.8	6.8	183.8	30mT	tuff	60.8 ± 4.8
GAR3	4	-108.3	-29.4	6.0	233.8	30mT	W.T.	
GAR0	10	45.0	73.0	12.3	16.5	10mT	tuff	
Kasagatake Rhyolite								
KRG4	5	123.5	-43.5	7.6	102.4	410° C	lava	57.3 ± 5.2
Omodani Rhyolite								
FOR0	9	-79.8	-55.3	7.8	44.1	15mT	W.T.	
FOR1	10	-112.5	-30.7	14.6	12.0	20mT	W.T.	
FOR2	8	-118.9	-67.2	8.6	42.7	25mT	tuff	
FOR3	5	-108.5	-32.5	9.6	64.0	25mT	tuff	

Table 1. Paleomagnetic results and geological informations of present study. Site: site name, N: number of data; D, I: declination and inclination after tilt correction; α_{95}, k: Fisher's 95 % confidence angle and precision parameter (Fisher, 1953); ODF, ODT: optimul demagnetizing step.

According to the results of demagnetization of pilot specimens, sampling sites were divided into three groups by their nature of remanent magnetization. A stable magnetic component that was successfully separated from relatively unstable components which were removed in the earlier demagnetizing steps, from 13 sites belonging to the first group (shown in Fig. 2a). The direction of stable component separated by AFD, shows almost the same direction of that obtained by ThD. In some cases, the stable direction of remanent magnetization was not observed. Such specimens were excluded from statistical calculations. As for the Site KRG4, only ThD was applied, and a stable magnetic component was successfully separated. From the other two groups, no stable magnetic component was separated by both of AFD and ThD (Fig. 2b, 2c). Then, they were excluded from farther experimental procedures. It is clarified from progressive demagnetization experiments of pilot specimens that both of AFD and ThD have almost the same effect to separate stable components. Since that, only AFD were applied to the remaining specimens of those thirteen sites. The demagnetizing field of a step, in which the Fisher's precision parameter k (Fisher, 1953) of the set of pilot specimens showed maximum value, is defined as the optimul demagnetizing field (ODF) for the site. Then mean direction and 95% confidence angle α_{95} (Fisher, 1953) obtained at ODF, are adopted as the paleomagnetic data. As for the Site KRG4, optimul demagnetizing temperature (ODT) was defined in the same way. Mean direction and Fisher's parameters at the ODT were calculated and cited as paleomagnetic data.

Tilt corrected mean paleomagnetic directions show better concentration than those before tilt correction, for each rock unit. The mean directions after tilt correction (shown in Table 1), so that, are considered to be the primary magnetic components and to reflect the geomagnetic field of the Late Cretaceous to Early Paleogene time.

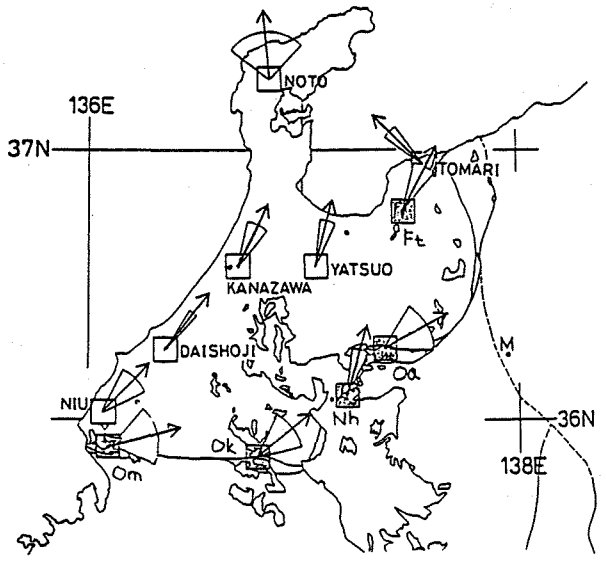

Figure 3. Area mean paleomagnetic declinations (arrow) of Late Cretaceous to Early Paleogene time (shaded square) and Early to early Middle Miocene time (hollow square) with declination error (fan) defined as $\alpha_{95} / \cos I$.

Discussion

Rock unit mean paleomagnetic declinations of above-mentioned 14 sites together with other reported paleomagnetic directions of the Nohi Rhyolite (Itoh, 1988) and the Futomiyama Group (Itoh and Itoh, 1988), are plotted on a map of tectonic terranes in Fig. 3. This shows clearly that the paleomagnetic declination has a certain angle to the elongation axis of the Circum-Hida terrane at all of the sites. This fact indicates that the Circum-Hida, and very probably some parts of the Hida and the Mino terranes alongside of the Circum-Hida terrane too, were straight in shape at Late Cretaceous to Early Paleogene when the volcanic activities of the Nohi Rhyolite and its correlatives were in their main phase. The terranes were deformed into present shape in some time after those volcanic activities. Hirooka *et al.* (1985) already suggested this kind of bending tectonics in this region from paleomagnetic observations of Triassic to Early Cretaceous rocks. The results of the present study make their suggestion to be more plausible.

It is difficult to reveal when the deformation occurred, because there is no post-Paleogene rocks in the Circum-Hida terrane and its adjacent area. Paleomagnetic studies were, however, carried out in the areas of north to the studied Rock units, such as Niu, Daishoji, Kanazawa, Noto, Yatsuo and Tomari (Hirooka *et al.*, 1972, 1986, 1990, in preparation; Itoh, 1986, 1988; Itoh and Hayakawa, 1988, 1989; Itoh and Ito, 1989; Itoh and Watanabe, 1988; Nakajima and

Rock Unit or Area	N	D (°)	I (°)	α_{95} (°)	k	dD (°)
Late Cretaceous to Early Paleogene						
Nh	12	16.2	53.0	6.5	45.1	10.8
Ok	3	50.4	56.6	14.0	78.8	25.4
Oa and Ks	5	60.6	51.3	20.6	14.8	32.9
Om	4	76.9	47.2	24.0	15.6	35.3
Ft	5	25.2	55.6	7.5	106.2	13.2
Early Miocene to early Middle Miocene						
Niu	22	44.0	49.8	11.4	8.3	17.7
Daishoji	12	38.8	51.7	4.2	107.9	6.8
Kanazawa	7	25.6	49.3	11.0	31.1	16.9
Noto	6	-4.8	70.9	15.9	19.0	48.7
Yatsuo	12	15.3	49.2	6.1	51.1	9.4
Tomari	3	-44.8	56.4	5.0	600.1	9.1

Table 2. Area mean paleomagnetic directions. N: number of Sites; D, I, α_{95}, k: see caption of Table 1; dD: uncertainty of declination defined as $\alpha_{95}/\cos I$. Nh: Nohi Rhyolite, Ok: Okumino Acid Igneous Complex, Oa: Oamamiyama Group, Ks: Kasagatake Rhyolite, Om: so-called 'Omodani Rhyolite', Ft: Futomiyama Group.

Hirooka, 1986). 62 paleomagnetic data of about 26 to 15 Ma (Early to early Middle Miocene epoch), are complied to compare with the data from the Nohi Rhyolite and its correlatives. The mean directions of these data are shown in Fig. 3 and Table 2. Mean paleomagnetic declinations of Early Miocene rocks show almost the same declination of nearby rock units of the Late Cretaceous to Early Paleogene time. To eliminate the poler wandering effect, the expected geomagnetic field directions at the locality of 36° N, 137° E are calculated referring to the pole positions at 20 Ma and at 60 Ma which estimated from Northern Eurasia by Irving and Irving (1982). These two expected declinations are almost the same. This indicates that the tectonic rotation did not occur during the Paleogene and Early Miocene time. The timing of the tectonic deformation around the Circum-Hida terrane, therefore, must be in some time after Early Miocene age. Further, paleomagnetic directions after about 14 Ma from northern area (*e.g.* Itoh, 1988) , except Tomari area (Itoh and Watanabe, 1988), are the same as the direction of geocentric dipole field. Since that, it is plausible that timing of the deformation may be the same as which of the opening of the Sea of Japan. Itoh and Ito (1989) suggested that the studied region was ductilely deformed to simple bow-shape, and that deformation is originated by the collision of the Izu-Bonin Arc. Paleomagnetic data obtained by present study indicates more intricate deformation occurred around the Circum-Hida terrane before it was deformed into the present shape.

In western part of the studied region, the Late Cretaceous to Early Paleogene declinations slightly deflect to the east, as compared with those of the Early Miocene. This may indicate the clockwise rotation of the Southwest Japan started at the earlymost Miocene time, as suggested by Nakajima *et al.* (1990).

This study is still in progress. Now, the authors are measuring samples from the Oamamiyama Group, the Futomiyama Group and the Ishizaka Rhyolite, which are distributed in east part of studied region.

References

Fisher, R. A. (1953) *Proc. Roy. Astr. Soc. London*, **217A**, 295-395.

Harayama, S., Y. Koido, K. Ishizawa, Y. Nakai and T. Kutsukake (1985) *Earth Science* (*Jour. Assoc. Geol. Collabor. Japan*), **39**, 345-357 (in Japanese with English abstract).

Hirooka, K., S. Uchiyama, T. Date, H. kanai and T. Nakajima (1985) in Howell. D. G. ed., *'Tectonostratigraphic terranes of the Circum-Pacific region'* (the Circum-Pacific Council for Energy and Mineral Resouces, Huston), 391-399.

Hirooka, K., H. Sakai, T. Takahashi, H. Kinoto and A. Takeuchi (1986) *Jour. Geomag. Geoelectr.*, **38**, 311- 323.

Hirooka, K., R. Yamada, M. Yamashita and A. Takeuchi (1990) *Paleogeogr. Paleoclimtol. Paleoecol.*, **77**, 345-354.

Hirooka, K., H. Iwano, T. Takai and K. Ogasawara, in prepalation.

Irving, E., and G. A. Irving (1982) *Geoophys. Surveys*, **5**, 141-188.

Itoh, Y. (1986) *Jour. Geomag. Geoelectr.*, **38**, 325-334.

Itoh, Y. (1988) *Jour. Geophys. Res.*, **93, B**, 3401-3411.

Itoh, Y., and H. Itoh (1988) *Jour. Geol. Soc. Japan*, **94**, 11-18 (in Japanese with English abstract).

Itoh, Y., and M. Watanabe (1988) *Jour. Geol. Soc. Japan*, **94**, 457-460 (in Japanese).

Itoh, Y., and H. Hayakawa (1988) *Jour. Geol. Soc. Japan*, **94**, 515-525 (in Japanese with English abstract).

Itoh, Y., and H. Hayakawa (1989) *Jour. Geol. Soc. Japan*, **95**, 133-136 (in Japanese).

Itoh, Y., and Y. Ito (1989) *Tectonophysics*, **167**, 57-73.

Iwano, H., K. Hirooka and T. Nakajima (1989) *Abstracts of the 96th annual meeting of Geol. Soc. Japan*, 511 (in Japanese with English abstract).

Nakajima, T., and K. Hirooka (1986) *Jour. Geomag. Geoelectr.*, **38**, 513-522.

Nakajima, T. and H. Iwano (1987) *Jour. Geol. Soc. Japan*, **93**, 925-928 (in Japanese).

Nakajima, T., H. Iwano and K. Hirooka (1988) *Mem. Fac. Educ., Fukui Univ.*, **Ser.2**, **38**, 87-100 (in Japanese with English abstract).

Nakajima, T., Y. Sawada, T. Nakagawa, A. Hayashi and T. Itaya (1990) *Jour. Japan Assoc. Mineral. Petrol. Econ. Geol.*, **85**, 45-59 (in Japanese with English abstract).

Otofuji, Y., and T. Matsuda (1983) *Earth Planet. Sci. Lett.*, **62**, 349-359.

Otofuji, Y., and T. Matsuda and S. Nohda, (1985) *Earth Planet. Sci. Lett.*, **75**, 265-277.

Yamada., N., Y. Teraoka and M. Hata (Chief eds., 1982) *'Gological Atras of Japan'* (Geological Survey of Japan, Tsukuba), 8-15.

Zijderveld., J. D. A. (1967) in Collinson, D. W., K. M. Creer and S. K. Runcorn eds., *'Methods in Paleomagnetism'* (Elsevier, Amsterdam), 254-286.

PALEOMAGNETISM OF THE EARLY MIOCENE KANI GROUP IN SOUTHWEST JAPAN AND ITS IMPLICATION FOR THE OPENING OF THE JAPAN SEA

[Extended abstract]

Akira HAYASHIDA and Takako FUKUI
Laboratory of Earth Sciences, Doshisha University, Kyoto 602

Masayuki TORII
Department of Geology and Mineralogy, Kyoto University, Kyoto 606

Paleomagnetic directions of the Early Miocene to early Middle Miocene sequences distributed in inland basins of Southwest Japan (the Setouchi Miocene Series) are characterized by clockwise declination shift. In the Mizunami area, the late Early Miocene members of the Setouchi Series show the deflections exceeding 50°, whereas the early Middle Miocene member showed declination shift less than 30° [Hayashida, 1986]. The clockwise deflection of the paleomagnetic directions has been explained by rotation of Southwest Japan relative to Eurasia, and then attributed to back-arc opening of the Japan Sea. Compilation of paleomagnetic and chronological data of Southwest Japan [Otofuji et al., 1985] suggested that the southwestern part of the Japan Sea was opened at about 15 Ma.

There are some difficulty, however, in assuming that the whole of the Japan Sea was formed during a short period around 15 Ma, as discussed by Kono [1987]. Recently, Leg 127 and 128 of Ocean Drilling Program succeeded in penetrating thick sediments on the basement at four sites in the Japan Sea, and provided preliminary micropaleontological data suggesting the age of sediment/basalt contacts between 14 and 19 Ma [Ingle et al., 1990; Tamaki et al., 1990]. This result suggests that the Yamato basin was initiated into rifting in the middle Early Miocene and widen in the late Early to early Middle Miocene. The widening of the Yamato Basin in this period seems concordant with the paleomagnetic view from Southwest Japan, but the ODP result also implies that the Sea of Japan had been existed to some extent before 15 Ma.

The Setouchi Miocene Series of the Kani Basin (the Kani Group), west of the Mizunami basin, includes lacustrine deposits correlative to the lower part of the Mizunami Group, and underlying volcanic rocks (the Hachiya Formation) dated at about 22 to 20 Ma [Torii, 1982; Nomura, 1986]. Volcanic product of this age is unique in the Setouchi Miocene Series, and thus the Kani Group provides an opportunity to assess possibility of rotation of Southwest Japan in the period from 20 to 16 Ma. Paleomagnetic results from 6 sites of the Kani Group gave the total mean (of normal polarity): Declination = 49.9° and Inclination = 53.2° with α_{95} = 9.7°. Our data were obtained from high temperature magnetization components from various lithology, corrected for paleo-horizontal plane, and include both normal and reversed polarities. We could not find significant differences among the site mean data of the Kani Group ranging from 22 to 16 Ma, and also between the means of the Kani Group and the Mizunami Group mostly dated 17 to 16 Ma.

Our results suggest that no detectable rotation of Southwest Japan occurred between 22 and 16 Ma. As the early Middle Miocene Oidawara Formation of the Mizunami Group shows declination shift less than 30° [Hayashida, 1986], the timing of the rotation can be assigned to the *Denticulopsis lauta* zone of diatom biostratigraphy (14.85 - 15.7 Ma) [Koizumi, 1985], or N.9 of the planktonic foraminifera zone. This assignment is concordant with the rotation of about 40° between 16.1 and 14.3 Ma determined by Otofuji et al. [1990] in the San'in area.

How can be the timing of rotation of Southwest Japan between 16 and 14 Ma correlated with the earlier formation of the Japan Sea from 19 to 14 Ma suggested by the ODP Leg 127 results? A possible solution is a parallel drifting of Southwest Japan before 16 Ma. Fitting of the Kita-Yamato Bank to the 200 to 2000 m isobath of the Asian continental margin suggests parallel opening of the western part of the Japan Basin, by which southeastward translation of Southwest Japan could be caused. In this stage, initial spreading of the Yamato Basin might have occurred. The southeastward translation of Southwest Japan of about a few degrees of latitude is not detected by the present data of paleomagnetic inclinations. The clockwise

rotation of Southwest Japan between 16 and 14 Ma is probably explained by extension in the southwestern part of the Japan Sea including the Yamato Basin. Assuming the southward drift of Southwest Japan before 16 Ma, we should place the pole of the clockwise rotation inside Southwest Japan, not to the west as previously suggested by Otofuji and Matsuda [1983]. Our model implies that convergence between the western end of Southwest Japan and the Korean Peninsula occurred around 15 Ma, and may explain the counter-clockwise deflection of paleomagnetic directions of the Tsushima Islands and their surroundings observed by Ishikawa et al. [1989].

References

Hayashida, A., *J. Geomag. Geoelectr.*, ***38***, 295-310, 1986.

Ingle, J. C., Jr, K. Suyehiro, M. T. von Breymann, et. al., Proc. ODP, Init. Repts., ***128***, pp. 652, Ocean Drilling Program, College Station, TX, 1990.

Ishikawa, N., M. Torii and K. Koga, *J. Geomag. Geoelectr.*, ***41***, 797-811, 1989.

Koizumi, I., *J. Geol. Soc. Japan*, ***91***, 195-211, 1985.

Kono, M., *Trans. Am. Geophys. Union (EOS)*, ***68***, 1146, 1987.

Nomura, T., *J. Geol. Soc. Japan*, ***90***, 73-76, 1986.

Otofuji, Y., A. Hayashida and M. Torii, in *Formation of Active Ocean Margins*, edited by N. Nasu et al., 551-566, Terrapub, Tokyo, 1985.

Otofuji, Y., T. Itaya and T. Matsuda, *Geophys. J. Internat.*, in press., 1990.

Otofuji, Y. and T. Matsuda, *Earth Planet. Sci. Lett.*, ***62***, 349-359, 1983.

Tamaki, K., K. Pisciotto, J. Allan, et al., Proc. ODP, Init. Repts., ***127***, pp. 844, Ocean Drilling Program, College Station, TX, 1990.

Torii, T., in *History of Inuyama City*, ***2***, 23-56, Education Committee of Inuyama City, 1982.

(Submitted to *Geophys. Res. Lett.*)

AN ANGLE OF A BLOCK ROTATION CAUSED BY LEFT-LATERAL FAULTING IN THE INNER BELT OF CENTRAL JAPAN

Yuji KANAORI*, Shin-ichi KAWAKAMI** and Kenji YAIRI*

*Department of Geological Sciences, Faculty of General Education, Gifu University, 1-1 Yanagido, Gifu City 501-11
**Department of Earth and Planetary Sciences, Faculty of Education, Gifu University, 1-1 Yanagido, Gifu City 501-11

Introduction

NW-SE and ENE-SWS aligned active faults have been systematically developed in the Inner belt of central Japan between the Itoigawa-Shizuoka (ISTL) and Tsurugawan-Isewan(TITL) tectonic lines. Active faults aligned in NW-SE have a predominant left-lateral strike slip component, while those in an ENE-SWS alignment predominantly have a right-lateral strike slip component. Central Japan can be divided into four blocks by the rough boundaries that connect NW-SE active faults (Kanaori et al., 1990b). A given block boundary is not defined by a single fault, but consists mainly of a few active faults arranged en echelon.

Rotational movements must be accompanied by strike-slip motions of parallel aligned faults (Nur and Beccelia, 1990). Although it has been well known that active faults bounding the NW-SE blocks moved left-laterally during the Quaternary period (Matsuda, 1976), the rotational movement of the blocks has previously been overlooked. In this short article, rotational angles of the blocks are calculated from the displacement amounts of basement rocks, based on a geometrical model of block rotation caused by strike-slip faulting (Ron et al., 1984).

Block Rotation by Strike-Slip Faultings

Central Japan between the ISTL and TITL consists of four blocks, 20 to 80km wide and approximately 200km long, which are bounded by the Nekomata-Sakaitoge (NS), Miboro-Atera (MA) and Fukui-Neodani (NF) block boundaries (BB). Each block in central Japan is inferred to have been rotated in a clockwise manner due to the left-lateral movement of the faults which constitute block boundaries (Fig. 1a). The small blocks found between the ENE-SWS faults which in turn are located between the MABB and NSBB,

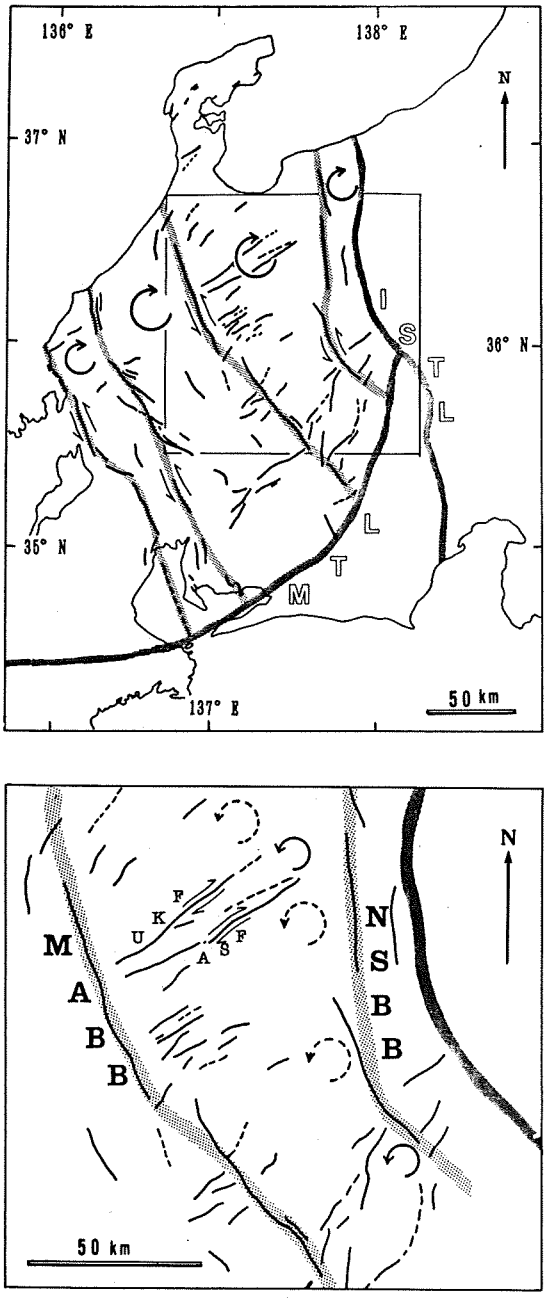

probably have been rotated counterclockwise. This resulted from the right-lateral slip of the fault, such as the Ushikubi and Atotsugawa faults (Fig. 1b). Kanaori et al.(1990a) proposed a nested fault model for central Japan based a hierarchical distribution of faults ranging from outcrops to regional scales. Within the model, the NW-SE and ENE-SWS aligned faults are interpreted as primary and secondary block faults, respectively. While the MTL is defined as the southern primary bounding fault, a northern bounding fault, the counterpart of the MTL, does not appear in central Japan. The northern primary bounding fault is believed to the Sikhote-Alin fault (Kanaori,1990).

When a contraction occurs perpendicular to the primary bounding fault, an extension is exerted parallel to the primary block fault. This results in an extension parallel to the secondary bounding faults. If the primary block faults, such as the Atera and Sakaitoge faults, generate left-

Fig. 1. An inferred block structure in central Japan(Kanaori et al.,1990b). (b) is a magnified view of the rectoangular area in (a). ASF=the Atotsugawa fault. UKF=the Ushikubi fault. The distribution of active fault was simplified from Kato and Sugiyama (1985) and Sangawa et al.(1983).

lateral slip when acting as the secondary bounding fault,a right-lateral slip is introduced to the secondary block faults. This would occur for example, in the Atotsugawa and Ushikubi faults having the opposite sense to that of the primary block faults (Nur et al., 1986; Ron et al.,1986; Martel et al., 1988).

Amount of Quaternary Rotation

A block rotation model associated with left-lateral faulting is schematically illustrated in Fig. 2. If it is assumed that a contraction occurs perpendicular to the bounding fault having no rotation while extension can occur parallel to the fault, then the following geometrical relationship is represented (Ron et al., 1984);

$$D / W = \frac{\sin \psi}{\sin \alpha \ \sin(\alpha - \psi)} = \cot(\alpha - \psi) - \cot \alpha$$

among the width of block (W), displacement along the block fault (D), the original angle α between the block and bounding fault before rotation, and the rotational angle ψ with left-lateral slip.

The amount of basement rock displacement along the block boundaries in central Japan was estimated from that of active faults which mainly constitute the block boundaries (Table 1). The rotational angles of blocks were calculated from the dispalcement (D) given in Table 1 and block width (W) measured from Fig. 1, by using the above equation, assuming that the angle α was 90° . The rotational angles calculated are 3° to 7° in a clockwise direction (Table 2). The present angles ($\alpha - \psi$) between the blocks and bounding faults range from 70° in the west to 90° in the east.

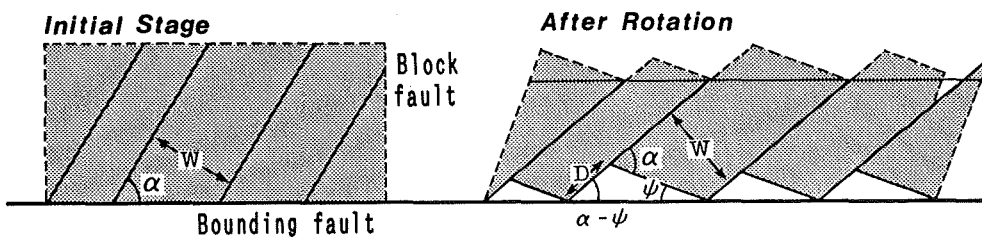

Fig. 2. A geometric model showing the quantitative relation between the left-lateral displacement and the rotation of the faulted blocks (modified after Ron et al., 1984). For explanation, see text.

Since the block width is more than ten times larger than the displacement, large rotational movement was not predicted, suggesting that the assumption of angle was reasonable.

The rotational angles of the two eastern blocks are larger than those of the two westernmost blocks. However, the rotational angles of all blocks would be the same when predicted by the present model. The differences in the actual rotation angles are possibly caused by errors in estimating the amount of displacement and by contributions from the bending of the MTL abd Southwest Japan (Faure and Lalevee, 1987).

Table 1. The amount of left-lateral displacement of block boundaries in central Japan

Block boud.name	Main fault of the block	Displacement (km)	Reference
TITL	Yanagase fault	1	Sugimura(1963)
FNBB	Neodani fault	3 ～ 5	Matsuda(1974)
MABB	Atera fault	5 ～ 7	Sugimura and Matsuda(1965)
NSBB	Sakai-toge fault	3 ～ 4．5	Kano and Sato (1988)

Table 2. Width of the block W and an angle of the block rotation ψ.

Block name	Boundary displacement(km)	Average width of the block, W (km)	rotation angle* ψ
TI-FN	1	25	3°
FN-MA	3 ～ 5	70	3° ～ 4°
MA-NS	5 ～ 7	60	4° ～ 7°
NS-IS	3 ～ 4．5	40	4° ～ 7°

* The intial angle between the bounding fault and block fault(α) is assumed to be 90°.

Discussion and Conclusions

Central Japan is of great significance in interpreting the structural evolution and to further understand the Quaternary tectonics of island arcs, since it is located on the inflection point of the bow-like Japanese Islands. Central Japan has a characteristic block structure, divided by major active faults. Movements of the MTL generated by the oblique subduction of the Pacific plate (Karig, 1980), created left-lateral faultings of the block boundaries, resulting in a clockwise rotation of the blocks.

Itoh (1988) compiled paleomagnetic declination data of rocks dated before the Miocene epoch from central Japan. Distinct differences in the declinations can be found between the eastern and western areas bounded by the MABB. In the western region the declinations are oriented more than 45° east, while they are north with no directional changes between the Late Cretaceous and Miocene rocks in the eastern area.

Although the western blocks underwent a clockwise rotation of 45° since the Middle Miocene, the amount of rotation due to left-lateral fault motions was only 3° to 7° during the Quaternary period. Thus, a great deal of rotation must have occurred between the Middle Miocene and Quaternary periods. Otofuji and Matsuda (1983) argued that the major clockwise rotation of Southwest Japan occurred during the opening of the Sea of Japan. In order to obtain the net amount of rotation of central Japan from paleomagnetic declination, rotational angles calculated from the displacement of the basement rocks along the block faults plus the rotation contributed by the MTL and Japanese Islands, must be subtracted from the angles inferred from the declinations.

On the other hand, the eastern blocks exhibited no significant paleomagnetic changes between the Late Cretaceous and Middle Miocene epochs. This can be explained by the nested fault model proposed by Kanaori et al. (1990a). Since faults ranging from an outcrop to regional scales form a nested fault system, a reciprocal block rotation occurs in each scale (Kanaori et al., 1990a). Moreover, only the rigid rotation, that is, not including plastic deformation of blocks, was taken into consideration in the estimation of rotational amount. When crustal rotations based on paleomagnetic data are discussed, regional structures including the sampling localities and surveyd areas should be clarified. The paleomagnetic data can then be evaluated, with respect to the regional structures, in interpreting the crustal rotations of the Japanese Islands.

In conclusion, the Inner belt of central Japan was deformed by block rotations caused by strike-slip faulting, which cancealed the strain on

the island arc due to the compression generated by the subduction of the Pacific and Philippine Sea plates.

References

Faure,M. and F.Lalevee (1987) Geology, 15, 49.

Itoh,Y. (1988) J. Geophys. Res., 93, 3401.

Kanaori,Y. (1990) Tectonophysics, 177, 381.

Kanaori,Y.,Y.Endoh, K.Yairi and S.Kawakami (1990a) Tectonophysics, 177,401.

Kanaori,Y.,K.Yairi, S.Kawakami and T.Takeshita (1990b) Zishin 2, 43, 77.

Kano,K. and H.Sato (1988) J. Geol. Soc. Japan, 94, 51.

Karig,D.E. (1980) J. Geol., 88, 27.

Kato,H. and Y.Sugiyama (1985) 1:500,000 Neotectonic Map Sheet 10 Kanazawa, Geol. Surv. Japan.

Martel,S.T.,D.D.Pollard and P.Segall (1988) Geol. Soc. Am. Bull., 100,1451.

Matsuda,T. (1974) Bull. Earthq. Res. Inst., Tokyo Univ., 14, 85.

Matsuda,T. (1976) J. Geodet. Soc. Japan, 22, 252.

Nur,A. and M.Boccaletti (1989) EOS Trans. Am. Geophys. Union, 70, 807.

Nur,A., H.Ron and O.Scotti (1986) Geology, 14, 746.

Otofuji,Y. and T.Matsuda (1983) Earth Planet. Sci. Lett., 62, 349.

Ron,H., A.Aydin and A.Nur (1986) Geology, 14, 1020.

Ron,H., R.Freund and Z.Garfunkel (1984) J. Geophys. Res., 89, 6256.

Sangawa,A., Y,Sugiyama and Y.Kinugasa (1983) 1:500,000 Neotectonic Map Sheet 11 Kyoto, Geol. Surv. Japan.

Sugimura,A. (1963) Quater. Res., 2, 220.

Sugimura,A. and T.Matsuda (1965) Geol. Soc. Am. Bull., 76, 509.

(Submitted to Tectonics)
(In press in Zishin 2)

PALEOMAGNETIC POLE FROM LATE CRETACEOUS KOTO RHYOLITES, SOUTHWEST JAPAN

Kouji FUKUMA and Masayuki TORII

Departmemt of Geology and Mineralogy, Kyoto University, Kyoto 606, Japan

Introduction

For paleo-reconstruction, it is essential to establish apparent polar wander paths from cratonic blocks. However reliable paleomagnetic poles cannot be easily obtained on active continental margins such as eastern Eurasia. This report presents a study to obtain a paleomagnetic pole position from late Cretaceous igneous rocks forming the rigid part of Southwest Japan.

The Koto Rhyolites is a part of the late Cretaceous felsic volcano-plutonic complex surrounding Lake Biwa at the mid-eastern part of Southwest Japan. Felsic igneous rocks distribute on the pre-Cretaceous accretionary terranes throughout the southwestern half of the Japanese island arc (e.g., Yamaguchi and Go river area, Nohi area). The Mesozoic felsic magmatism, as an overview, took place widely along the eastern margin of the Eurasia continent related to the past oceanic plate subduction. Such felsic igneous rocks amalgamated allochthons with the past continental margin to form a crustal backbone such as of the present Japanese island arc [*Takahashi, 1983*].

The geology of the Koto Rhyolites is well documented [e.g., *Nishikawa et al., 1983*] (Fig. 1). The exposed area is subdivided into two parts. The main mass is situated on the eastern flank of the Suzuka Mountains forming a hilly backyard of Lake Biwa, and more than ten small masses are sporadically distributed on the coastal alluvial plain or in Lake Biwa as inlets. Lithologically the Koto Rhyolite is composed of ash flow tuff and felsic intrusive rock. Ash flow tuff, most of which is densely welded, covers the extensive area and is divided into two units separated by the lacustrine sediments. Felsic dike rock intruded ash flow tuff along the double ring fracture and made the contact aureoles in the surrounding ash flow tuff. Stratigraphic correlation between the main mass and the small masses has been so far ambiguous due to their isolated distributions.

Geochronological studies were carried out on the various rock units with the biotite K-Ar method [*Sawada and Itaya, 1988*] and the zircon fission track (FT) method [*Ito, 1989*]. Both methods give a variety of age values from 55 Ma to 70 Ma. Those age data from each ash flow tuff unit are consistent and while intrusive rocks show the scattered results. The younger ages may imply the slow cooling of the deeper part of the rock body. Taking account of the low closure temperature of the K-Ar biotite

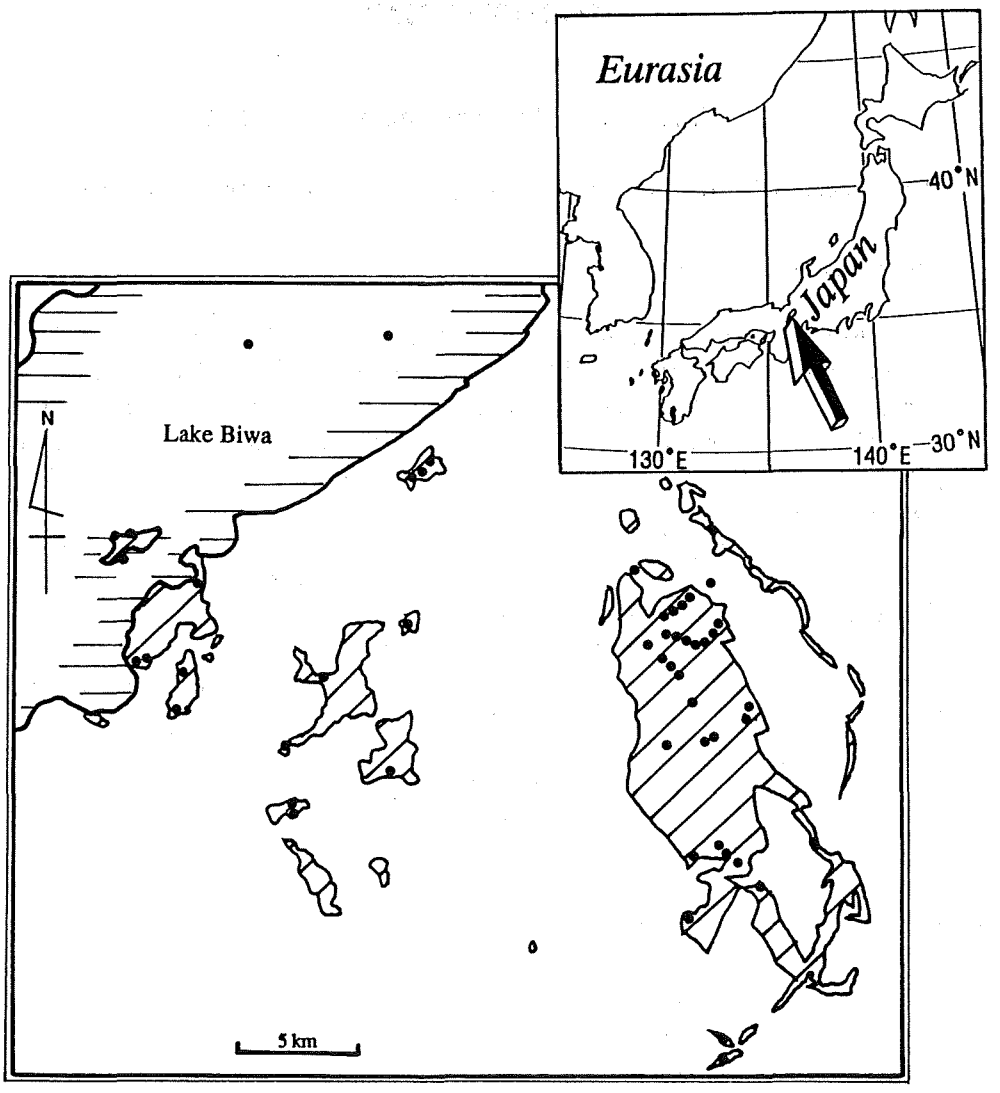

small masses in Koto Plain

site (KH)	Rock Unit
05,06,07,09 10	felsic intrusive rocks
01,02,03,04 08,11,12,13 14,15,17,19	Kamewariyama Welded Tuff
18	sediments
16,KY08,KY09	Azuti Welded Tuff

main mass

Rock Unit		site KT	site KY
Inugami Granite Porphyry	outer arc	14,24	04,05
	inner arc	05,15,23	06,07
Yatsuoyama Pyroclastics		02,19,20,16 17	01,02,10,11 12,13,14
sediments			
Hatasho Quartz Porphyry		03,07,08,09 13	
Kaiwara (Same) Welded Tuff		01,04,06,10 11,12,18,21 22,25,26	03,15

Fig. 1 A sketch map and stratigraphic table of the Koto Rhyolites showing sampling sites (dots and numbers) for the paleomagnetic study. Geological map is simplified after Nishikawa et al. (1983).

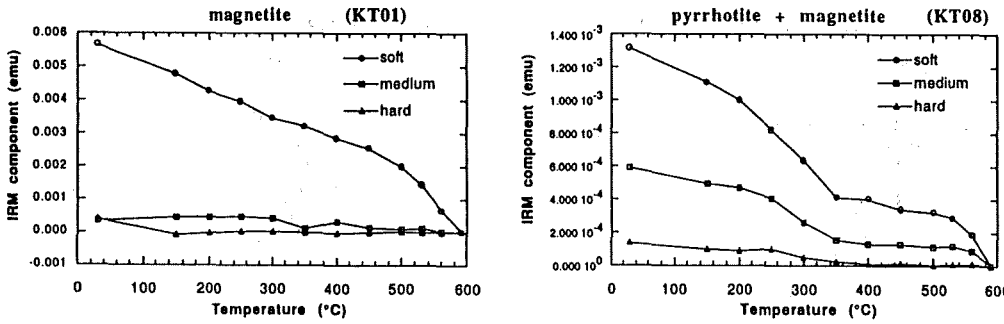

Fig. 2 Mutually orthogonal IRM intensity variation during the progressive thermal demagnetization. upper: ash flow tuff containing nearly pure magnetite, lower: intrusive rock closely related to the ash flow tuff showing pyrrhotite and magnetite. Soft, medium and hard represent the IRM components induced in the direct field of <0.12T, 0.12-0.4T and 0.4-1.3T respectively.

and FT zircon, the oldest age, 70 Ma, is correspond to the timing of emplacement.

Paleomagnetic analysis

Paleomagnetic samples were collected at 60 sites which were distributed over the whole area of the Koto Rhyolites and cover the representative rock units (Fig. 1): 40 sites from ash flow tuff, 19 sites from intrusive rock and 1 sites from the sediments. At each site, 10 or less oriented hand samples were taken with a magnetic compass. Orientations of the eutaxitic structure were measured for ash flow tuff at 20 sites. Dipping angles of ash flow tuff are smaller than 30 degrees.

Rock magnetic analyses were made on some representative samples. To identify magnetic minerals, we measured the temperature dependence of strong field magnetization and initial susceptibility. Progressive thermal demagnetization of orthogonal IRM [*Lowrie, 1990*] was also done. Most of ash flow tuffs and intrusive rocks were found to contain nearly pure magnetite (Fig. 2). Some intrusive rocks contain pyrrhotite associated with magnetite. The red pigmented ash flow tuff reveals the presence of titanohematite as opacites originated from olivine or pyroxene.

Modified Lowrie-Fuller tests were performed to estimate the domain structure for magnetite bearing samples. Ash flow tuffs represent the single domain or pseudo-single domain characteristics. Intrusive rocks reveal the multi-domain behaviors [*Dunlop, 1983*].

For each site, progressive thermal demagnetization for three specimens and progressive alternating field demagnetization for one specimen were performed to identify the components of the remanent

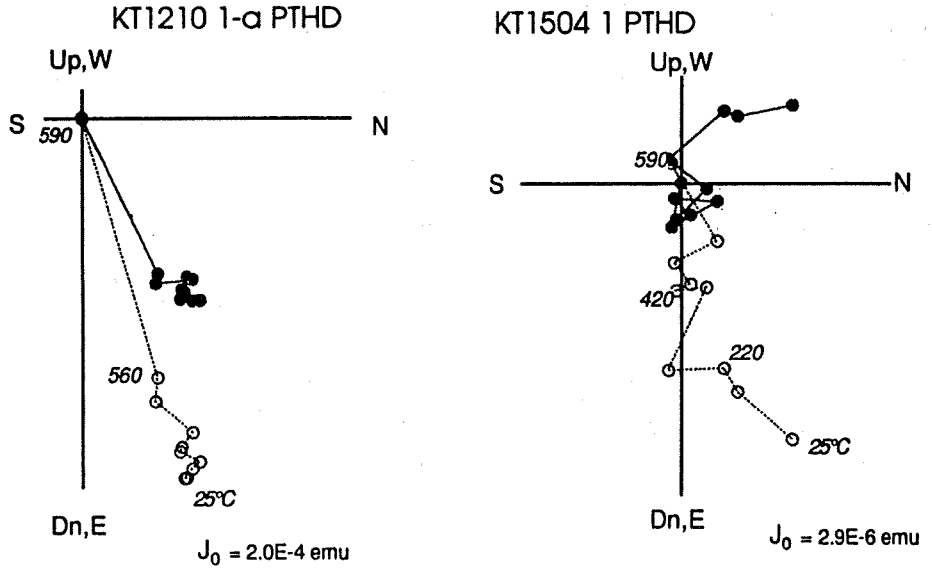

Fig. 3 Vector demagnetization diagrams representing the thermal treatments. left: ash flow tuff with high unblocking temperature magnetization, right: intrusive rock with low and wide distribution of unblocking temperature magnetization.

magnetization. Thermal demagnetization was more effective to isolate characteristic remanent magnetizations (ChRM) for most specimens (Fig. 3). Most of ash flow tuffs have a high unblocking temperature (>500°C) component carried by magnetite except for a low unblocking temperature component which is parallel to the present geomagnetic field. The range of the unblocking temperature of intrusive rock is broad and over relatively low temperature (<500°C). During the high temperature treatment the remanent magnetizations of intrusive rocks showed erratic behaviors. Site mean ChRM directions were determined through a blanket thermal demagnetization at the optimum level or progressive thermal demagnetizations of all specimens of each site with the principal component analysis.

Paleomagnetic Pole

Site mean ChRMs were obtained through the thermal demagnetization from 33 sites (Fig. 4). ChRMs have normal polarities at 25 sites and reversed polarities at 8 sites. ChRM directions of normal polarity as well as reversed polarity are well clustered. Normal and reversed mean directions are almost antipodal each other. Each rock unit shows consistent polarity. According to the stratigraphic succession, normal-reversed-normal polarity changes are observed for the main mass and for the small masses in the plain.

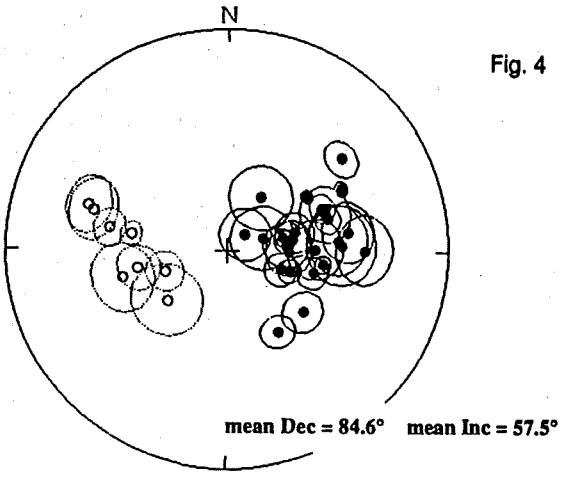

Fig. 4 Equal area projection of *in situ* site mean directions with 95% confidence cones of characteristic remanent magnetizations.

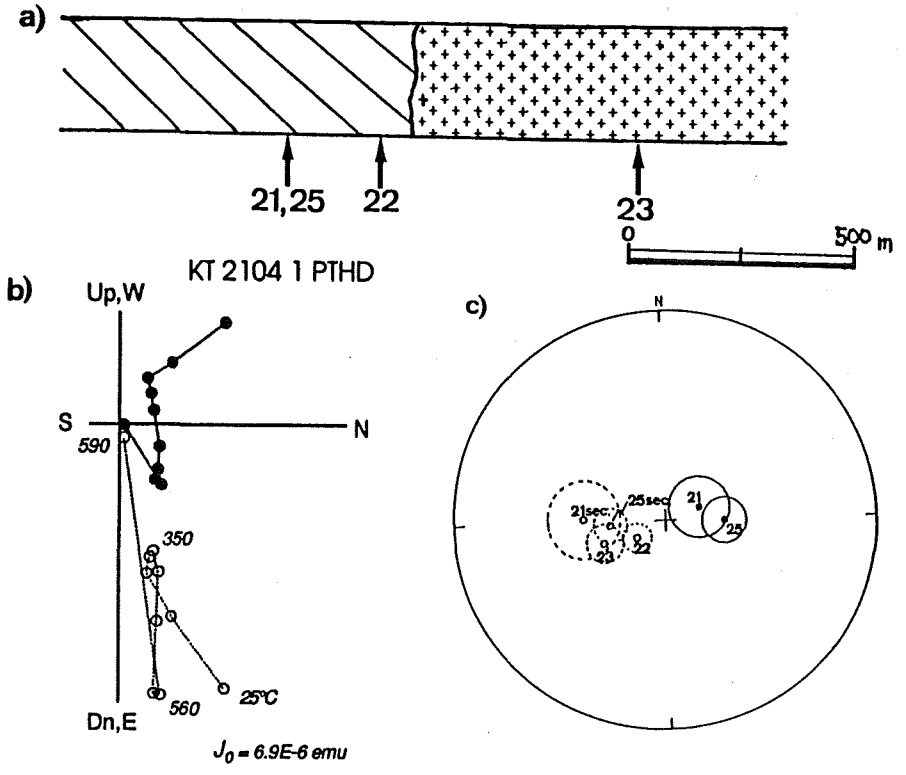

Fig. 5 Schematic view of the baked contact zone and the magnetizations around this zone. a) Schematic view of the contact zone. left: ash flow tuff, right: intrusive rock. Numerals represent the site numbers. b) Typical example of the multi-component magnetization. c) Directions of the components of magnetization. The numerals of 21, 22, 23 and 25 denote the characteristic remanent magnetizations of site21, site22, site23 and site25 respectively. 21sec and 25 sec denote the low unblocking temperature component of site21 and site25.

The intrusive rocks gave contact metamorphism to the ash flow tuff in the southern part of the main mass. The magnetization of ash flow tuff varies as a function of the distance from the contact (Fig. 5). The samples from the very contact have single component magnetizations which is parallel to the ChRM of the intrusive rock. To the contrary, almost antiparallel two components of magnetization are observed at the sites about 250 m apart from the contact. The high temperature component is parallel to the ChRM of the unmetamorphosed ash flow tuff and the low temperature component is parallel to the ChRM of the intrusive rock. This fact suggests a positive contact test, that is, the ChRM of the ash flow tuff is dated before the intrusion.

Directions of ChRM at 14 sites were corrected based on the eutaxitic structure of ash flow tuff. Dispersion, however, increased after the correction (Fig. 6). This negative tilt test indicates that the ChRMs of ash flow tuff were acquired after taking the present bedding attitude. The acquisition of magnetization may be related to the growth of fine magnetites in volcanic glass [*Schlinger et al., 1988*]. Positive reversal test, well defined polarity sequence and positive contact test suggest that the acquisition of ChRM shortly followed collapse and tilting of ash flow tuff within the Koto Rhyolites "caldera".

The orientations of eutaxitic structure of ash flow tuff are almost random and their average is nearly horizontal. The overall area of the Koto Rhyolites has not suffered the regional tilting up to the present time. The average of virtual geomagnetic poles calculated from the uncorrected ChRM directions safely provides the paleomagnetic pole position of the Koto Rhyolites in late Cretaceous time (25.6°N, 165.9°W, a_{95}=7.1°, Fig. 7). This pole position is in good agreement with that of 60 Ma and 80 Ma

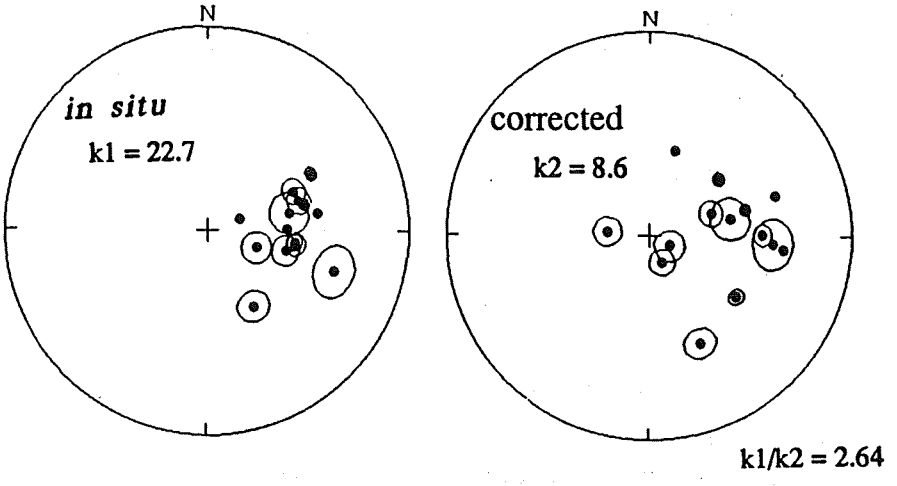

Fig. 6 Equal area projections of the *in situ* and tilt corrected directions from ash flow tuffs.

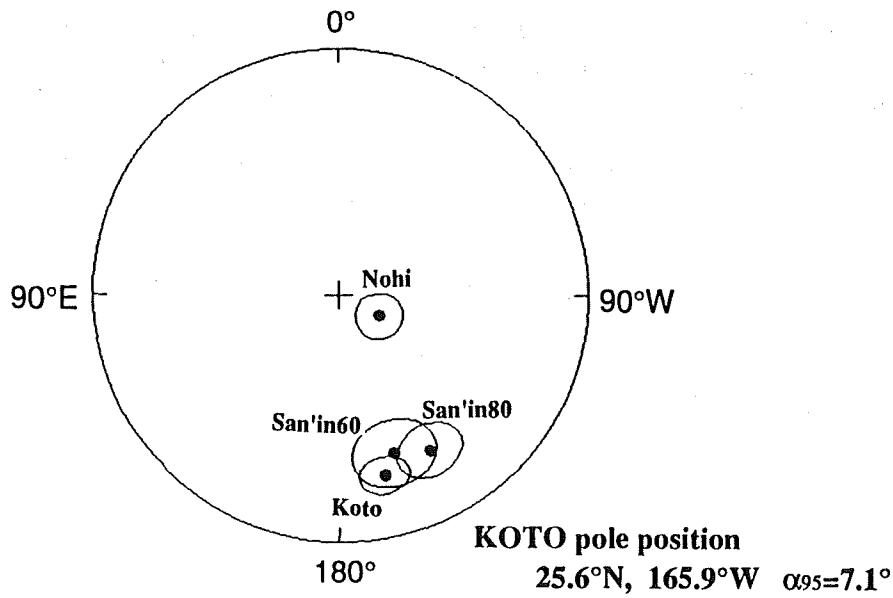

Fig. 7 Equal area projection in the northern hemisphere paleomagnetic pole positions from the Koto Rhyolites (Koto), the Yamaguchi and Go-river area whose age is about 60 Ma and 80 Ma [Otofuji and Matsuda, 1987](San'in60, San'in80) and the Nohi Rhyolites [Itoh,1988](Nohi).

obtained from Yamaguchi and Go river area, the western part of the Southwest Japan [*Otofuji and Matsuda, 1987*]. On the other hand, the pole position from the Nohi Rhyolites [*Itoh, 1988*], the eastern part of Southwest Japan, is largely departed from the Koto's pole position. This discrepancy of pole positions indicates that Koto area and Nohi area relatively rotated after their formations. The bending motion of the eastern part of Southwest Japan, which occurred between 15 Ma and 12 Ma, can explain this rotation [*Itoh, 1988*].

Koto area and Yamaguchi and Go river area, sharing the common paleopoles, have been united as a single coherent block since late Cretaceous time. The paleomagnetic pole obtained from late Cretaceous Koto Rhyolites gives a reliable data for the apparent polar wander path of Southwest Japan.

References

Dunlop, D. J., *Earth Planet. Sci. Lett.*, 63, 353-367, 1983.
Ito, H., *J. Geol. Soc. Japan*, 95, 479-482, 1989.
Itoh, Y., *J. Geophys. Res.*, 93, 3401-3411, 1988.
Lowrie, W., *Geophys. Res. Lett.*, 17, 159-162, 1990.
Nishikawa, K., T. Nishibori, T. Kohayakawa, T. Tajima, M. Joshima, K. Mimura, and M. Katada, *J. Jap. Assoc. Min. Petr. Eco. Geol.*, 77, 51-64,1983.

Otofuji, Y., and T. Matsuda, *Earth Planet. Sci. Lett.*, 85, 289-301, 1987.
Sawada, A., and T. Itaya, *Geol. Soc. Jap. Abstr. Programs*, 95, 323, 1988.
Schlinger, C. M., J. G. Rosenbaum and D. R. Veblen, *Geology*, 16, 556-559, 1988.
Takahashi, M., in *Accretion Tectonics in the Circum-Pacific Region*, edited by M. Hashimoto and S. Uyeda, TERRAPUB, Tokyo, 69-88, 1983.

DIFFERENTIAL ROTATION OF THE WESTERN PART OF SOUTHWEST JAPAN: PALEOMAGNETIC STUDY IN THE NORTHERN PART OF THE KYUSHU ISLAND

Naoto ISHIKAWA

Dept. Earth Sciences, College of Liberal arts and Sciences,
Kyoto Univ., Kyoto 606

Pre-Neogene geologic units in the main part of Southwest Japan show ENE-WSW trending zonal arrangements (Ozawa et al., 1985). This zonal structure is continuously traced to the the northern and eastern parts of the Kyushu Island, showing *approximately* same structural trend. Recent paleomagnetic investigations in the main part of Southwest Japan revealed the Middle Miocene clockwise (CW) rotation of the area through about 50° (Otofuji et al., 1985). Based on the zonal structure as mentioned above, Southwest Japan including the northern and eastern parts of the Kyushu Island has been regarded as a rotated rigid block at the first approximation (Otofuji and Matsuda, 1983, 1987). In order to assess this approximation, we carried out paleomagnetic studies in the northern part of the Kyushu Islands.

We collected samples for paleomagnetic measurement at 13 sites from the late Cretaceous granitic rocks and at 18 sites from sedimentary rocks of the Oligocene Ashiya Group (Figs. 1 and 2). The Cretaceous granitic rocks intrude into the basement rocks of the Permian Sangun metamorphic rocks, the Paleozoic sedimentary rocks, and late Cretaceous Kanmon Group, which belong to the geologic units showing the above-mentioned zonal structure. The K-Ar ages from the granitic rocks range from 76 Ma to 97 Ma with the peak occurrence of 90 Ma (Shibata and Karakida, 1965; Kawano and Ueda, 1966; Nozawa, 1970). The Ashiya Group is the upper unit of Paleogene sequences overlying the granitic rocks and the above-mentioned basement rocks. The

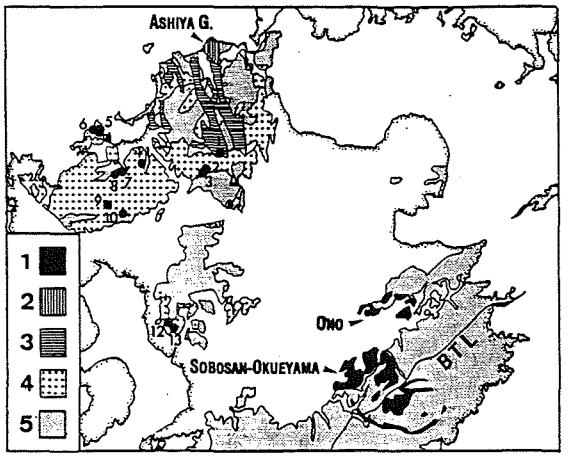

Fig. 1. Index map of studied area in the northern and eastern parts of the Kyushu Islands. Solid circles with numerals denote sampling sites of Cretaceous granitic rocks. 1: Middle Miocene igneous rocks. 2: the Ashiya Group. 3: Paleogene non-marine sediments (the Otsuji and Nogata Groups). 4: Cretaceous granitic rocks. 5: other pre-Neogene geologic units. BTL: Butsuzo Tectonic Line.

Ashiya Group is divided into three formations, and each formation is lithologically subdivided into two or three members as shown in Fig. 2. The geologic age of the Ashiya Group has been estimated by biostratigraphic data. Calcareous nannoplankton assemblages from the Norimatsu shale member were correlated to CP 18 (Saito and Okada, 1984). Tsuchi et al. (1987) obtained planktonic foraminifera assemblages from five horizons in the Norimatsu, Aisaka and Tomoro members (Fig. 2). These horizons were included in the basal part of Zone P.21. These micropaleontological data indicate that the whole Ashiya Group is probably assigned to the Oligocene in age (Tsuchi et al., 1987).

Block samples were collected from granitic rocks. Sedimentary rock samples of the Ashiya Group were collected using a gasoline-powered core drill. Six to fourteen oriented block or core samples were obtained at each site. One or two cylindrical specimens of 24 mm in diameter and 22 mm in height were prepared from each sample for the paleomagnetic measurements. Remanent magnetization was measured by a cryogenic magnetometer (ScT C-112) at Department of Geology and Mineralogy, Kyoto University. Stability of remanence was assessed through progressive alternating field (AF) and thermaldemagnetization experiments. Two or three pilot specimens at each site were subjected to each demagnetization experiment.

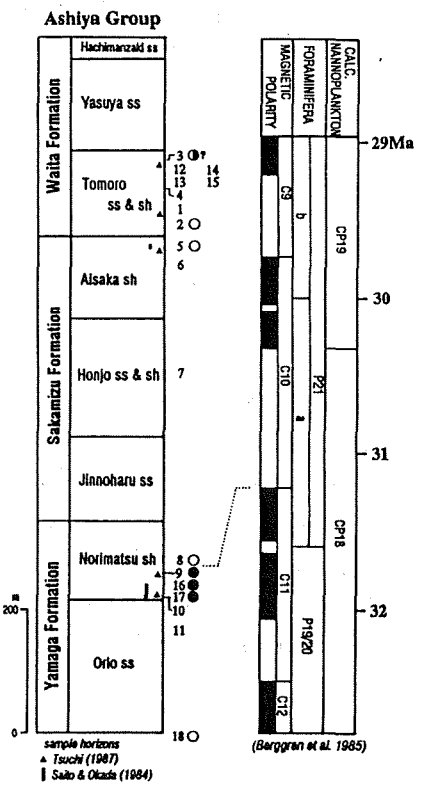

Fig. 2. Diagrams showing the stratigraphy of the Ashiya Group and distribution of sampling horizons for micropaleontologic (Saito and Okada, 1984; Tsuchi et al., 1987) and paleomagnetic studies. Numerals indicate the names of the paleomagnetic sampling sites. Solid and open circles denote normal and reversed polarity, respectively. Cenozoic time scale of Berggren et al. (1985) was adopted.

Demagnetization results

Cretaceous granitic rocks

Pilot specimens of four sites among the 13 sites of the granitic rocks yielded stable magnetic components at the demagnetization levels approximately above 500 °C and/or 20 mT (Fig. 3). The stable components were regarded as a linear trend toward the origin of the vector-demagnetization diagram. Pilot demagnetization results of the rest sites provided erratic behaviors or linear trends which did not decay toward the origin of the diagram. All remaining specimens of the four sites were demagnetized at several demagnetization levels which yielded the stable component decaying toward the origin in

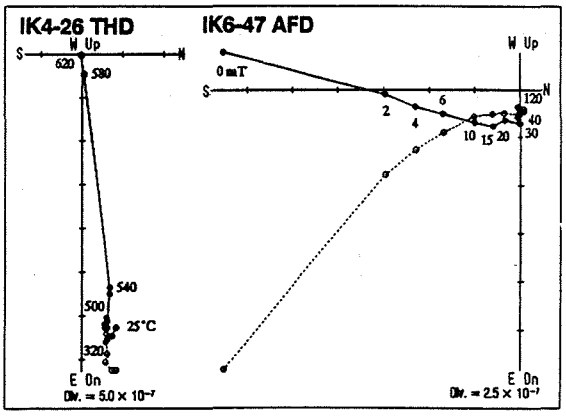

Fig. 3. Vector-demagnetization diagrams of progressive thermal (THD) and alternating field (AFD) demagnetizations of Cretaceous granitic rocks. Solid and open symbols are projection on horizontal and N-S vertical planes, respectively. Numerals attached to symbols are demagnetization levels. Div.: one division of coordinate (Am^2).

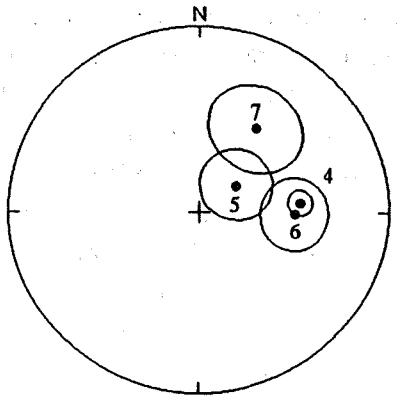

Fig. 4. Equal-area projection of site- mean directions from Cretaceous granitic rocks. Ovals around the mean directions denote 95% confidence limit. Numerals indicate site numbers. Solid (open) symbol is on the lower (upper) hemisphere.

the respective pilot specimens. The site-mean direction and associated statistic parameters were calculated for each demagnetization level. The mean direction with the minimum dispersion was selected as a characteristic direction of the site. The characteristic directions of the four sites are listed on Table 1 and shown in Fig. 4. All characteristic directions showed easterly-deflected direction with normal polarity. A mean direction was calculated: D=67.4°, I=54.4°, α_{95}=24.5°, k=15.1.

Table 1. Paleomagnetic data from Cretaceous granitic rocks.

Site	N	level	D	I	α_{95}	k
4	8	540°C	84.4°	45.3°	5.5°	101.6
5	8	500°C	53.0°	69.7°	15.8°	13.3
6	8	30mT	91.7°	47.7°	15.7°	13.4
7	8	500°C	33.6°	44.5°	19.7°	8.8
mean	4		67.4°	54.4°	24.5°	15.1

N: number of specimens or sites. level: demagnetization level, D, I: declination and inclination in in-situ coordinates, respectively. α_{95}: radius of 95% confidence circle. k: precision parameter. mean: mean calculated from in- situ site-mean directions.

The Ashiya Group

Sedimentary rock specimens yielded erratic behaviors of remanent magnetization at the demagnetization levels approximately above 400°C or 25 mT. Below these levels, several pilot demagnetization results implied the existence of two components; one (the lower component) was mainly isolated below about 240°C or 10mT, and the other (the higher component) above the demagnetization levels (Fig. 5). The two components were not clearly isolated by AF and thermal demagnetization methods. The higher component was recognized as a curved line decaying toward the origin on the vector-demagnetization diagram. Remanent directions of the pilot specimens changed along a great circle on the equal-area projection. The remagnetization circles of pilot specimens seemed to converge into a direction at each site. These phenomena indicate the overlapping of unblocking temperature or coercivity of the two component. In order to estimate the direction into

which the remagnetization circles converged, that is, the direction of the higher component, all remaining specimens were progressively demagnetized by the thermal or AF method. The AF demagnetization was used only when pilot demagnetization results between the thermal and AF method were in good agreement. Remagnetization circle of each specimen was fitted to a least-square great circle. A direction into which the fitted least-square great circles converged was calculated at each site using the method of McFadden and McElhinny (1988). This direction was regarded as a characteristic direction of the site.

We obtained the characteristic directions from eight sites among the 18 sites (Fig. 6 and Table 2). We performed tilt correction for these directions. All characteristic directions except that of site 3 showed a better antipodal relationship with the NE-SW trend after tilt correction (Fig. 6 and Table 2). The untilted directions of the seven sites were regarded as the directions of the primary magnetic components acquired at the formation of the Ashiya Group. An anomalous direction of site 3 may be attributed to a record of the transitional field during

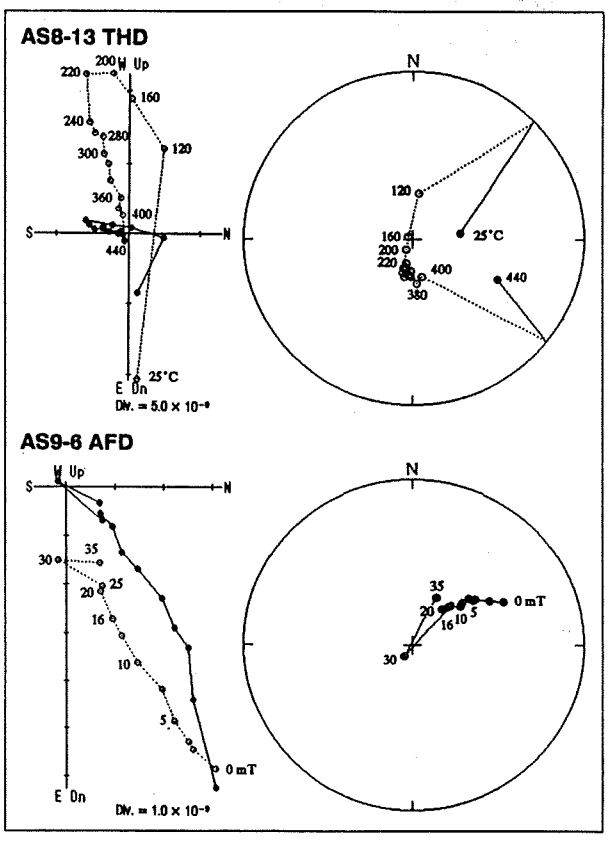

Fig. 5. Vector-demagnetization diagrams and equal-area projection stereograms of progressive demagnetization of sedimentary rocks from the Ashiya group. Solid (open) symbols on the stereogram denote positive (negative) inclination. See Fig. 4 for explanation.

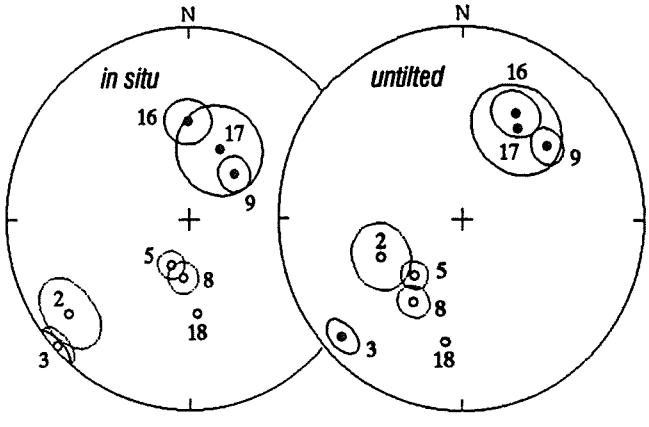

Fig. 6. Equal-area projection of in situ and untilted site-mean directions from the Ashiya Group. See Fig. 5 for explanation.

a geomagnetic reversal or a local tectonic disturbance around site 3. The latter was probably less possible because the bedding of strata at site 3 show approximately same trend to the general trend of the Ashiya Group. A mean direction was calculated from the untilted direction of the seven sites: D=35.9°, I=45.7°, α_{95}=11.5°, and k=28.7. This direction was regarded as a paleomagnetic direction of the Oligocene Ashiya Group.

Table 2. Paleomagnetic data from the Ashiya Group.

Site	N	levels	D	I	D*	I*	α_{95}	k
2	7	0-20mT	-126.9°	-18.1°	-114.5°	-49.8°	13.7°	29.5
3	7	120-320°C	-132.4°	-1.9°	-133.6°	11.1°	6.8°	116.8
5	8	120-280°C	-156.7°	-68.6°	-139.0°	-57.6°	6.1°	112.7
8	6	120-360°C	-173.6°	-64.6°	-148.8°	-47.8°	7.0°	255.0
9	9	0-20mT	46.7°	61.1°	51.2°	39.4°	7.5°	62.5
16	5	2-20mT	-0.8°	47.3°	28.5°	37.9°	10.3°	118.8
17	4	0-20mT	25.3°	56.5°	33.2°	43.0°	19.7°	81.5
18	6	120-320°C	174.5°	-48.8	-171.8°	-35.3°	1.6°	4618.4
mean	7		22.8°	54.6			17.1°	13.4
mean*	7				35.9°	45.7°	11.5°	28.7

levels: demagnetization levels at which a least-square great circle was fitted to the demagnetization result. D*,I*: declination and inclination after tilt correction. mean*: mean calculated from untilted site-mean directions. See Table 1 for explanation.

Discussion

The micropaleontological data indicate that the Norimatsu member is correlated to CP 18 of the calcareous nannoplankton biostratigraphy (Saito and Okada, 1984) and to the basal part of Zone P.21 (P.21a) of the planktonic foraminifera one (Tsuchi et al., 1987). The characteristic directions obtained from the Norimatsu shale member showed a change of the polarity (Fig. 2). In conjunction with the above-mentioned micropaleontological data, the polarity change in the Norimatsu shale member is correlated to that between Chron 10 and Chron 11 of the magnetostratigraphy after Berggren et al. (1985). The age of the Norimatsu member can be assigned to about 31.2 Ma. The paleomagnetic direction of the Ashiya Group obtained in this study are thus regarded as the paleomagnetic direction of around 30 Ma in the northern part of the Kyushu Island.

The paleomagnetic direction of the Ashiya Group show a CW deflection (Fig. 7). We compared this direction with the expected direction calculated from the 30 Ma mean paleopole of northern Eurasia (Irving and Irving, 1982). Based on the definition of Beck (1980), the anomalies of declination and inclination are 27.8° ± 17.8° and 11.1° ± 12.4°, respectively. The significant declination anomaly indicates a CW rotation of the area including the Ashiya Group through about 28° relative to northern Eurasia after about 30 Ma.

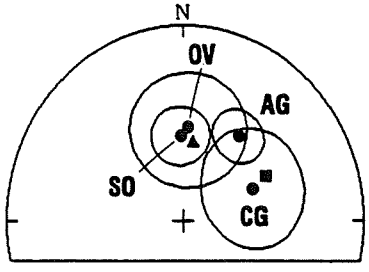

Fig. 7. Paleomagnetic data from the northern and eastern parts of the Kyushu Island. AG: the Ashiya Group. CG: Cretaceous granitic rocks. SO: the Sobosan-Okueyama volcano-plutonic complex. OV: the Ono volcanic rocks. Triangle and square symbols show the expected directions calculated from the 30 Ma Eurasia mean paleopole (Irving and Irving, 1982) and from the 30 Ma mean paleopole of Southwest Japan (Otofuji and Matsuda, 1987), respectively, at 34.90°N and 130.68°E.

The mean remanent direction of the Cretaceous granitic rocks also show a CW deflection (Fig. 8). This deflection can be not simply attributed

to a CW rotation around a vertical axis because tilt correction can not be performed for the direction of the granitic rocks. However, the CW-deflected paleomagnetic direction is obtained from the Ashiya Group, which is the upper unit of Paleogene sequences overlying the granitic rocks and other basement rocks. The CW deflection of the remanent direction from the granitic rocks supports the interpretation that the area including the granitic rocks and the other basement rocks, that is, the northern and eastern part of the Kyushu Island, were subjected to the CW rotation shown by the paleomagnetic direction of the Ashiya Group.

Paleomagnetic data have been reported from the two units of Middle Miocene igneous rocks at the eastern part of the Kyushu Island: One is from the Ono volcanic rocks and the other from the Sobosan-Okueyama volcano-plutonic complex (Torii and Ishikawa, 1986). These igneous rocks intrude or overlie the zonal structure of pre-Neogene geologic units (Fig. 1). The times of these igneous activities have been estimated at about 13-14 Ma based on the K-Ar radiometric age data (Shibata and Ono, 1974; Shibata, 1978; Tatsumi et al., 1980). The paleomagnetic directions from these Middle Miocene igneous rocks pointed parallel direction with the present north (Fig. 7), which indicates that the area including the igneous rocks has not suffered any regional rotation since the Middle Miocene igneous activity. It can be said that the CW rotation of the northern and eastern parts of the Kyushu Island had occurred between 30 Ma and 14 Ma.

The CW rotation of the main part of Southwest Japan occurred at about 15 Ma. The northern and eastern parts of the Kyushu Island is assumed as a western part of Southwest Japan based on the structural trend of pre-Neogene geologic units. The CW rotation of the northern and eastern parts of Kyushu Island is probably attributed to that of the main part of Southwest Japan, that is, Southwest Japan including the northern and eastern parts of the Kyushu Island suffered a CW rotational movement at about 15 Ma.

It is noted that rotation angle of the western part of Southwest Japan indicated from the paleomagnetic data of the Ashiya Group is smaller than that of the main part of Southwest Japan. Compared with the expected direction calculated from the 30 Ma paleopole of the main part of Southwest Japan (Otofuji and Matsuda, 1987), the paleomagnetic direction of the Ashiya Group shows a significant declination anomaly ($-28.2^\circ \pm 18.6^\circ$). It is suggested that the differential rotation occurred between the Kyushu Island and the main part of Southwest Japan during the CW rotation of Southwest Japan at about 15 Ma. Murata (1987a,1987b) and Kano et al. (1990) pointed out a discrepancy in structural trend of the pre-Neogene geologic units between the eastern part of the Kyushu Island and the main part of Southwest Japan: the structural trend is $N55^\circ \pm 5^\circ E$ in the eastern part of the Kyushu Island and is $N75^\circ \pm 5^\circ E$ in the main part of Southwest Japan (Kano et al. 1990). The amount of the discrepancy in the structural trend is approximately consistent with that of the differential rotation between the Kyushu Island and the main

part of Southwest Japan deduced by the paleomagnetic data. The first approximation that the whole Southwest Japan behaved as a rigid block during its CW rotation should be modified.

The zonal structure of pre-Neogene geologic units is bent to NNE-SSW in the southern part of the Kyushu Island. Kano et al. (1990) suggested that this bending structure was formed by horizontal compression with vertical or subvertical σ_2 axes associated with the CW rotation of Southwest Japan. Ishikawa and Tagami (1991) suggested that the Tsushima Strait area between the Kyushu Island and the Korean Peninsula suffered a compressive deformation coeval with the CW rotation of Southwest Japan. The CW rotation of Southwest Japan seems to have caused the compressive tectonic situations in the two area. It is perhaps why the rotation angle of the western part of Southwest Japan was smaller than that of its main part.

References

Beck, M. E., Jr. (1980), J. Geophys. Res., **85**, 7115.

Berggren, W. A., D. V. Kent, J. J. Flynn, and J. A. Van Couvering (1985), G. S. A. Bull., **96**, 1407.

Irving, E. and G. A. Irving (1982), Geophys. Surv., **5**, 141.

Ishikawa, N. and T. Tagami (1991), J. Geomag. Geoelectr., **43**(in press).

Kano, K., K. Kosaka, A. Murata, and S. Yanai (1990), Tectonophysics, **176**, 333.

Kawano, Y. and Y. Ueda (1966), J. Pet. Min. Econ. Geol., **56**, 191.

McFadden, P. L. and M. W. McElhinny (1988), Earth Planet. Sci. Lett., **87**, 161.

Murata, A (1987a), J. Geol. Soc. Japan., **93**, 91.

Murata, A (1987b), J. Fac. Sci. Univ. Tokyo, II, **21**, 333.

Nozawa, T. (1970), J. Geol. Soc. Japan, **76**, 493.

Otofuji, Y. and T. Matsuda (1983), Earth Planet. Sci. Lett., **62**, 349.

Otofuji, Y. and T. Matsuda (1987), Earth Planet. Sci. Lett., **85**, 289.

Otofuji, Y., A. Hayashida, and M. Torii (1985), in 'Formation of Active Ocean Margins', eds., N. Nasu et al., TERRAPUB, Tokyo, 551.

Ozawa, T., A. Taira, and F. Kobayashi (1985), Kagaku (Science), **55**, 4.

Saito, T. and H. Okada (1984), in 'Biostratigraphy and International Correlation of the Paleogene System in Japan', eds., T. Saito et al., 85.

Shibata, K. (1978), Bull. Geol. Surv. Japan, **85**, 551.

Shibata, K. and Y. Karakida (1965), Bull Geol. Surv. Japan, **16**, 443.

Shibata, K. and K. Ono (1974), Bull. Geol. Surv. Japan, **25**, 663.

Tatsumi, Y., M. Torii, and K. Ishizaka (1982), Bull. Vol. Soc. Japan, **25**, 171.

Torii, M. and N. Ishikawa (1986), Rock Mag. Paleogeophys., **13**, 1.

Tsuchi, R., T. Shuto, and M. Ibaraki (1987), Rep. Fac. Sci. Shizuoka Univ., **21**, 109.

PALEOMAGNETIC EVIDENCE FOR NORTHWARD DRIFT AND CLOCKWISE ROTATION OF THE IZU-BONIN FOREARC SINCE THE LATE OLIGOCENE

Masato Koyama[1], and Stanley M. Cisowski[2]

1: Institute of Geosciences, Shizuoka University, 836 Oya, Shizuoka 422, Japan
2: Department of Geological Sciences, University of California at Santa Barbara, Santa Barbara, CA93106, U. S. A.

A paleomagnetic study was made on the deep-marine sediments and volcanic rocks drilled by Ocean Drilling Program (ODP) Leg 126 from the Izu-Bonin forearc region (Sites 787, 792, and 793, Fig. 1). This study evaluates the sense and amount of the tectonic drift and/or rotation associated with the evolution of the Philippine Sea plate and the Izu-Bonin arc. Alternating field and thermal demagnetization experiments show that many of the samples have stable remanence and are suitable for paleomagnetic studies. Paleomagnetic declinations were recovered by two methods of core-orientation, one of which uses a secondary viscous magnetization vector of each specimen as an orientation tool, and the other is based on the data of dowonhole microresistivity measurement using a formation microscanner (FMS).

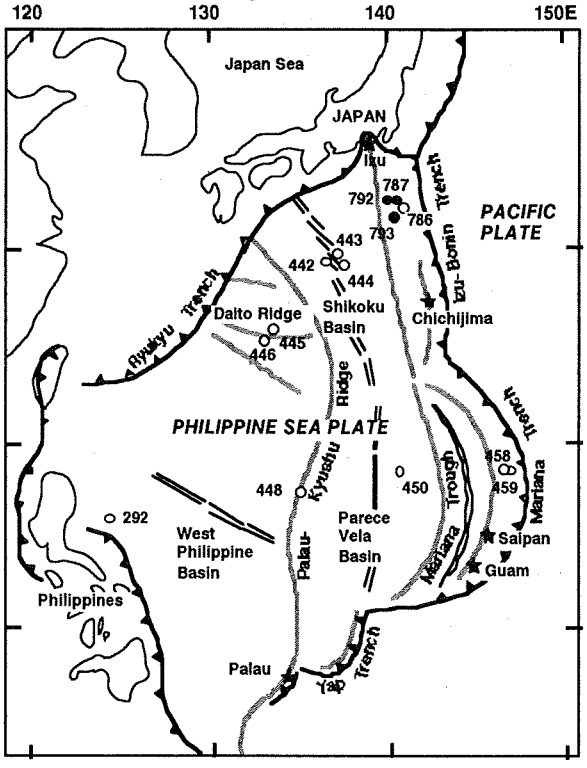

Figure 1. Tectonic features in and around the Philippine Sea at present. Thick solid line with teeth shows an active convergence boundary between plates. Thick gray line traces a ridge crest of active or non-active volcanic arc in the Philippine Sea. Double lines show the locations of spreading centers of active or non-active marginal basins. Sites examined by the present and previous paleomagnetic studies are shown with symbols: solid circle, ODP Leg 126 forearc site highlighted in this paper; open circle, other ODP or IPOD drill site; star, onland site.

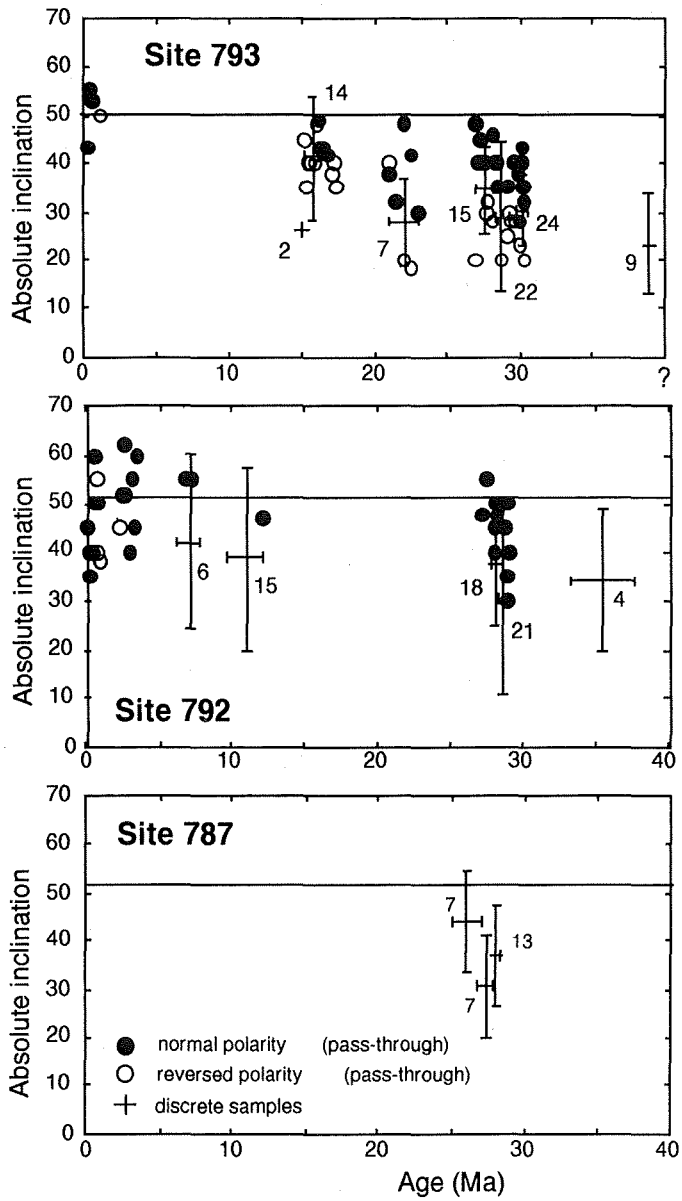

Figure 2. Relationship between remanence inclinations and their ages for each forearc site. Reversed inclinations were converted to normal ones. Cross with error bar shows the mean inclination of discrete samples after AF demagnetization. Number shows the number of samples. In Sites 792 and 793, mean inclinations measured with the long-core pass-through cryogenic magnetometer on the ship are shown with circles. Solid and open circles correspond to normal and reversed intervals, respectively. Long-core pass-through data from highly disturbed cores were not shown. Solid line shows the inclination of virtual geocentric dipole field for the present location of each drill site.

Oligocene to early Miocene samples show 10° to 15° shallower remanence inclinations than that of the present (Fig. 2). Middle Miocene to early Oligocene samples show progressive clockwise deflections (up to ~90°) of remanence declination (Fig. 3). These results suggest large northward drift and clockwise rotation of the Izu-Bonin forearc region since the early Oligocene time. Considering the previous paleomagnetic results from the other regions in the Philippine Sea, this motion implies the large clockwise rotation of the whole Philippine Sea plate over the last 27 Ma.

(submitted to *Proc. ODP, Scientific Results*)

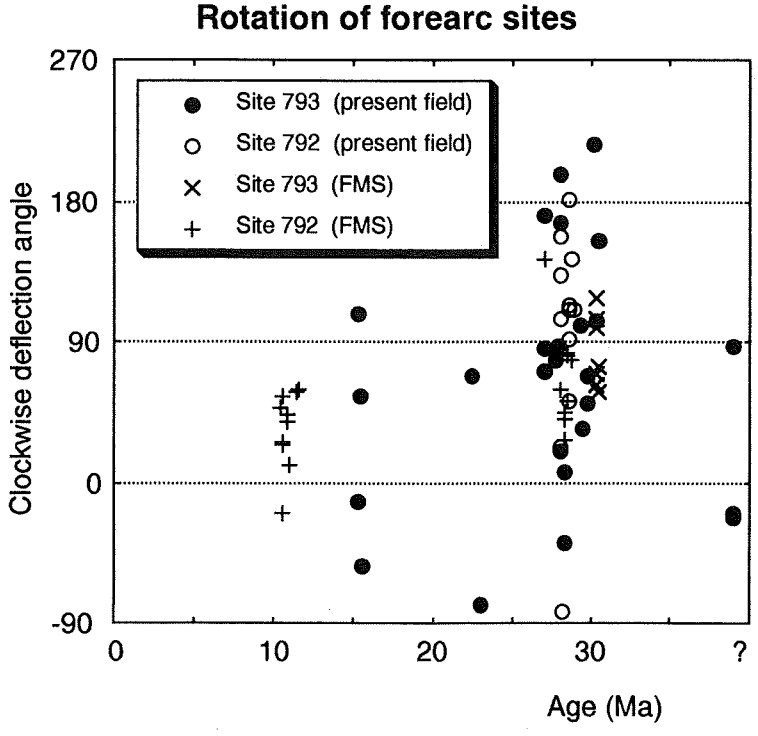

Figure 3. Relationship between azimuthally orientated declinations of remanence and their ages. Vertical axis shows the clockwise deflection angle from the geographic north. Circles correspond to the declinations orientated by the "present field" method using a secondary viscous magnetization of each sample. Crosses correspond to the declinations orientated by the "FMS" method.

TECTONICS OF AN ARC-ARC JUNCTION: PALEOMAGNETIC STUDY ON NORTHERN TAIWAN

Masako MIKI[1], Masahide FURUKAWA[1], Yo-ichiro OTOFUJI[2], Shuhjong TSAO[3] and Tunyow HUANG[3]

1. The Graduate School of Science and Technology, Kobe University, Kobe 657, Japan
2. Departmemt of Earth Sciences, Faculty of Science, Kobe University, Kobe 657, Japan
3. Central Geological Survey, Ministry of Economic Affairs, P.O.Box 968, Taipei, Taiwan, Republic of China

Taiwan lies on an arc-arc junction between the Philippine sea plate and the Eurasian plate. The Ryukyu arc and The Luzon arc join in Taiwan by means of the collision of the Luzon arc. Both arcs have undergone tectonic rotations since Miocene. Paleomagnetic and geochronological studies were carried out on Taiwan, in order to understand the kinematic history of this arc-arc junction.

Almost rocks sampled in this study are irregular tuffaceous intercalations in Miocene sedimentary sections in northern Taiwan. They are distributed at different horizons of the Miocene strata, as lenses or irregular beds of varying thickness. The extruding is contemporaneous with the deposition of the sedimentary strata (Ho, 1986). Samples of tuffs and basaltic lava flows were collected from 14 sites in early to late Miocene strata (Fig. 1). Samples were also collected from Chilung Volcano Group, the age of which ranges from 0.2 to 1.7 Ma (Juang and Bellon, 1984). Dacite lavas were sampled from one sites.

K-Ar dating was done on two samples from the Miocene volcanic rocks (site NT24 and NT43) and one sample from Chilung Volcano Group (site NT40). The samples are believed to be fresh enough for determining the extruding age. The obtained ages from Miocene volcanic rocks are 7.9±0.45 Ma and 10.1±0.61 Ma. The age from the sample of Chilung Volcano Group is 1.20±0.07 Ma. These ages are consistent with the field evidence.

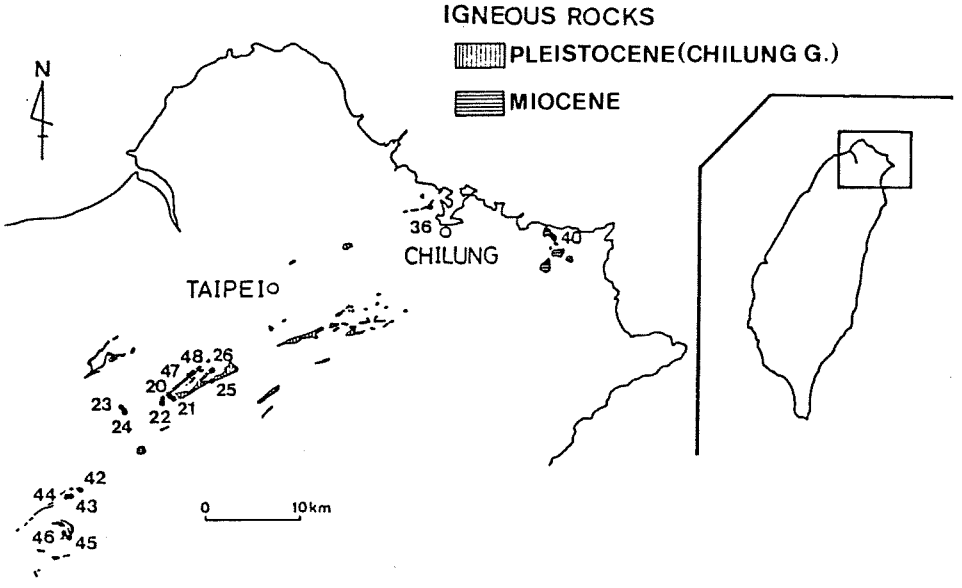

Fig. 1. Sketch map of sampling locarities (solid circles) in northern Taiwan.

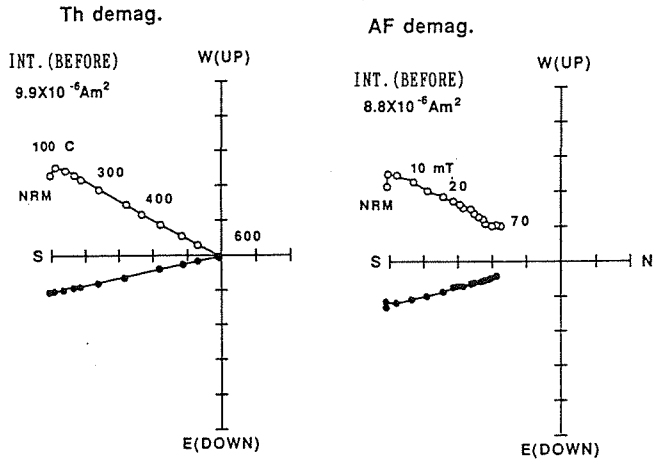

Fig. 2. Orthogonal projection plots for NRM stability examinations. Typical example of comparison between behaviours during progressive thermal and AF demagnetization for pilot specimens. Open (solid) circles are on the vertical (horizontal) plane.

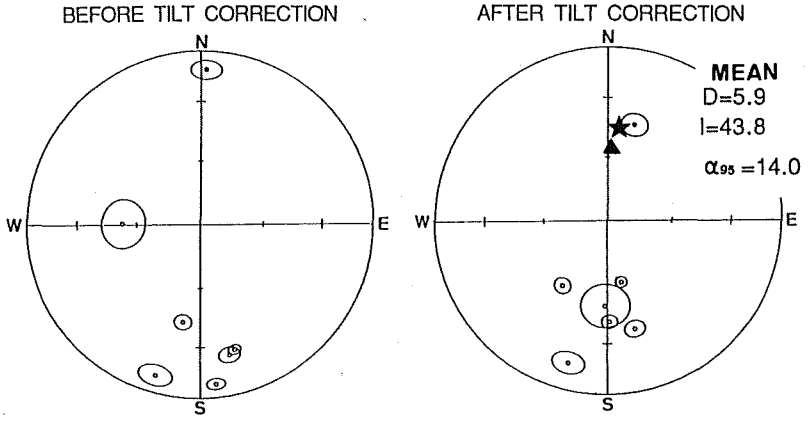

Fig. 3. Paleomagnetic directions from northern Taiwan. Comparison between site mean directions before and after tilt corrections are shown for the Miocene volcanics (Circles). Tilt correction has not been applied to the direction from Chilung Volcanic Group (triangle). Star shows the mean direction for the seven sites of the Miocene volcanics.

The natural remanent magnetization (NRM) was analyzed with the standard demagnetization technique. Two or three samples were chosen for pilot study. One specimen from each pilot sample was subjected to stepwise thermal demagnetization at up to 600°C. Another specimen was subjected to stepwise alternating field (AF) demagnetization, up to a maximum peak field of 100 mT.

Demagnetization behavior is relatively simple (Fig. 2). One or two components of magnetization can be distinguished in most samples using orthogonal demagnetization diagrams. A small low temperature component is removed up to 200 °C. The remaining high temperature component is stable up to 600 °C, at which the magnetization is completely removed. We regarded the high temperature component as the characteristic direction of each specimen. The characteristic direction is also isolated by the alternating field demagnetization. The hard component after demagnetization in the field of 5 mT is similar in direction to that of the high temperature component.

The characteristic direction of each specimen was determined by the principal component analyses (Kirschvink, 1980) using more The great majority of the samples have maximum angular dispersion (MAD) values of less than 5°, indicating the straightness of each

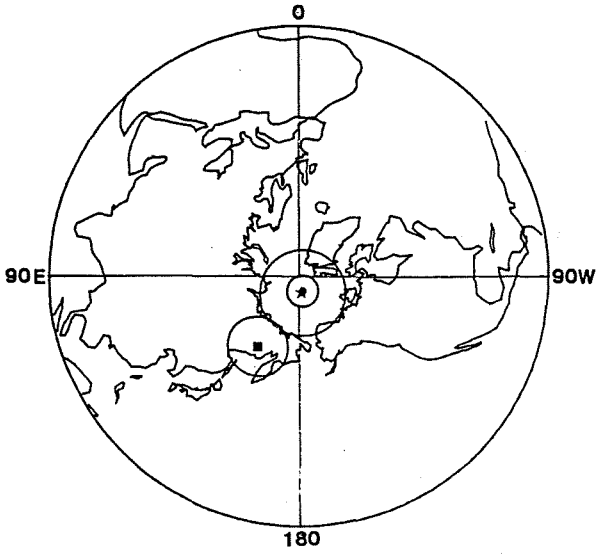

Fig. 4. Equal-area projections of Tertiary poles with 95 % confidence circles. Circle; the pole for 10 Ma Taiwan (this study), star; the pole for Neogene north China block (Zhen et al., 1990), square; the pole for Eocene south Ryukyu arc (Miki et al., 1990).

demagnetization path. Only samples with MAD values smaller than 10° were included in the site mean calculations.

The reliable paleomagnetic directions were obtained from seven sites of Miocene volcanic rocks and one site of Chilung volcanics (Fig.3). the mean direction of the 7 sites of Miocene volcanics is D=5.9°, I=43.8° with the radius of 95% confidence circle, 14.0°. The scatter of the mean directions became smaller after tilt corrections. The direction from the Chilung volcanics site is D=2.5°, I=53.3°

The pole position in this study for Miocene northern Taiwan is in excellent agreement with the pole determined for Neogene north China block by Zhen et al.(1990; Fig. 4). The Neogene pole for the north China Block can be regarded as the pole for the whole china block, because it is the pole after the amalgamation of north china block and south china block, which has been completed in middle Julassic (Zhen et al., 1990). The agreement indicates that the Taiwan has undergone neither tectonic rotation nor north-south translation respect to China block since 10 Ma. Taiwan has been a part of Asian continent since 10 Ma.

The paleomagnetic poles for the island arcs in both side of Taiwan are quite different from that of Taiwan. the South Ryukyu arc has rotated clockwise since 10 Ma, due to the Okinawa Trough opening (Miki et al., 1990). Luzon has undergone complicated rotations due to the interaction between the Philippine Sea plate and the South China Sea (McCabe et al., 1987; Fuller et al., 1989).

Taiwan is situated on an island arc junction making a cusp. Almost all of the island arcs have undergone tectonic rotations, along the island arc chain in western Pacific margin. Nevertheless, Taiwan has not gone through any tectonic rotation nor translation since 10 Ma. the paleomagnetic data strongly indicates that Taiwan is a part of continent, although Taiwan is a part of island arcs geographically. This means that the island arc cusps are happened in the position where the continental margin strongly connect the mother continent.

References

Fuller, M., R. Haston and J. Almasco (1989) Tectonophysics, 168, 171.
Juang, W.S. and H. Bellon (1984), Oroc. Geol. Soc. China, 27, 86.
Ho, C.S. (1986), Tectonophysics, 125, 1.
Kirschvink, J.L.(1980) Geophys. J. R. Astron. Soc.,62, 699.
McCabe R.J. et al., (1987) J. Geophys. Res., 92, 555.
Miki, M., T. Mathsuda and Y. Otofuji (1990) Tectonophysics, 175, 335.
Zhen, Z. et al.,(1990) Geophys. J. International, in press.

(To be summitted to Tectonophysics)

THE AMALGAMATIVE HISTORY OF EASTERN ASIA INFERRED FROM PALEOMAGNETISM OF THE NORTH CHINA

Zhong ZHENG*, Masaru KONO* and Ji'an SHAO**

* Department of Applied Physics, Tokyo Institute of Technology
Ookayama 2-12-1, Meguro-ku, Tokyo 152
**Department of Geology, Peking University, Beijing, China

1. Introduction

It is now widely believed that China is composed of tectonic collage formed through successive amalgamation of terranes since Paleozoic time (e.g., McElhinny et al. 1981; Zhao et al. 1990; Lin and Fuller 1990, Fig. 1). Since the completion of the collage of the Chinese continent, an accretionary process developed along the eastern continental margin of Asia (Mizutani et al., 1990) and later in Miocene age the Japan sea opened (Otofuji et al., 1985). The paleomagnetic investigation in the Northern and Northeastern China will enable a detailed reconstruction of such complicated process.

In this paper, We present the Paleomagnetic results of the Mesozoic sedimentary and Cenozoic basalts from the Northern and Northeasternmost China, and discuss their implications. The present model will make better understanding of the tectonic evolutionary history of Eastern Asia.

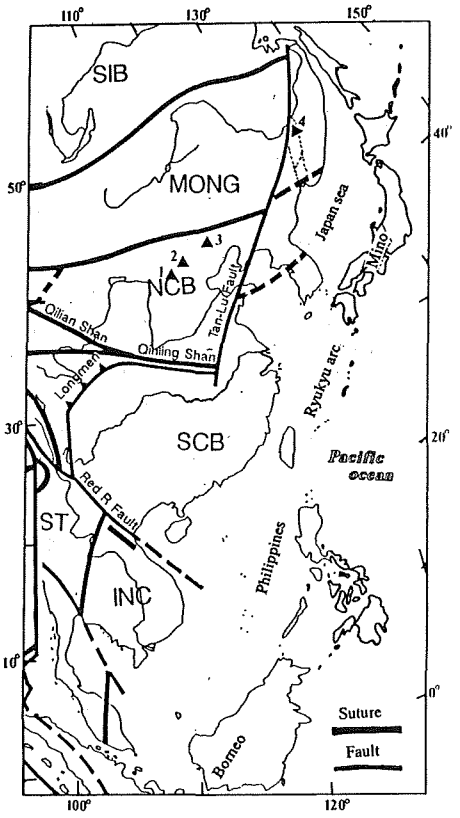

Figure 1. Generalized tectonic map of the Eastern China (base map by Enkin et al 1990) with sampling localities shown by numbers and triangles: 1: Datong, Shanxi, 2: Zhangjiakou, Hebei, 3: Chifeng, Innermongolia, 4: Nadanhada, Heilonjiang.

2. Paleomagnetic sampling and measurement

2.1 Datong area, Shanxi Province
(sampling central location at 40.1°N, 113.1°E)

Shanxi platform is in the center of the North China Block (NCB) and is one of the most stable part of that Block (Fig. 1). The sedimentary layers with Paleozoic and Mesozoic ages are widely distributed, and they are gently folded due to later tectonic movements. Datong area is located in the north-central part of Shanxi platform. In Zuoyun quarry, a very flat lenticular Cretaceous limestone about 30 m thick (Zuoyun

formation) overlies Cretaceous-Jurassic andesite (Baiqi formation) and middle Jurassic sandstone and mudstone of Yungan formation. Core samples were obtained at four sites from Zuoyun formation, one site from Baiqi formation, and two sites from Yungang formation . Besides the sites at Zuoyun quarry, sandstones of Jurassic age (Datong formation and Yungang formation of middle Jurassic and Yongdingzhuang formation of early Jurassic) were sampled at eight sites along the highway from Datong city to Yungan cave.

Middle Jurassic paleomagnetic direction

For the Jurassic rocks, the NRMs from mudstone (site ID DZ07) and sandstone (site ID DY07) showed a very queer phenomenon. The original remanence points to south and upward, a very typical "reversed" direction. Upon demagnetization, however, it reverts to normal direction by heating only to 100°C (Fig. 2a). By demagnetization at 150°C, the intensity of remanence became less than 1/10 of the original NRM. After that, the NRM stays in the north and downward direction to 650°C without further changes. Remarkably similar behaviors were observed for both sandstone (DY07) and mudstone (DZ07) samples. The low temperature component which can be demagnetized at 100°C seems to be carried by goethite. The weak but very stable high temperature components must be carried by hematite, and give a direction which is significantly different from the present magnetic field direction. The sandstone layer DZ06, which overlies the mudstone DZ07, has a very stable remanence persisting up to 600°C, with a direction similar to the high temperature components of DY07 and DZ07. While from other seven site no reliable results were obtained.

Following the demagnetization experiments, we conclude that primary direction was obtained from these three sites. The mean direction of magnetization is I=58.7°, D=17.9° (N=3, α_{95}=5.9°, k=443) and the VGP at 76.2°N, 199.9°E with the 95% confidence limit of A_{95}=4.2°. This Jurassic direction is not substantiated by fold test or reversal test, because all the rocks have normal polarity and the accepted layers are nearly horizontal. As the NRM in these rocks are very stable, and as the overprinting in both mudstone and sandstone sites show similar behavior in reversed and not normal direction, we may conclude that these data are acceptable as the middle Jurassic magnetic direction.

Cretaceous paleomagnetic direction

In the Cretaceous samples, behavior of the natural remanent magnetization (NRM) against thermal demagnetization depended on the intensity of the NRM, which ranged between 10^{-3} to 10^{-5} A/m. In weakly magnetized rocks (~ 10^{-5} A/m), the NRM showed two components, of which the direction of the low temperature components was erratic (Fig. 2b). The remanence directions became noisy again at temperatures higher than about 600°C. On the other hand, the strongly magnetized rocks (≥ 10^{-4} A/m) showed single and stable component of magnetization. Such contrasting behaviors were observed even among samples obtained at the same site.

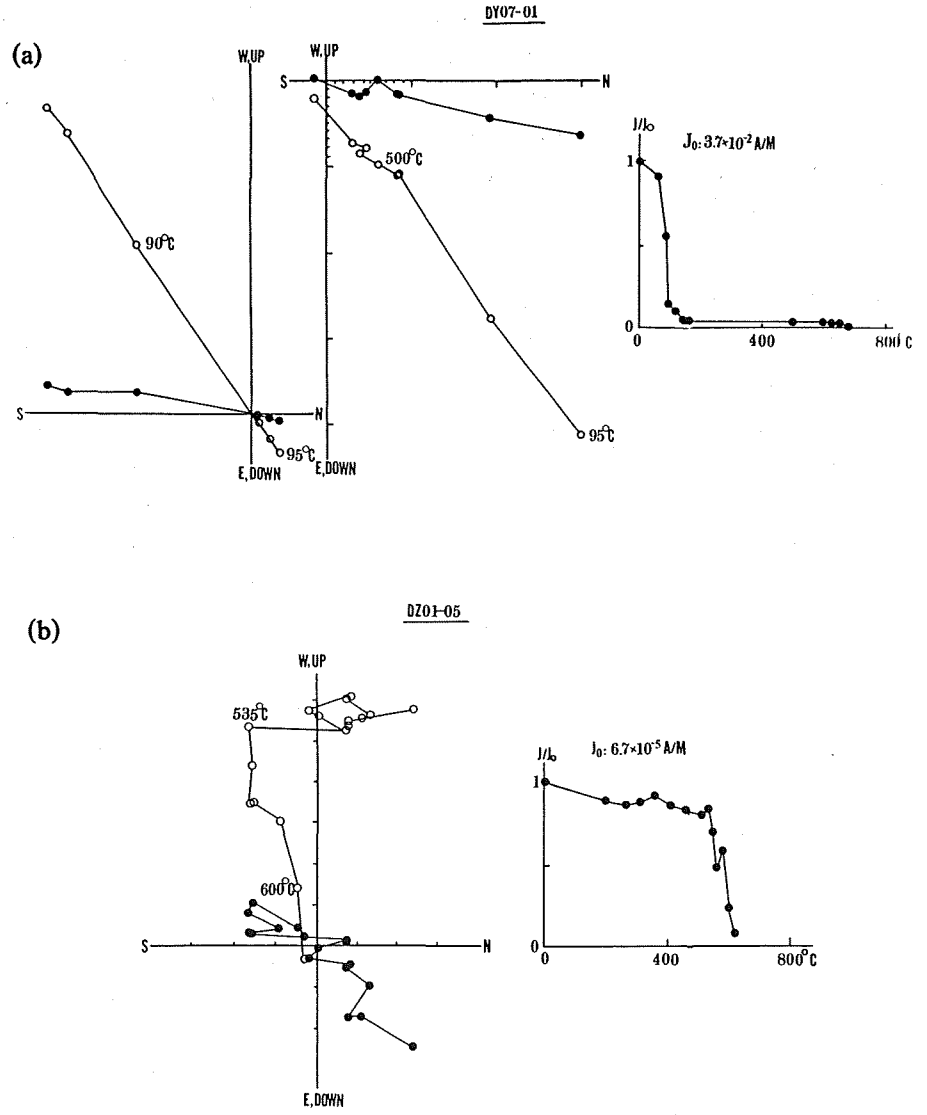

Figure 2. Examples of orthogonal projections of the magnetization vectors in Mesozoic rocks in Datong area during the course of thermal demagnetization. Insets show the decay of intensity of remanence by demagnetization. In the orthogonal projections, solid (open) circles are those projected on the horizontal (vertical) plane in geographical coordinates. The initial NRM intensities are given in the figures. (a) DY07-1 from sandstone of Yungan formation, (b) DZ01-05 from limestone of Zuoyun formation. The unit on the vector plot scales is 10^{-4} A/m for (a) and 10^{-5} A/m for (b).

For the four sites, the uppermost site (DZ01) contained reversely magnetized rocks: among the twelve samples measured, nine were reversed and three were normal. The two directions are approximately antipodal . These samples were collected from a layer approximately 0.5 m in height in the thick limestone exposed at the Zuoyun quarry. We conclude from the mixed polarity of DZ01 that both normally and reversely magnetized layers exist in close succession. Three other Cretaceous sites showed normal polarity with very stable

magnetizations which did not change its direction in thermal demagnetization up to 670°C, suggesting that these remanences are carried by hematite.

In the NRM of Baiqi formation (upper Jurassic to lower Cretaceous), a single stable component was observed. AF demagnetization was effective for this formation, but thermal method was more powerful in demagnetizing all the remanence. The mean direction of magnetization is very steeply inclined compared with all the other directions of NRMs from Jurassic and Cretaceous rocks in this study. As this formation was sampled from a single basaltic andesite lava flow, this direction should be regarded as a spot sampling of the secular variation at that age. For this reason, the results from Baiqi formation was excluded from further discussion.

The mean direction for four sites of Zuoyun formation was calculated to be D=12.4°and I=63.4° (N=4, α_{95}=4.2°, k=468) and the VGP at 79.6°N, 170.1°E with the 95% confidence limit of A_{95}=5.8°. In view of the existence of the reversed magnetization and very stable behavior of the remanences in demagnetization experiments, it is concluded that these directions are primary.

2.2 Neogene to Quaternary basalts in Chifeng, Inner Mongolia (sampling central location at 42.3°N, 118.9°E) and Zhangjiakou, Hebei Province (sampling central location at 41.1°N, 114.7°E)

The Cenozoic flood basalts are widely distributed in the northernmost Hebei Province and southeastern Inner Mongolia. Their ages were determined to be Neogene to late Pleistocene by K-Ar method (Zhou et al., 1988) and stratigraphic evidence (Sun, 1987). At one basalt platform in the very sampling area, we observed Malan loess of late Pleistocene age at 40 meter depth when a well was being drilled. So the ages of these basalt was suggested to be Neogene to Quaternary.

Samples were collected at 42 sites in Chifeng area, and at 10 sites in Zhangjiakou area. Columnar joints are well developed and formed basaltic platforms, most of them are vertical, but slanted ones are also observed in some of the platforms. It is an interesting question if the slanting is the original feature or caused by some local tectonic movement. Care was taken to sample several sites for each platform. Where vertical as well as slanted columnar joints were observed, samples were obtained from both places in the hope of performing a kind of fold test to see if the slanting of the column occurred later than the eruption.

The basalt samples from Chifeng and Zhangjiakou areas contain NRMs which are quite stable and well behaved. Almost all the samples showed single component of remanence in thermal and AF demagnetizations. As the NRMs are very well behaved in demagnetizations, there is no difficulty in choosing primary directions for these rocks. In four platforms, samples were collected at both vertical and slanted columns, and fortunately the results are in good agreement when the slanted columnars were rotated to vertical. We therefore used the tilt corrected data in this study.

In most of the measurements for basaltic rocks, different sites belonging to the same platform gave very similar results, while different platforms showed different directions even with distance of less than 15 Km. This suggests that, while the center of volcanic activity migrated with time, each platform was built within a short time before significant secular variation occurred. The data from 49 sites (40 in Chifeng, 9 in Zhangjiakou) out of 52 sites are used in present study. Three sites were unsuccessful; one site in Zhangjiakou was very much weathered and well-defined direction was not obtained by stepwise demagnetization, and the NRM from two slanted columnar joint sites in Chifeng are exceptional for our tilt correction method. Normal and reversed directions were obtained from 29 sites and 20 sites, respectively. The normal and reversed directions are almost antipodal, which confirms that these remanences are stable and reliable. The overall mean direction obtained from 49 site mean directions is I=61.5°, D=8.2° with α_{95}=4.2° and the VGP at 85.2°N, 192.5°E with the 95% confidence limit of A_{95}=5.1°.

2.3 The late Jurassic to early Cretaceous sedimentary rocks from Nadanhada Range, Northeasternmost China (sampling location at 47.3°N, 134.2°E)

Black and grey siltstone and shale are well exposed at the food preventing channel under the foot of Nanshan mountain, Donganzhen village, Raohe county, Helongjiang Province (Fig. 1). Vast amount of Buchia fossils of margin sea origin were found at this 105 m length of the section. Sun et al. (1989), after studying the features of the Buchia found at this very section, suggested that the formation (named Donganzhen FM.) should be divided into the upper formation with the age of early Cretaceous and the lower formation with the age of late Jurassic. A core sample was collected along the strata roughly by every three meter, and totals of fifteen and twelve samples were obtained from the upper and lower strata, respectively.

Stepwise AF demagnetization was not effective; there was hardly any changes in the NRM directions and intensities even at the maximum demagnetizing field (80 mT). Thermal demagnetization, however, isolated a very stable and simple shallow inclination component; The unblock temperature is dominated in a very narrow range 310°-345°C, and the intensity of remanence decreased to less than 1/20 of the initial NRM, but it kept the direction until heated to 490°c when the direction became erratic because of the noise of VRM.

As the NRMs in these rocks were very stable and the directions before the tilt correction are significantly different from the present or Brunhes normal epoch mean field direction, we suggest they are essentially primary, though the further study is necessary. The secular variation should be averaged out sufficiently because the sample were collected from a strata in which the age covers the long period of from late Jurassic to early Cretaceous. So we conclude fairly low paleolatitudes for the Nadanhada terrane between late Jurassic to early Cretaceous time.

3. Discussion and conclusions

Table 1 lists the paleomagnetic poles obtained in the present study for the NCB. It also includes poles for Siberia-Europe block, the NCB and the South China Block (SCB) for Jurassic to Tertiary reported from other paleomagnetic studies. For the SCB, we use the data compiled by Lin (1990), but rejected the data from the South Korea. For Siberia-Europe block, the compilation by Sasajima & Maenaka (1989) is used which was obtained by critical assessment of data listed by Irving and Irving (1982) and by Khramov (1984). Westphal et al. (1986) also gave a good data compilation. When their data used in place of Sasajima & Maenaka compilation, our conclusions are not significantly changed because the two data sets are not much different. Following Zhao et al. (1990), we assumed that Europe, Siberia, and Kazakhstan were amalgamated before Jurassic.

Table 1 Paleomagnetic pole positions since the Jurassic for the North Eurasia, the North and South China Blocks.

Age	North Eurasia			North China Block			South China Block		
	lat.	Lon.	A95	lat.	Lon.	A95	lat.	Lon.	A95(α_{95})
Q-N				85.2	192.5	5.1			
N2	85.4	215.1	2.5						
N1	84.9	192.8	2.9						
E							85.2	173.8	(11.9)
K2	75.1	163.7	8.3	79.6	170.1	5.8	76.3	172.6	10.3
K1	72.4	164.9	5.1				76.2	225.7	4.8
J3	75.0	158.9	9.5				73.0	213.7	12.6
J2	68.5	142.2	10.0	76.2	199.9	8.3	71.5	201.1	5.8
J1	74.4	130.5	9.7						
Tr3	58.2	137.4	33.7				62.7	197.2	2.6

The amalgamation of Asia continent

From the comparison of the APWPs for Siberia-Europe block, the NCB, and the SCB, it can be seen that the middle Cretaceous poles are very close to each other but the Siberian middle Jurassic pole is displaced from the contemporary Chinese poles (Fig. 3). Based on the polar wander paths since Carboniferous, Zhao et al. (1990) suggested that North China Plate including Outer Mongolia, Inner Mongolia, and the North China block collided with the Siberia-Europe block sometime in the late Permian near the western end of the Southern Siberian fold belt. After this initial collision, the North China Plate rotated by about 117° anticlockwise, closing the sea between the two blocks

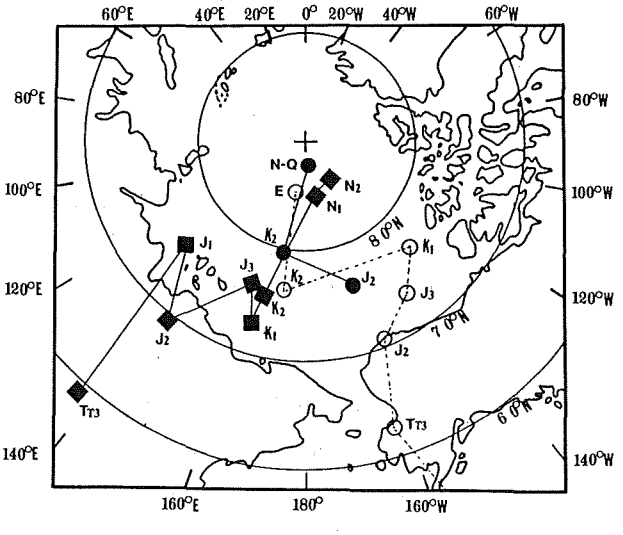

Figure 3. The combined APWPs for the NCB (solid circles), SCB (open circles) and Siberia-Europe Block (squares) for the period of Jurassic to Tertiary

starting from the western end and migrating eastward with time. Zhao et al. (1990) concluded that the suturing and rotation were almost completed by the late Jurassic.

Kimura et al. (1990) proposed that the two Chinese blocks collided in Late Triassic and the suturing continued through Jurassic until early Cretaceous. The present data are consistent with this model: the paleomagnetic poles from the NCB and SCB are quite different in Paleozoic (Lin 1990; Zhao et al. 1990), but their displacement decreases with time in Mesozoic and their poles become very close in Jurassic. Our data suggests that the two blocks were firmly connected by the middle of Jurassic. The collision with Siberian block, on the other hand, seems to have taken place a little later. The difference of the pole positions in Jurassic is still significant, but that in Cretaceous is not. We can conclude that amalgamation of the three blocks was almost complete in Cretaceous. Minor adjustments may have still occurred after that within the three blocks, but the three blocks were essentially within the same tectonic framework since Cretaceous.

The accretion process along eastern Chinese continent

The paleomagnetic directions from upper and lower strata at Donganzhen section do not show any significant difference, and the corresponding paleolatitude at 27.4°N with 95% confidence limit of 2.4°, which is much lower than the present latitude of 47.3°N. Uchimura (1989) reported paleomagnetic result of almost the same age (middle Jurassic to early Cretaceous) from non-marine sandstone in Qitaihe area (45.8°N, 131.1°E), one part of the NCB about 300 Km to southwest of Donganzhen. The direction passed reversal and marginally fold tests and yielded at I=64.3°, D=-23.6°, α_{95}=8.0°, the corresponding paleolatitude at 46.1°N with 95% confidence limit of 10.2°. According to the paleolatitudes, Qiteihe was located near the present position, while Nadanhada situated at more than 2000 Km south of the present location. The upper Mesozoic sedimentary rocks developed in Nadanhada were marine formations while those found in Qiteihe were not. Considering these facts, the two terranes must have different evolutionary history. Interesting enough, paleomagnetic investigation on Mesozoic sedimentary formations of the Mino terrane (Hirooka et al.1983, Shibuya and Sasajima 1986, Fig.1) indicate that the Mino terrane was also much south than the present position, and did not drift beyond 12°N until late Jurassic.

Mizutani et al. (1990) compared the radiolarian fossils and the lithological and the structural features among the formations from Nadanhada, Mino terrane of the Japanese Island, Ryukyu arc, the Philippines and Borneo. They concluded that these terranes including the Western Sikhote-Alin constituted a belt of accretionary complexes during late Jurassic and/or early Cretaceous time along the eastern continental margin of Asia after completion of the Triassic collage of the Chinese continent. The present paleomagnetic result coincide with their idea: In late Jurassic to early Cretaceous time, accretionary process developed along western margin of Pacific after completion of the amalgamation of Chinese continent, when Nadanhada terrane was near the South China and to the south situated the Mino terrane. In middle to late Cretaceous time, horizontal compress-shear displacement occurred and the Nadanhada and the

Mino superterrane moved northward to the easternmost China continental border. And in Neogene time the Japan sea opened.

References

Enkin, R.J., Y.Chen, V.Courtillot, J.Besse, L.Xing, Z.Zhang, Z.Zhuang and J. Zhang (1990) J. geophys. Res., in press.

Hirooka, K., T.Nakajima, H.Sakai, T.Date, T.Nittamachi and I.Hattori (1983) Accretion Tectonics in the Circum-Pacific Region, edited in M,Hashimoto and S.Uyeda, 179-194.

Irving, E. and G.A. Irving (1982) Geophys. Surv., 5, 141-188.

Khramov, A.N. (1984) Paleomagnetic Directions and Pole Positions, Soviet Geophysical Committee, USSR Academy of Sciences, Moscow. (in Russian)

Kimura, G., M.Takahashi and M. Kono (1990) Tectonophysics, **181**, 15-23.

Lin, J. and M. Fuller (1990) Phil. Trans. R. Soc. Lond. A **331**, 589-598.

McElhinny, M.W., B.j.j. Embleton, X.H. Zhang and Z.K. Zhang (1981) Nature, **293**, 212-216.

Mizutani, S., J. Shao and Q. Zhang (1990) Acta Geological Sinica, vol. **3**, No. 1, 16-29.

Otofuji, Y., T. Matsuda and S. Nohda (1985) Nature, **317**, 603-604.

Sasajima, S. and K. Maenaka (1989) Research Rept. Hanazono Univ., **20**, 1-19, 1989. (In Japanese with English abstract)

Shibuya, H. and S.Sasajima (1986) Jour. Geophys. Res., vol. **91**, 14105-14116.

Sun, G., J.Sha, Y.Wang, F.Yuan, X.Xong and T.Piao (1989) Acta paleontological Sinica, vol. **28**, No. 25, 579-589.

Sun, J. (1987) Research on Recent Crustal Movement 3, 157-164, Institute of Geology, State Seismological Bureau, Seismological Press, Beijing. (in Chinese)

Uchimura, H. (1989) master thesis, Tokyo Institute of Technology.

Westphal, M., M.L.Bazhenov, J.P.Lauer, D.M.Pechersky and J.C.Sibuet (1986) Tectonophysics, **123**, 37-82.

Zhao, X., R.S. Coe, Y. Zhou, H. Wu and J.Wang (1990) Tectonophysics, **181**, 43-81.

Zhou, X.H., B.Q. Zhu, R.X.Liu and W.J. Chen (1988) in Macdougall, J.D. ed.,"Continental Flood Basalts", pp. 311-330, Kluwer Academic, Dordrecht, Netherlands.

DEFORMATION OF SOUTHERN TIBET: PALEOMAGNETIC STUDY OF THE QUXU PLUTON OF THE GANDESE BELT

Yo-ichiro OTOFUJI*, Jun KADOI*, Shoubu FUNAHARA*, Fumiyuki MURATA* and Xilan ZHENG**

* Department of Earth Sciences, Faculty of Science, Kobe University, Kobe 657, Japan
** Institute of Geology, Academia Sinica, Beijing, China

Forty five samples have been collected at 9 sites from the 42.5 Ma Quxu pluton of the Gandese belt (Fig. 1). The sampling localities are located within 31 km from the Indus-Zangbo suture zone. Low temperature component with northerly direction are removed by thermal demagnetization at about 300 °C. High temperature components appear in four sites. Two sites preserve primary paleomagnetic direction, whereas the other sites have secondary magnetization which is produced during cataclastic metamorphism.

The primary paleomagnetic direction shows westerly deflection in declination (D= -48° and -82°). These directions are consistent with the paleomagnetic directions which are observed in rocks distributed along the Indus-Zangbo suture zone (Pozzi et al 1984; Otofuji et al. 1989) (Fig. 1). This indicates that the Quxu pluton of the Gandese belt was also subjected to the 'Domino-style' deformation since 42.5 Ma. The domino-style deformation occurred in the narrow zone along the suture zone from 82°20'E to 90°58'E. The deformed zone exceeds 840 Km in length. The deformation propagated into the interior of the Eurasian continent at 31 Km from the Indus-Zangbo suture zone. This deformation is ascribable to the collision of the Indian continent.

References

Otofuji,Y., S.Funahara, J.Matsuo, F.Murata, T.Nishiyama, X.Zheng and K.Yaskawa(1989) Earth Planet. Sci. Lett., 92, 307.

Pozzi,J.P., M.Westphal, J.Grardean, J.Besse, Y.X.Zhow, X.Y.Chen and Li.s.Xing(1984) Earth Planet. Sci. Lett., 70, 383.

(To be submitted to Earth Planet. Sci. Lett.)

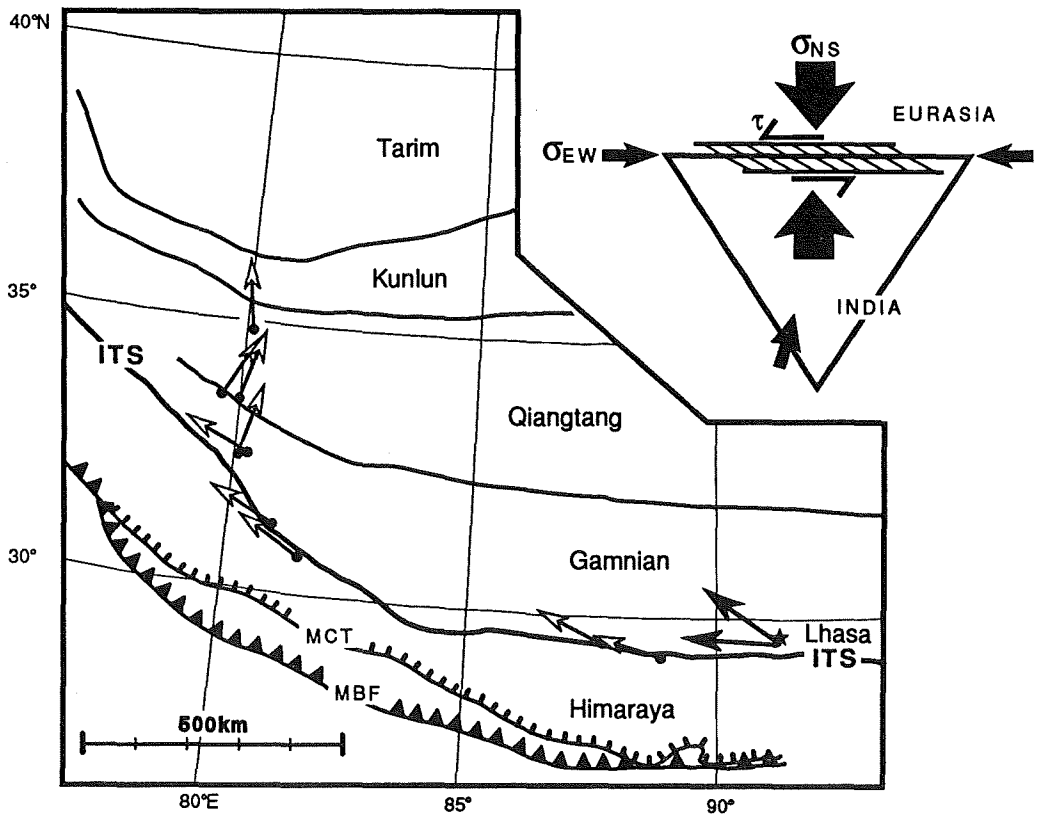

Fig. 1. Paleomagnetic directions found along the Indus-Zangbo suture zone (ITS). The solid arrows are obtained from the Quxu pluton and the open arrows from the previous studies (Pozzi et al 1984; Otofuji et al. 1989) . The major tectonic units and the geologic provinces are also indicated. Barbed lines are continental thrust (MCT=Main Central Thrust : MBF= Main Boundary Fault). The inset shows the 'Domino-style' deformation model proposed by Otofuji et al. (1989).

A STUDY OF GROUND MAGNETIC AND APPARENT SUSCEPTIBILITY SURVEY AROUND GOZAISHO-TAKANUKI METAMORPHIC ROCKS

Rie MORIJIRI, Masahiko MAKINO, Shigeo OKUMA and Tadashi NAKATSUKA

Geophysics Dept., Geological Survey of Japan
1-1-3 Higashi, Tsukuba City, Ibaraki 305, Japan

1. Introduction

Ground magnetic survey is one of very useful methods to investigate shallow crustal structures. Though this method tends to be affected by magnetic noise caused by artificial structures and quite local anomalies, it can supply informative data to estimate subsurface structures by measured at very close to ground surface. We have been trying to get better data to distribute survey points densely and to apply this method more.

We carried out Ground magnetic and susceptibility surveys around the middle part of the central Abukuma mountains in 1989 and 1990.

2. Methods

A portable proton precession magnetometer, EG&G GeoMetrics G856, was used to get total magnetic intensity data, at area 'X' and 'Y' in Fig.1(after Kano et al.,1973). Moreover, susceptibility meters SCINTREX SM-5 and KAPPAMETER KT-3 were used in-situ measurement of outcropped rocks at points 'A'-'U' in Fig.1.

Areas 'X' and 'Y' were situated on very gentle slopes of meadows. In the area 'X'(100m × 115m), we set 24 observation lines in the direction of N64° E. The length of each line was 100m, the line spacing was 5m. Along each line, total magnetic intensities were measured every 2m. And the sensor height was 2.5m. In order to correct the time variation of the geomagnetic field, we marked a base point in the area, and we got magnetic data at this point soon before and soon after observation along each line. In the area 'Y'(100m × 20m), we set 5 observation lines in the direction of N30° E, and the observation was carried out in the same way as in the area 'X'.

Susceptibilities were measured at several points on each outcropped rock. And we measured some large enough rocks at each observation site.

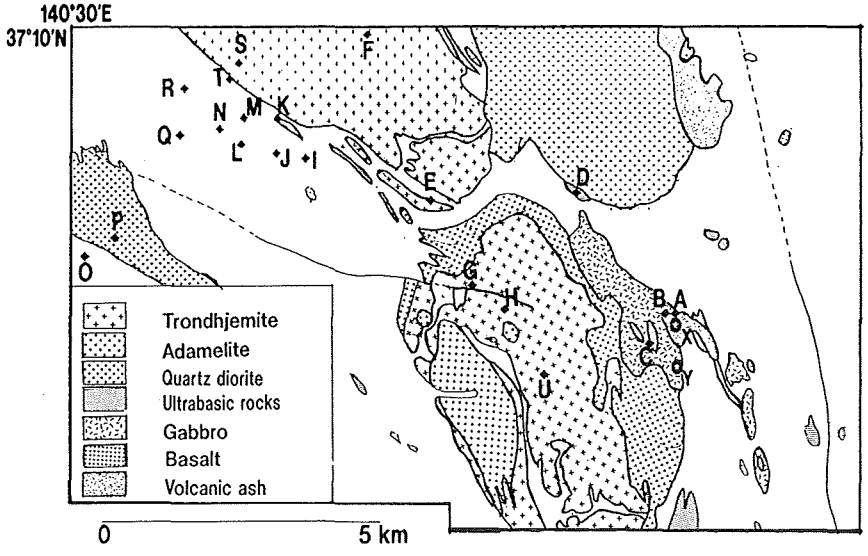

Fig.1 Ground magnetic survey areas;X,Y susceptibility survey points;A-U

surface geology from Kano *et al.* (1973)

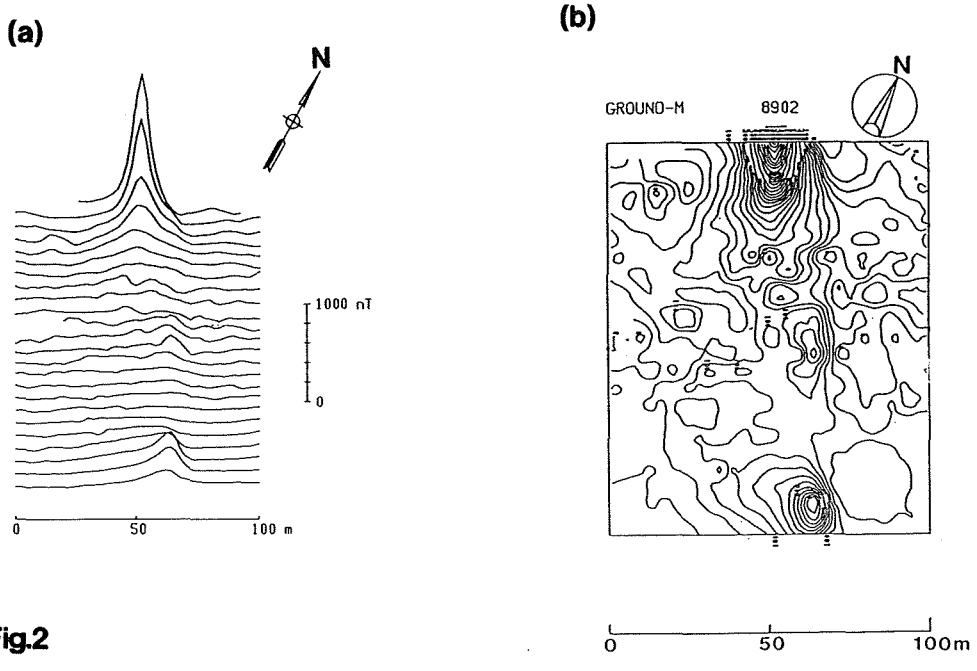

Fig.2

magnetic anomaly in the area X

Makino *et al.* (1989)

(a):profiles along each line
(b):contoured map

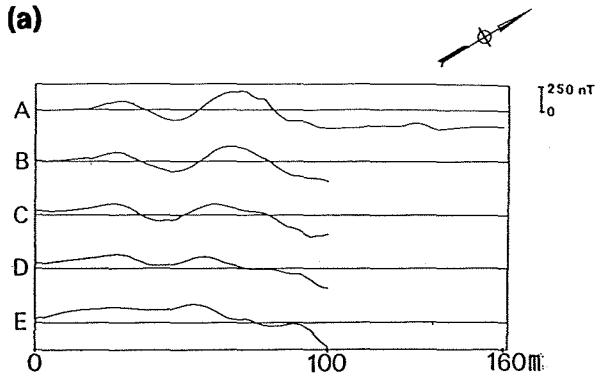

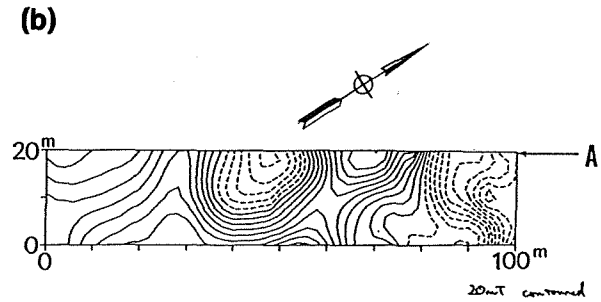

Fig.3
magnetic anomaly in the area Y

(a):profiles along each line
(b):contoured map

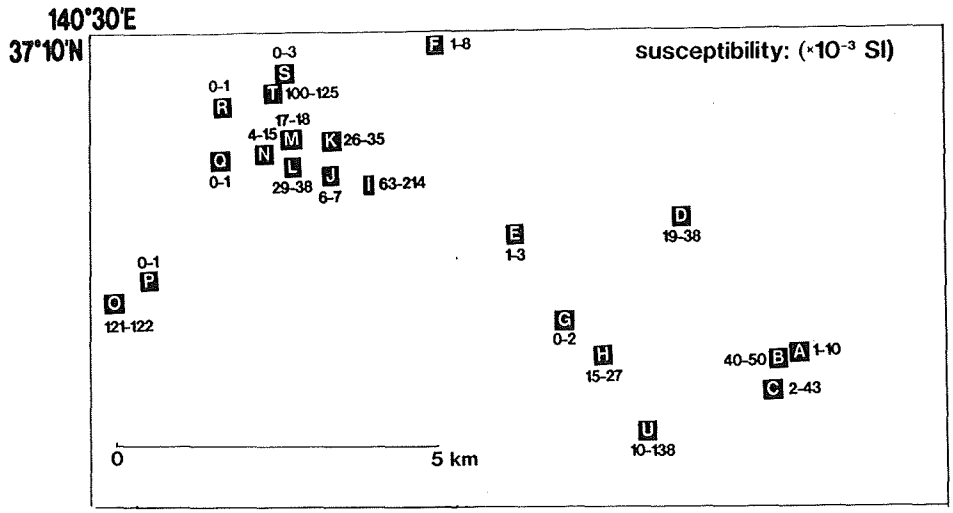

Fig.4 results of susceptibility survey
A-U: survey points

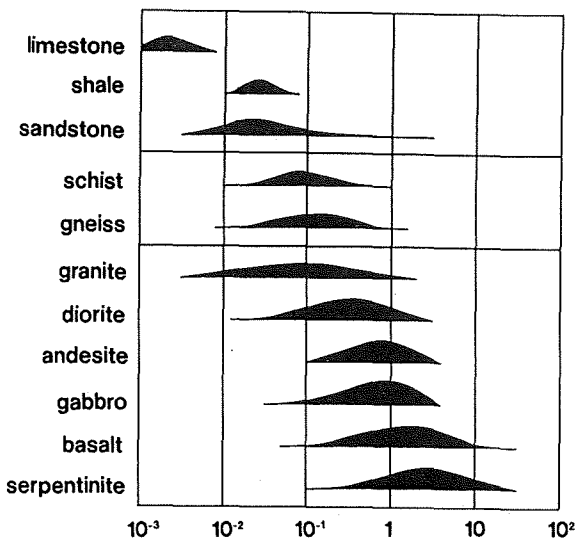

Fig.5 susceptibilities of rocks

SEGJ(1989)

3. Results and Discussion

Fig.2-a(Makino et al., 1989) indicates the magnetic anomaly profiles along each line in the area 'X'. Data were corrected only for the time variation of the geomagnetic field, not filtered. And Fig.2-b(Makino et al., 1989) indicates the contoured map derived from these data.

Fig.3-a and Fig.3-b indicate the profiles and the contour map of magnetic anomaly in the area 'Y' after the same process as in the area 'X'.

In the area 'X', we see very steep positive anomaly patterns with width of 16m, and its amplitude is about 1,400nT. It is estimated that there is something like a dike extending NNW-SSE in the shallow. In the area 'Y', we can see similar positive anomaly patterns which also suggest the existence of other shallow body like a dike.

According to the surface geology(Fig.1 after Kano et al., 1973), survey areas are mostly covered with tuff and there are some intrusive Gabbros and Ultrabasic rocks whose strikes are N20°W - N30°W. The direction corresponds with the strike estimated by magnetic anomaly patterns. Therefore, the shallow dike-like bodies mentioned above can be interpreted as ultrabasic rocks.

Moreover, as is shown in Fig.4, susceptibilities of rocks around the part where we recognized positive anomalies are higher than surroundings.

We recognize that susceptibility data in Fig.4 are scattered. Before this survey, we measured the susceptibilities of some rock samples at Geological Museum to check up our instruments, and the result agreed with the report by Kanaya(1987). Therefore we convince that our susceptibility survey data are also sufficiently reliable.

As is evident from Fig.5(SEGJ,1989), it is well known that susceptibility values of rocks have wide range, and we can not identify rock species only by susceptibility. When we interpret subsurface structure by magnetic anomaly patterns, we can get a condition if we have susceptibility data. In-situ measurement of rock susceptibility is very easy. The combination of ground magnetic survey and susceptibility survey is useful.

References

Kanaya,H. (1987) Bull. Geol. Surv. Japan, **38(4)** 203-216

Kano,H.,Y.Kuroda,K.Uruno,T.Nurei,S.Kanisawa,T.Maruyama,H.Umemura, H.Mitsukawa,N.Seto,Y.Ohira,S.Sato, and N.Isshiki (1973) Quadrangle Series, scale 1:50,000, **70** Geol.Surv.Japan

Makino,M.,S.Okuma,R.Morijiri, and T.Nakatsuka (1989) Proceedings of the 80th SEGJ Conference

Society of Exploration Geophysicists of Japan (1989) Graphics:Geophysical Exploration

THE CRUSTAL STRUCTURE OF THE SOUTHERN PART OF BOSO PENINSULA BASED ON MAGNETIC ANOMALY STUDY

Toshiya FUJIWARA[1], Sumio OGURA[2], Rie MORIJIRI[3] and Hajimu KINOSHITA[4]

1 Ocean Research Institute, University of Tokyo, Tokyo 164, Japan
2 NTT co. ltd., Tokyo 100, Japan
3 Geological Survey of Japan, Ibaraki 305, Japan
4 Earthquake Research Institute, University of Tokyo, Tokyo 113, Japan

The Boso Peninsula is located in the boundary area among three plates, i.e., North American Plate, Philippine Sea Plate, and Pacific Plate. These three large plates meet topographically at the trench-trench-trench Triple Junction off Boso Peninsula. The geology of the Boso Peninsula must be caused by complicated tectonic mechanism of three plates. Structural studies can provide clue to understand phenomena occurring in the boundary between continental and oceanic lithosphere in the Boso Peninsula. This study attempts to investigate the magnetic structure.

The on-land magnetic survey using a proton precession magnetmeter in the southern part of Boso Peninsula was conducted from March 1985 to March 1989. All the data points of the magnetic survey are displayed in Fig. 1. The area of the magnetic survey extends from 34°54' to 35°10'N, and from 139°45' to 140°10'E. The observation was made at 1212 points and spacing between data points were about 500m in average. A magnetic profile along a ship track in Tokyo Bay west off Boso Peninsula was obtained during DELP (Dynamics and Evolution of Lithosphere Program) 1987 cruise (Isezaki *et al.*,1989).

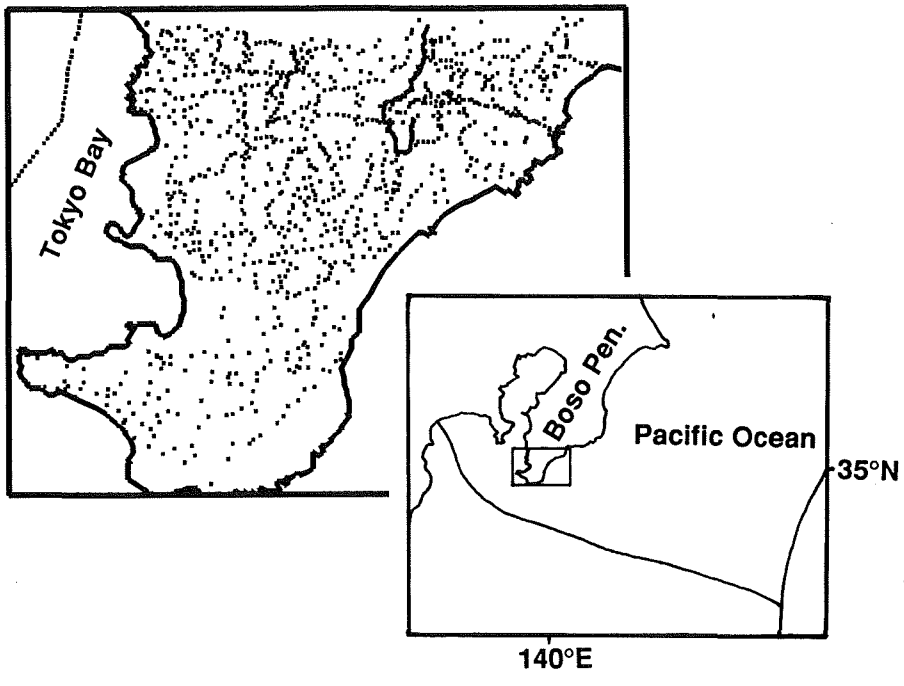

Fig. 1 Index map of the study area. Dots indicate observation points.

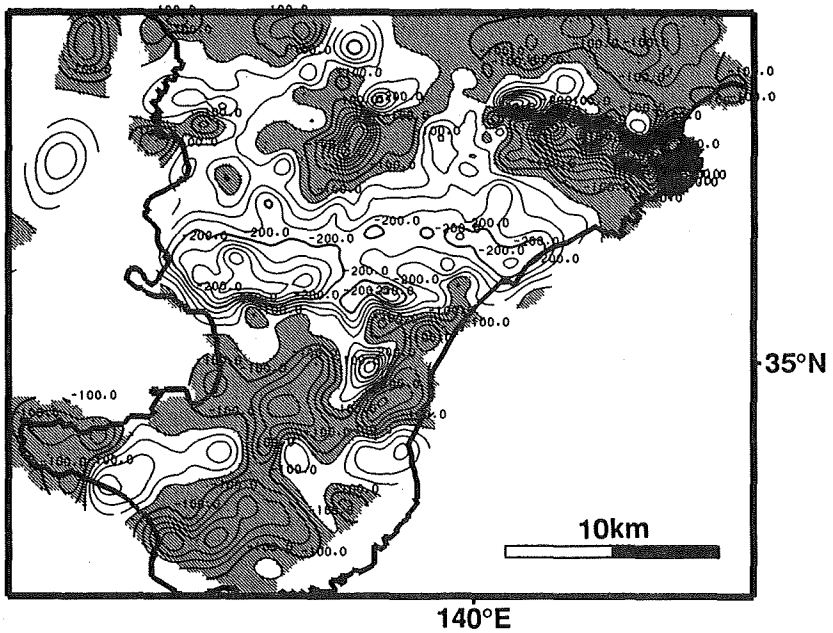

Fig. 2 Magnetic anomaly map continuated upward on a level of 460m. Contour interval is 20 nT. Positive anomaly area is shaded.

Fig. 2 is the magnetic anomaly map reduced by IGRF (International Geomagnetic Reference Field) 1985 model (IAGA Div. I WG. 1, 1985) and daily variation obsereved at Kano-zan Geodetic Station, Geographical Survey Institute. A general feature of magnetic anomalies in the survey area is characterized by a parallel alignment of positive and negative anomaly pattern with E-W strike. Positive anomalies in the southside of survey area is gentle with relatively long wavelength and the magnitude is about 100nT. Negative anomalies in the middle of survey area have an magnitude of about -300nT. Negative anomalies extend along WNW-ESE direction from a magnetic anomaly on a ship track in Tokyo Bay. Positive anomalies in the northside of survey area are prominent with short wavelength and the magnitude range from 200 to 300nT. These positive anomalies are caused by the ophiolitic rocks (especially serpentinite and basalt) associated with the geological trend of Mineoka belt (Kanehira *et al.*,1968). The Mineoka belt extends geologically to the Hayama belt in the Miura Peninsula on the opposite side of Tokyo Bay as is geomagnetically shown as the positive magnetic anomaly on the ship track.

Observed magnetic anomaly was devided into longer wavelength anomaly and shorter wavelength anomaly. Two wavelength components were analysed by different techniques. Magnetic basement undulation for the regional structure was inferred from low pass magnetic anomalies using two layer model inversion (Okuma *et al.*,1989). Magnetic anomalies involving short wavelength are interpreted by magnetized block using prism-shaped model calculation (Bhattacharyya,1964). As for parameters of the analysis, the direction of ambient geomagnetic field was assumed to be constant all over the area for the calculation. The values of declination of -6° and inclination of 48° were adopted referring IGRF 1985 model (The values at 35°N, 140°E). In the analysis of inversion, the magnetized direction is assumed to be the same as the ambient geomagnetic field. A contrast of magnetized intensity was set to be 2A/m. A mean depth was assumed to be 2804m. In the forward modeling, the magnetized directions and intensities is arbitrary.

Fig. 3 is a map of magnetic basement undulation derived from two-layer inversion of long wavelength geomagnetic anomalies. Depth of magnetic basement is ranging from 2km to 4km below the ground surface. The obtained magnetic basement is characterized by some features. The magnetic basement is shallow beneath the southside of study area. In the middle of study area where intervals of contour lines distribute densely in the figure, the magnetic basement is dipping steeply toward north with E-W strike. Beneath the Mineoka belt in the northside of study area, the magnetic basement rapidly becomes shallower than the surrounding area and forms sheet-like shape standing almost vertically with the E-W strike.

Two examples of the results of model calculations based on short wavelength geomagnetic anomalies are displayed in Fig. 4. Magnetized intensities are ranged from 0.5 to 1.8A/m. In Profile 1, prism-shaped magnetized block is located beneath the Mineoka belt. This represents sheet-like magnetic blocks the size of which is about 500m in horizontal N-S direction and is about 4000m in vertical. This block has deep magnetized inclination. In Profile 2, the solution reveals the structural change from south to north. As is shown in the figure, sheet-like magnetic block's array is extending horizontally. These magnetic blocks were sinking toward north. Their magnetized inclination are low angles. A difference of depth of magnetized blocks are recognized at the horizontal distance of 16-20km. The depth of the area where the magnetic basement is inclined steeply. This array sinks about 3000m below the surface. In the northside of study area, magnetized blocks become shallow. The magnetized inclination change to deep angles.

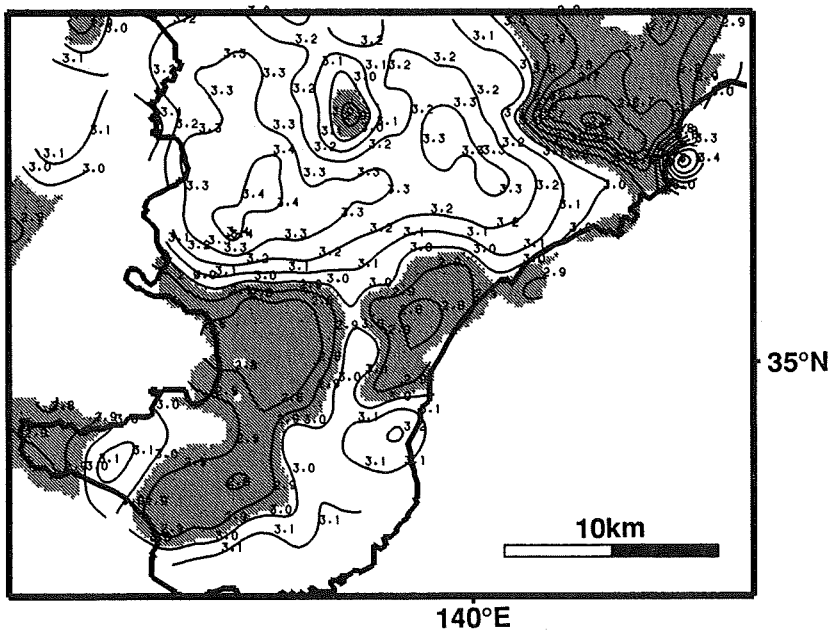

Fig. 3 Magnetic basement depth map. Contour interval is 0.1km. Relatively shallow basement area is shaded.

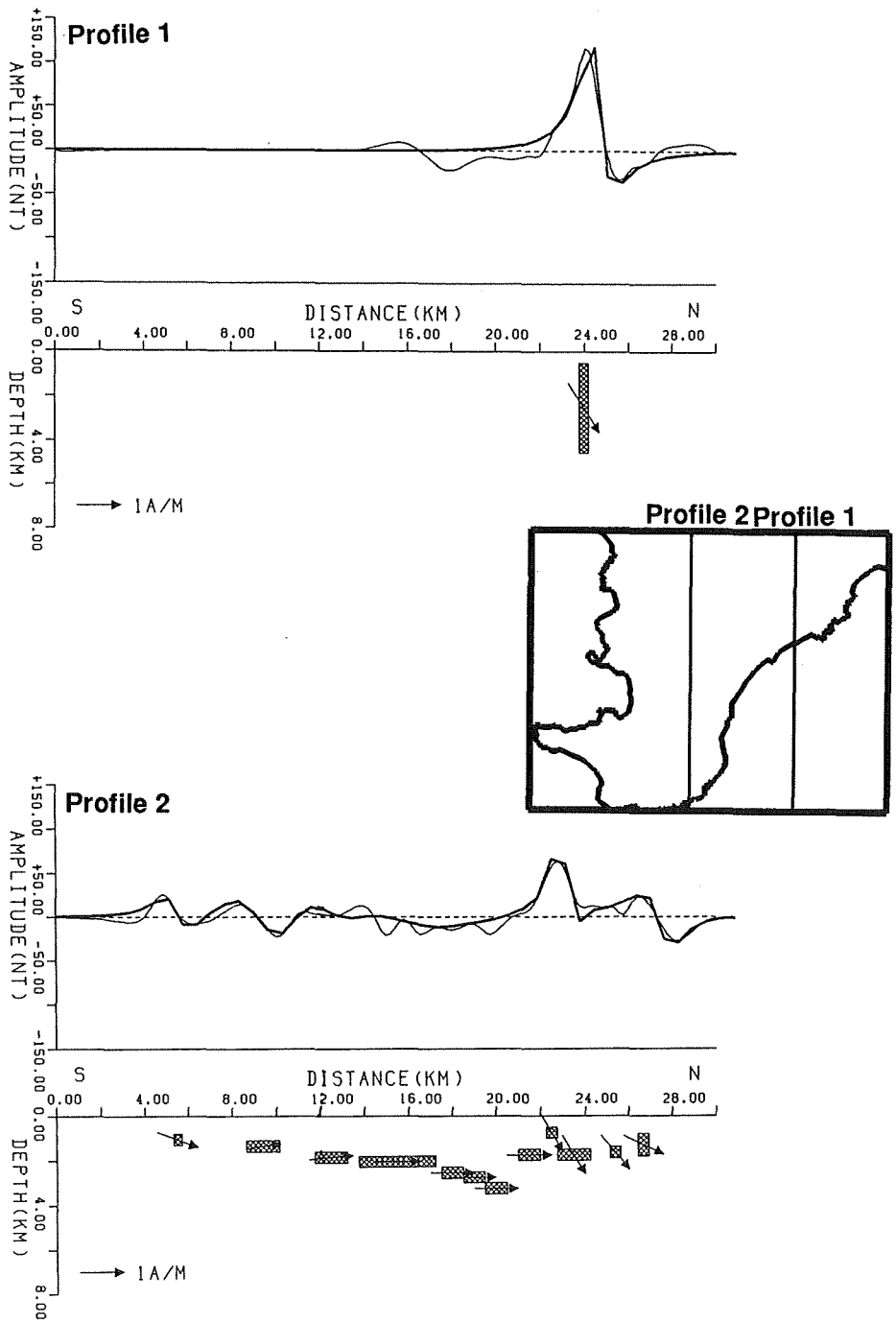

Fig. 4 Prism-shaped models which satisfied short wavelength magnetic anomalies. Upper part indicates short wavelength component of observed anomaly (plain) and a calculated anomaly (bold) profile. Lower part indicates a model structure. Rectangles indicate the position and size of magnetized models. Arrows indicate magnetized intensities and inclinations.

Positive anomalies in the southside of survey area are considered due to shallow magnetic basement and blocks. Magnetized inclinations in this area have low angles generally. The magnetic basement is inclined steeply in the middle of study area. In the same area, magnetic blocks have a difference of depth. This feature is considered as the cause of negative anomalies. Positive anomalies in the northside of study area are considered due to a shallow magnetic basement and standing sheet-like magnetic blocks. Their magnetized inclination are deep angles in contrast to southward area's results. The results of magnetic block's are sheet-like shape with thickness of about 500m and magnetized intensities of about 1-2A/m. Magnetic material origin are supposed to be oceanic origin from geological setting. Their scale and magnetic character are in good agreement with oceanic layer 2. Magnetic blocks are considered as pieces of oceanic crust. Magnetic basement is considered as emplacement and concentration of oceanic crust. Magnetized direction of magnetic blocks are regarded as due to Natural Remanent Magnetism of oceanic crust which indicates paleoposition. Low angle inclinations indicates that their are carried from low latitude. Variety of polarization and depth of magnetic blocks and layer are regarded as the result of emplacement of oceanic crust underplating, obducting or structural deformation in tectonic process. The oceanic crust was detached at trench and placed in sediments in process of accretion. Their locating depth become deep as away from the trench. In the Mineoka belt which is a boundary between ocean origin and land origin, magnetized directions were tilted and depth of magnetic material is very shallow. This feature is considered as the result of catastrophical collision, obduction or uplifting of oceanic crust.

REFERENCES

Bhattacharyya,B.K. (1964), Geophys., **29**, 517-531

IAGA Division I Working group 1 (1985), J. Geomag. Geoelectr., **37**, 1157-1163

Isezaki,N., H.Inokuchi, H.Ishikawa, K.Takahashi, Y.Inoue and K.Sugimoto (1989), Bull. Earthquake Res. Inst. Univ. Tokyo, **64**, 179-222

Kanehira,K., Y.Oki, S.Sanada, M.Yabe and F.Ishikawa (1968), J. Geol. Soc. Jpn., **74**, 529-534

Okuma,S., M.Makino and T.Nakatsuka (1989), Butsuri-Tansa, **42**, 82-96

(To be submitted to J. Geomag. Geoelectr.)

INTERMITTENT UPWELLING OF ASTHENOSPHERE BENEATH THE KENYA RIFT

Yoshiyuki TATSUMI and Nobukazu KIMURA

Department of Geology and Mineralogy, Kyoto University, Kyoto 606, Japan

The Kenya Rift is part of the Eastern African Rift system, which joins the worldwide oceanic ridge system at its northern end. It offers an opportunity to evaluate the role of mantle activity in the breakup of continents. Previous studies (Williams, 1972; King and Chapman, 1972; Norry et al., 1980; Wendlandt and Morgan, 1982) have reported decreasing degree of silica-undersaturation and incompatible element contents in alkaline basalts from the Miocene to the present. However, the absence of a data set including both age and basalt composition makes it difficult to detect the detailed secular variation of lava chemistry. This contribution examines the compositional variation of basalts with time, and discusses tpossible thermal causes in the upper mantle beneath the Kenya Rift.

Basalt samples were systematically collected from the lava stratigraphy within a small area (30 x 30 km) of the Samburu Hills on the northern frank of the Kenyan dome. It is assumed that this minimizes possible spatial (along- and across-rift) variation in basalt chemistry (Baker, 1972). Fig. 1 confirms previous suggestion (Williams, 1972; Baker, 1972) that major basalt volcanism occurs at ~15 and ~6 Ma, and is followed by phases of voluminous phonolite/trachyte eruption. A marked hiatus in volcanism is also notable at 8-9 Ma (Fig. 1).

Relatively aphyric basalts with phenocrysts of olivine, clinopyroxene, and plagioclase, were analysed, which minimizes the effect of phenocryst accumulation on the bulk rock chemistry. The basalts show a marked secular variation in incompatible element concentration (Fig. 2), involving two phases of relative depletion. These variations do not correlate well with major element compositions controlling normative mineralogy. Based on these observations, basaltic volcanism in this region can be divided into four stages; stage 1 between 17.4-13.0 Ma, stage 2 between 13.0-10.9 Ma, stage 3 between 10.8-5.0 Ma, and stage 4 between 5.0-0 Ma (Fig. 2). Here we use the term, high- and low-incompatible-element basalts (HIB and LIB) for stages 1 and 3, and stages 2 and 4, respectively (Fig. 2). The LIB volcanism of stages 2 and 4 is coeval with updoming and voluminous felsic volcanism in the region (cf. Fig. 1).

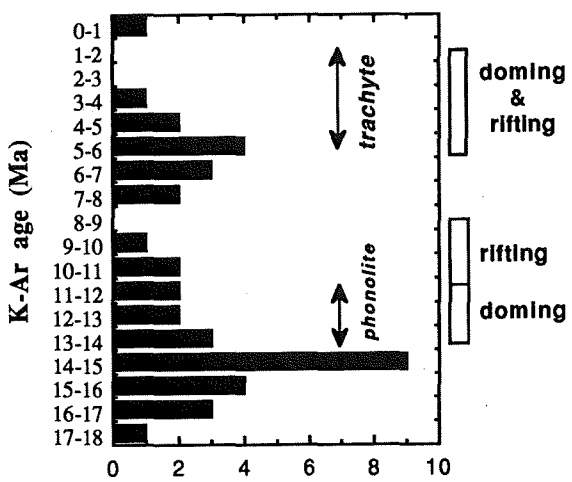

Figure 1. Frequency of K-Ar ages for basalts from the Samburu Hills. Ages of felsic volcanism and tectonic events are also shown. Major basaltic volcanisms occurred at 15 and 6 Ma and were followed by felsic volcanisms and domal uplift. A volcanic hiatus is notable at 8-9 Ma.

This secular variation in incompatible element concentration is most consistent with varying degrees of partial melting in the mantle source. Alternatively, HIB magmas are formed by more extensive fractionation or by greater contribution from incompatible-element-enriched materials. Fig. 3a,b suggest that HIB magmas cannot be produced from LIB magmas by fractionation of phenocryst phases. Possible incompatible-element-enriched contaminants are crustal materials, subcontinental upper mantle, trachyte or phonolite magma, and fluid phases. The formation of HIB magmas by greater involvement of the enriched mantle/crust materials is inappropriate, as representative African subcontinental upper mantle material, the source of Karoo picrites (Ellam and Cox, 1989), and continental crustal materials (Weaver and Tarney, 1981; Taylor and McLennan, 1981) have much higher K_2O/Nb ratios than Kenyan basalts (Fig. 3c). Formation of HIB magmas by mixing between LIB and trachyte/phonolite magmas is also unlikely, as these felsic magmas are more depleted in Sr than the basalt magmas (Fig. 3d). Norry et al. (1980) discussed the possible introduction of incompatible elements with a CO_2-rich fluid as a control on the compositional variation of basalts in the Kenya Rift. The more nepheline-normative (Eggler, 1974) and HIB magmas would then be generated when larger amounts of CO_2 are added to the magma source region. However, the absence of a sympathetic variation in normative nepheline and incompatible element concentrations (Fig. 2) does not support this.

If variation in the degree of partial melting is accepted as the principal cause of secular variation in incompatible element contents, then higher degrees of partial melting would be responsible for the more incompatible-element-depleted (Fig. 3b) and more magnesian (Fig. 3a) magmas of stages 2 and 4. The simple correlation between incompatible elements in Fig. 4 further suggests that the source mantle material for both HIB and LIB magmas is identical (i.e., source ratios remain constant). The divergence of only the lavas of highest Nb contents from the Th-Nb and Rb-Nb trends may be explained by the presence of residual phlogopite during their generation, an interpretation which is consistent with their generation at much smaller degrees of partial melting, as experimentally demonstrated by Mengel and Green (1986).

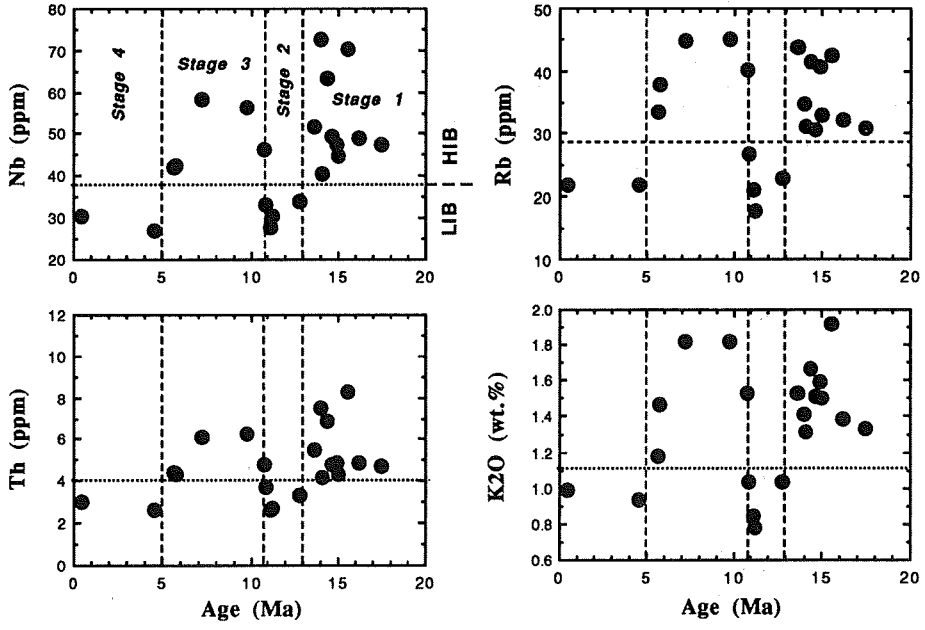

Figure 2. Secular variation of chemistry of aphyric basalts in the Samburu Hills. Two cycles of incompatible element relative depletion are recognized. A sympathetic variation in incompatible element concentrations and normative nepheline is absent. Basalts in stages are characterized by their higher incompatible element concentrations. HIB, high-incompatible-element basalts; LIB, low-incompatible-element basalts.

The occurrence of higher degrees of partial melting during stages 2 and 4 could be attributed to shallower and/or higher temperature melting of mantle material. In this context, it is notable that LIB magmas at stages 2 and 4 were produced soon after the peaks in basaltic volcanism at 14-15 and 5-6 Ma. These periods of extensive basaltic

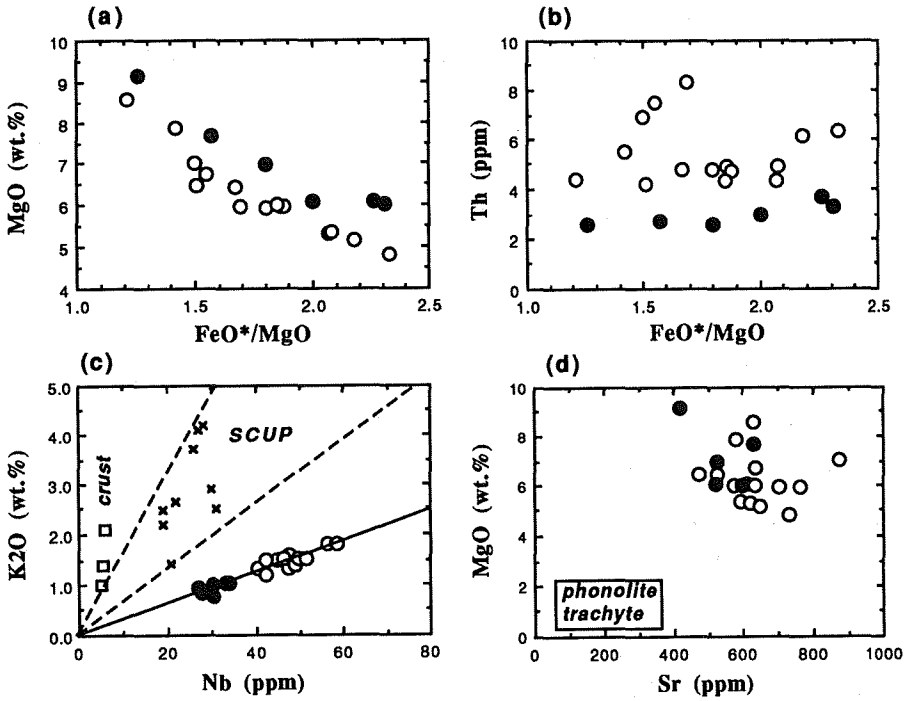

Figure 3. Examination of mechanisms producing HIB magmas (open circles) from and LIB magmas (filled circles) (see text). SCUP, subcontinental upper mantle.

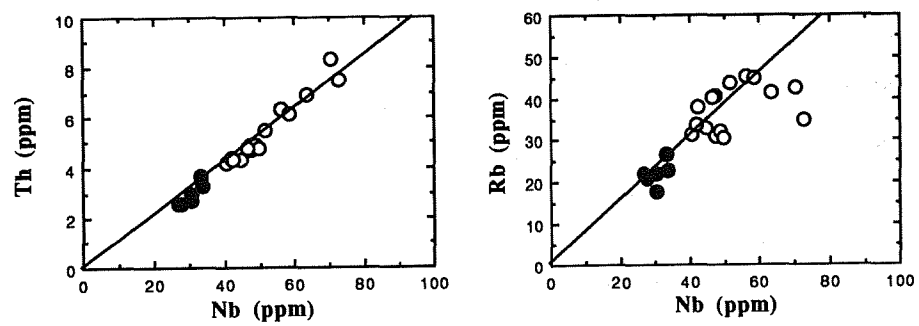

Figure 4. Incompatible element correlation in Samburu Hills basalts. HIB magmas (open circles) are produced by lower degrees of partial melting than LIB magmas (filled circles). Both magmas are derived from an identical incompatible element compositions with leaving phlogopite as a residual phase for highest-HIB magmas.

volcanism could be related to more intense mantle upwelling. This in turn will heat and lower the viscosity of surrounding and overlying mantle material and most likely result in thinning of the lithosphere (Spohn and Schubert, 1982). This enables further uprise of asthenospheric mantle which then segregate magmas at shallower levels, represented by stages 2 and 4. The hiatus in volcanism during stage 3 suggests a lull in mantle upwelling and generally cooler temperatures in the upper mantle. The stage 3 HIB magmas may correspond to lower degrees of partial melting at greater depths, possibly at the base of rethickened lithosphere.

The geological evolution of Kenya Rift may therefore be understood in terms of pulses of mantle upwelling following the onset of mantle melting. During the initial stage of volcanism at 18-17 Ma, the degree of partial melting was relatively small, due to deeper magma segregation beneath relatively thicker lithosphere. Asthenospheric upwelling reached its peak at ~15 Ma, yielding voluminous basalts. This phase of intense upwelling resulted in thermal thinning of the lithosphere. During the following period (13-10.9 Ma), upwelling material was able to ascend to shallower levels and melt to a larger degree. The injection of voluminous basalts into the crust since the onset of magmatism may have produced felsic magmas (trachyte/phonolite) by crustal anatexis (Bailey, 1964; Williams, 1971; Davies and Macdonald, 1987), though fractionation of basalt magmas may also have been responsible for the felsic magmas observed at this stage (Weaver et al., 1972; Baker et al., 1977; Price et al., 1985). The increased volume associated with crustal anatexis or the heat generation through crystallization of basalt magmas, and thermoelastic loading (McMullen and Mohraz, 1989) resulted in the expansion of crust and domal uplift of the surface. This was followed by the cracking of the brittle surface of the crust, and initiation of rifting (McMullen and Mohraz, 1989). Upwelling of asthenospheric mantle materials became weaker at 10.8-9 Ma, resulting in lithospheric cooling and thickening, with basalts magmatism during this stage being produced at greater depths and associated lower degree of partial melting. It is envisaged that this sequence of events was then repeated in the last 7 Ma.

References

Bailey, D. K. (1964) *J. Geophys. Res.* 69, 1103-1111.

Baker, B. H., Goles, G. G., Leeman ,W. P. & Lindstron, M. M. (1977) *Contri. Miner. Petrol.* 64, 303-332.

Baker, B. H., Mohr, P. A. & Williams, L. A. J. (1972) *Geol. Soc. Amer. Spec. Pap.* 136, 1-67.

Baker, B. H., Williams, L. A. J., Miller, J. A. & Fitch, F. J. (1971) *Tectonophys.* 11, 191-215.

Davies, G. R. & Macdonald, R. (1987) *J. Petrol.* 28, 1009-1034.

Eggler, D. H. (1974) *Yearb. Carnegie Inst. Wash.* 73, 215-224.

Ellam, R. M. & Cox, K. G. (1989) *Earth Planet. Sci. Lett.* 92, 207-218.

King, B. C. & Chapman, G. R. (1972) *Phil. Trans. R. Soc. Lond.* A271, 185-208.

McMullen, R. J. Jr. & Mohraz, B. (1989) *J. Geophys. Res.* 94, 13951-13962.

Mengel, K & Green, D. H. (1986) in *Kimberlites and related rocks*, Vol. 1, 571-581.

Norry, M. J., Truckle, P. H., Lippard, S. J., Hawkesworth, C. J., Weaver, S. D. & Marriner, G. F. (1980) *Phil. Trans. R. Soc. Lond.* A297, 259-271.

Price, R. C., Johnson, R. W., Gray C. M. & Frey, F. A. (1985) *Contri. Miner. Petrol.* 89, 394-409.

Spohn, T. & Schubert, G. (1982) *J. Geophys. Res.* 87, 4669-4681.

Taylor, S. R. & McLennan, S. M. (1981) *Phil. Trans. R. Soc. Lond.* A301, 381-399.

Weaver, B. L. & Tarney, J. (1981) *Earth Planet. Sci. Lett.* 55, 171-180.

Weaver, S. D., Sceal, J. S. C. & Gibson, I. L. (1972) *Contr. Miner. Petrol.* 36, 181-194.

Wendlandt, R. F. & Morgan, P. (1982) *Nature* 298, 734-736..

Williams, L. A. J. (1971) *Bull. Volcanol.* 34, 439-465.

Williams, L. A. J. (1972) *Tectonophys.* 15, 83-96.

(In press in *Earth Planet. Sci. Lett.*)

Authors Index

Channell, J. E. T. see Torii et al.
Cisowski, S. M. see Koyama and Cisowski
Fujiwara, T., S. Ogura, R. Morijiri, and H. Kinoshita 100
Fujiwara, Y. and T. Kanamatsu 38
Fukui, T. see Hayashida et al.
Fukuma, K. and M. Torii 65
Funahara, S. see Otofuji et al.
Funaki, M. and H. Sakai 5
Furukawa M. see Miki et al.
Hayashida, A., T. Fukui, and M. Torii 57
Hayashida, A. see Oda et al.
Hirooka, K. see Miki and Hirooka
Huang, T. see Miki et al.
Hyodo, M., W. Sunata, and E. E. Susanto 31
Hyodo, M. see Itota et al.
Ishikawa, N. 73
Itota, C., M. Hyodo, and K. Yaskawa 26
Kadoi, J. see Otofuji et al.
Kanamatsu, T. see Fujiwara and Kanamatsu
Kanaori, Y., S. Kawakami, and K. Yairi 59
Katsura, I. see Yamazaki et al.
Kawakami, S. see Kanaori et al.
Kimura, N. see Tatsumi and Kimura
Kinoshita, H. see Fujiwara et al.
Kono, M. see Zheng et al.
Koyama, M. and S. M. Cisowski 80
Maenaka, K. 21
Makino, M. see Morijiri et al.
Marumo, K. see Yamazaki et al.
Miki, D. and K. Hirooka 51
Miki, M., M. Furukawa, Y. Otofuji, S. Tsao, and T. Huang 83
Momose, H., M. Torii, and H. Tanaka 47
Morijiri, R., M. Makino, S. Okuma, and T. Nakatsuka 96
Morijiri, R. see Fujiwara et al.
Murata, F. see Otofuji et al.
Nakatsuka, T. see Morijiri et al.
Nishitani, T. 17
Oda, H., H. Shibuya, A. Hayashida, and M. Torii 42
Oda, H. see Torii et al.
Ogura, T. see Fujiwara et al.
Okuma, S. see Morijiri et al.
Otofuji, Y., J. Kadoi, S. Funahara, F. Murata, and X. Zheng 94
Otofuji, Y. see Miki et al.
Sakai, H. see Funaki and Sakai
Shao, J. see Zheng et al.
Shibuya, H. see Oda et al.

Sunata, W. see Hyodo et al.
Susanto, E. E. see Hyodo et al.
Tanaka, H. see Momose et al.
Tatsumi, Y. and N. Kimura 105
Torii, M., H. Oda, and J. E. T. Channell 11
Torii, M. see Fukuma and Torii
Torii, M. see Hayashida et al.
Torii, M. see Momose et al.
Torii, M. see Oda et al.
Tsao, S. see Miki et al.
Yairi, K. see Kanaori et al.
Yamazaki, T., I. Katsura, and K. Marumo 1
Yaskawa, K. see Itota et al.
Zheng, X. see Otofuji et al.
Zheng, Z., Kono, M., and J. Shao 86